Spring 5-10-2019

Role of the glycerophosphocholine acyltransferase, Gpc1, in phosphatidylcholine (PC) biosynthesis and remodeling in Saccharomyces cerevisiae

Sanket Anaokar

ROLE OF THE GLYCEROPHOSPHOCHOLINE ACYLTRANSFERASE, Gpc1, IN PHOSPHATIDYLCHOLINE (PC) BIOSYNTHESIS AND REMODELING IN *SACCHAROMYCES CEREVISIAE*

A Dissertation

Submitted to the Bayer School of Natural and Environmental Sciences

Duquesne University

In partial fulfillment of the requirements for

the degree of Doctor of Philosophy

By

Sanket Pramod Anaokar

May 2019

ROLE OF THE GLYCEROPHOSPHOCHOLINE ACYLTRANSFERASE, Gpc1, IN PHOSPHATIDYLCHOLINE (PC) BIOSYNTHESIS AND REMODELING IN *SACCHAROMYCES CEREVISIAE*

By

Sanket Pramod Anaokar

Approved February 4, 2019.

Dr. Jana Patton-Vogt Professor of Biological Sciences (Committee Chair)	Dr. Joseph McCormick Chair and Associate Professor of Biological Sciences (Committee Member)
Dr. Michael Jensen-Seaman Associate Professor of Biological Sciences (Committee Member)	Dr. Michael Cascio Associate Professor of Chemistry and Biochemistry (Committee Member)
Dr. Philip Reeder Dean, Bayer School of Natural and Environmental Sciences	

ABSTRACT

ROLE OF THE GLYCEROPHOSPHOCHOLINE ACYLTRANSFERASE, Gpc1, IN PHOSPHATIDYLCHOLINE (PC) BIOSYNTHESIS AND REMODELING IN *SACCHAROMYCES CEREVISIAE*

By

Sanket Pramod Anaokar

May 2019

Dissertation supervised by Dr. Jana Patton-Vogt.

Biomembranes are permeable barriers that enclose the cell and the intracellular organelles in a cell. The selective nature of these robust barriers acts as the first line of defense towards the harsh factors that can compromise cell survival. Biomembranes primarily consist of membrane lipids that are organized into layers to form a dynamic bilayer structure. The dynamic nature of the membrane requires the synchronized modulation of lipid composition through *de novo* synthesis, degradation, intracellular movement, and remodeling. Phospholipids are the major membrane lipid class, and phosphatidylcholine (PC) is the most abundant phospholipid in most eukaryotic biomembranes.

PC is primarily produced via two major pathways: the Kennedy and PE methylation pathways. Through a collaborative project, we have discovered a lipid-modifying enzyme, a glycerophosphocholine acyltransferase, Gpc1, involved in a new pathway for PC biosynthesis and

PC remodeling. Here, I have examined this alternative route for PC biosynthesis and remodeling using *Saccharomyces cerevisiae* (*S. cerevisiae*) as a model organism. First, I performed *in vivo* metabolic labeling studies to delineate the role of Gpc1 in the alternative route for PC biosynthesis. I have also determined the apparent molecular weight of this novel Gpc1 protein by constructing a C-terminal epitope tag followed by Western blot analysis. These studies are described in more detail in Chapter two.

In the second half of my dissertation, I have examined the physiological function and regulatory aspects of Gpc1. Using LC-MS analysis, I have determined the PC species profile generated via this alternative pathway. Gpc1 was found to be involved in a PC deacylation/reacylation remodeling pathway (PC-DRP) that results in an increase in monounsaturated PC species at the expense of diunsaturated PC species. Here, I report inositol, a phospholipid precursor, as a down-regulator for *GPC1* expression. Also, I have identified a phenotype associated with the loss of *GPC1.* Loss of *GPC1* results in decreased cell viability for cells at the stationary phase. These studies are described in detail in Chapter three. Overall, in Chapters two and three, I have identified Gpc1 as a member of PC-DRP, a pathway that increases the saturation state of the PC. This increase may impact on the physiochemical properties of the membrane.

ACKNOWLEDGEMENT

First, I would like to thank my advisor Dr. Jana Patton-Vogt for providing me the opportunity to work on this exciting project under her supervision. She has guided, helped and supported me right from my thesis proposal phase to attaining a post-doctoral position. Her guidance and encouragement allowed an overall development in me as a young scientist. I want to thank every member of Patton-Vogt Lab, present and past, specially Alexiy Nikiforov, Benjamin Jonik, Will King for all their support both during good and bad times.

Thanks to Dr. Joseph McCormick and Dr. Michael Seaman for providing valuable feedback on various aspects of my project. Thanks to Dr. Michael Cascio, for providing suggestions on the mass spectrometry aspects of my project. I want to acknowledge Dr. Ravindra Kodali, who helped us optimize and analyze the lipid samples using LC-MS.

I want to thank each person in the department who have helped me in my journey here at Duquesne. Especially to Sree Pullugula, Sumedha Sethi, Joe Sallmen, and Benjamin Robinson for all their help. Special thanks to my father Pramod Anaokar and mother Vrushali Anaokar for all their love and support. Thanks to my wife, Pratiksha for her patience, love, care, and help in the final year in my Ph.D.

TABLE OF CONTENTS

LIST OF FIGURES

Chapter 1

Chapter 2

Chapter 3

ABBREVIATIONS

CL	Cardiolipin
CDP-DAG	Cytidinediphosphate diacylglycerol
GPC or GroPCho	Glycerophosphocholine
GPE	Glycerophosphoethanolamine
GPI	Glycerophosphoinositol
GPCAT	Glycerophosphocholine acyltransferase
LPC	Lysophosphatidylcholine
OD(U)	Optical density (unit)
PC	Phosphatidylcholine
PA	Phosphatidic acid
PE	Phosphatidylethanolamine
PI	Phosphatidylinositol
PS	Phosphatidylserine
PC-DRP	PC deacylation/reacylation remodeling pathway
PG	Phosphatidylglycerol
qRT-PCR	Real-time quantitative-PCR
S. cerevisiae	*Saccharomyces cerevisiae*
SGD	*Saccharomyces* genome database
TAG	Triacylglycerol
WT	Wild type

Chapter 1: Introduction

1.1. *Saccharomyces cerevisiae* as a model organism to explore membrane lipids

Saccharomyces cerevisiae (*S. cerevisiae*) is a eukaryotic unicellular fungus known as the budding yeast. This unicellular fungus exists in both diploid and haploid states. Employing *S. cerevisiae* as a model organism has proven to be beneficial in understanding the biochemistry, molecular biology, and cell biology of lipids. There are many advantages to be gained by using *S. cerevisiae* as a model organism. For example, the doubling time for yeast is 90 minutes, this shorter generation time allows for faster culture saturation. The components in the medium can be altered depending on the aim of the experiment. The yeast deletion collection [1], auxotrophic markers, and drug-resistant markers are available for ease of genetic modification. The *Saccharomyces* Genome Database (SGD; http://www.yeastgenome.org), and linked websites such as Yeastract (http://www.yeastract.com) provide wealth of information on almost every aspect of characterized or uncharacterized ORFs. Accessible information includes potential transcription factors, cellular localization of gene products, gene expression data and protein-protein interactions.

The following are specific benefits of using *S. cerevisiae* as a model system to study lipids. First, the biochemical pathways necessary for cellular functioning in *S. cerevisiae*, including the lipid metabolism, show a high degree of similarity to the higher eukaryotes. *S. cerevisiae* lacks polyunsaturated lipids, making their lipid profile easier to study. The genetic tractability of this organism allows for the facile construction of the gene knockouts, overexpressors, and epitope tags. Components of the medium, such as the inclusion of inositol and choline, have a significant impact on the lipid profile. Thus, the ability to work with the defined medium allows the

researcher to have control over the physiological and biochemical parameters affecting the lipid profile.

1.2. Overview of the major classes of membrane lipids in *S. cerevisiae*

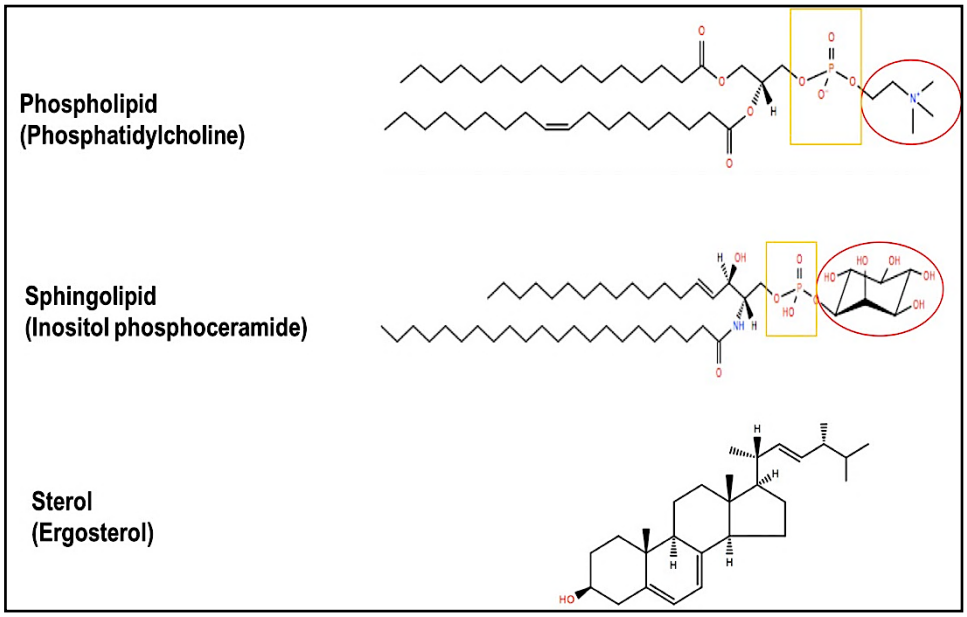

Figure 1. 1. Major classes of membrane lipids in yeast.
Phospholipids have a glycerol backbone, while sphingolipids have a ceramide backbone. Phospholipids have acyl chains at *sn-1* and *sn-2* positions of the glycerol backbone. Backbones and headgroups are highlighted in yellow boxes and red circles, respectively. Hydroxyl and oxygen moieties are denoted in red text. The structures were obtained from the LIPID MAPS database (https://www.lipidmaps.org/).

Biomembranes are bilayer structures consisting of lipids and proteins. Biomembranes act as barriers between the intracellular compartments of a cell and its cytosol, and between a cell and its environment. Each of these lipid layers has hydrophobic acyl chains directed inwards to create a hydrophobic core, while the hydrophilic headgroups interact with the outer or inner aqueous environment of a cell. The proteins associated with the lipid bilayer perform vital functions including the transportation of metabolites, responding to external stimuli and assistance in energy

transduction [2-4]. The major classes of membrane lipids (Fig 1.1) include phospholipids, sphingolipids and ergosterol [5, 6]. In yeast, phospholipids make up 70% of the membrane lipids, while sphingolipids and ergosterol account for the remaining amount [6].

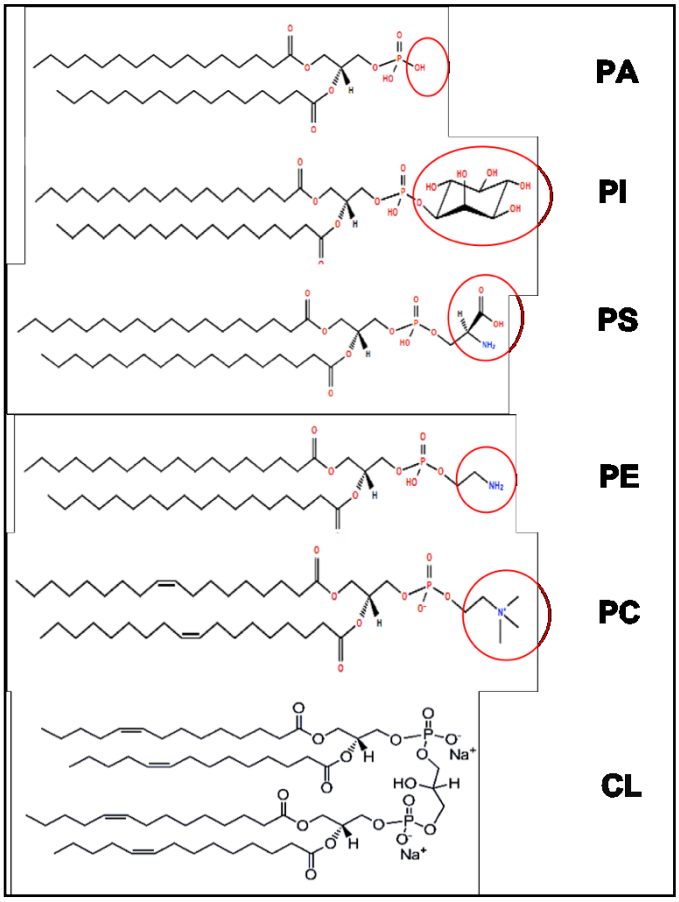

Figure 1. 2. Types of phospholipids.
Phospholipids are classified based upon the head group that is attached at the *sn-3* position of the glycerol backbone. The corresponding headgroup for each sub-class of phospholipids is denoted in red circles. Hydroxyl and oxygen moieties are denoted in red text. This figure was modified from reference [5]

Phospholipids are the primary lipid components of biomembranes. Phospholipids have a glycerol backbone that is esterified with acyl chains at the *sn-1* and *sn-2* positions and have a head group attached at the *sn-3* position (Fig 1.1). Phospholipids are categorized into sub-classes

depending on the type of the head group that is attached (Fig 1.2). The next major lipid class is the sphingolipids. Sphingolipids are based on a ceramide backbone to which an acyl chain is attached via an amide linkage. This class of membrane lipid accounts for almost 40% of the total inositol-containing lipids in the yeast [7]. Sphingolipids in yeast are classified into three major sub-classes: inositol-P-ceramide (IPC), mannose-inositol-P-ceramide (MIPC) and mannose-(inositol-P)$_2$-ceramide (M(IP)$_2$C) [2, 8]. The third major lipid class is the sterols. Ergosterol, the primary yeast sterol, is a four-ring structure with a hydrophilic hydroxyl group and an acyl side chain. The main structural difference in ergosterol with respect to cholesterol is that it has an extra carbon atom and one hydrogen in the side chain being replaced by methyl group [6]. Sterols, like ergosterol, are crucial in maintaining cell viability and membrane integrity in eukaryotic cells [6].

These major lipid classes along with membrane proteins form numerous specialized biomembranes such as the plasma membrane, the mitochondrial membrane, the endoplasmic reticulum, the Golgi apparatus membrane, the nuclear membrane, and the vacuolar and peroxisomal membranes. These membranes are involved in specialized functions including compartmentalization, metabolic energy generation, protein and lipid synthesis, and protection of genetic material.

1.3. Overview of phospholipid metabolism in yeast

The typical phospholipid composition of the plasma membrane (PM) is phosphatidylcholine (PC, 38%), phosphatidylethanolamine (PE, 30%), phosphatidylserine (PS, 4%), phosphatidylinositol (PI, 16%), cardiolipin (CL, 5%) and other minor phospholipids (7%) [6]. The other minor phospholipids include phosphatidic acid (PA), cytidine diphospho-diacylglycerol (CDP-DAG), phosphatidyldimethylethanolamine (PDME), phosphatidylmonomethylethanolamine (PMME), triacylglycerol (TAG) and diacylglycerol (DAG)

[6]. The lysophospholipids have a single fatty acid chain and make up a minor amount of the total lipid composition [6, 9].

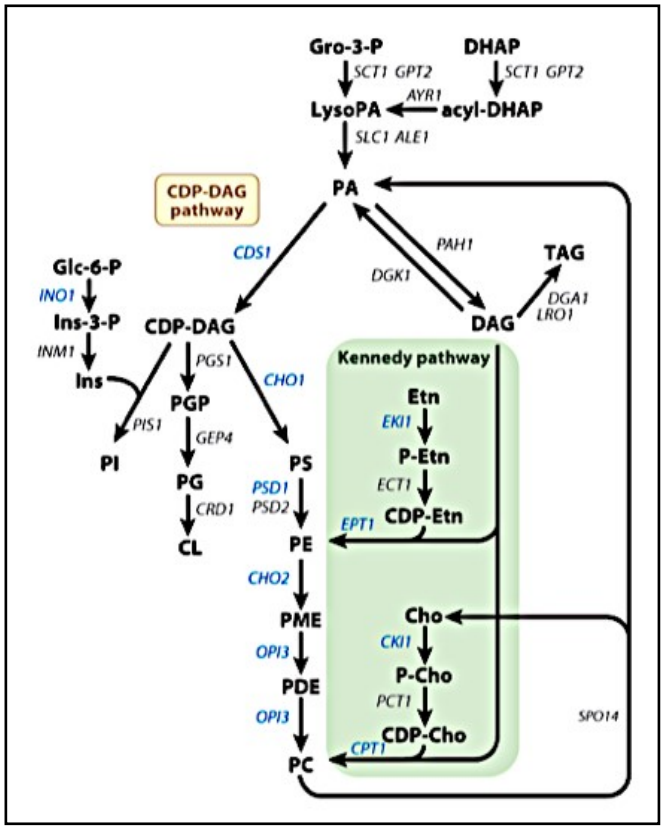

Figure 1. 3. Pathways for phospholipid synthesis in yeast.
The enzymes catalyzing each step are indicated in italics. The enzymes regulated by the Henry Regulatory Circuit are in blue. Abbreviation: G3P, glycerol-3-phosphate; LPA, lysophosphatidic acid; DHAP, dihydroxyacetone phosphate; acyl-DHAP, acyl dihydroxyacetone phosphate; PA, phosphatidic acid; TAG, triacylglycerol; PI, phosphatidylinositol; PS, phosphatidylserine; PE, phosphatidylethanolamine; PMME, phosphatidylmonomethylethanolamine; PMDE, phosphatidyl dimethylethanolamine; PC, phosphatidylcholine; Cho, choline; Cho-P, choline phosphate; Etn, ethanolamine; Etn-P, ethanolamine phosphate; PIP, phosphorylated phosphatidylinositol phospholipids; GPC, glycerophosphocholine; GPI, glycerophosphoinositol This figure was obtained from reference [5].

The pathways for phospholipid synthesis are interconnected with PA being the central lipid intermediate for the syntheses of other phospholipids [5]. PA is synthesized via the stepwise acylation of glycerol-3-phosphate (G3P) to lysophosphatidic acid (LPA) by the glycerol-3-

phosphate acyltransferases, Sct1 and Gpt2. LPA is then subsequently converted to PA by LPA acyltransferases, Slc1 and Ale1 [5, 6, 10-12]. PA is partitioned into making CDP-DAG and DAG by the enzymatic action of Cds1 and Pah1, respectively (Fig 1.3). CDP-DAG is used in the production of PI, CL, PG, and PS. DAG is used for CDP-choline and CDP-ethanolamine pathways for PC and PE synthesis, respectively (Fig 1.3). Along with the synthesis of phospholipids, DAG also enters the lipid storage pathway for TAG production. The detailed discussion of DAG and CDP-DAG utilization are reviewed below.

Synthesis and turnover of TAG: The PA phosphatase, Pah1 catalyzes the conversion of PA to DAG. DAG is a crucial precursor molecule in the synthesis of TAG [13]. Dga1 and Lro1 are acyl-CoA-dependent and phospholipid-dependent acyltransferases, respectively, that catalyzes the conversion of DAG to TAG [13]. In a nutrient deprivation stage of the cell cycle, such as the stationary phase, TAG is mobilized to produce fatty acids that are important for the synthesis of phospholipids and sphingolipids [14]. The TAG lipases such as Tgl1, Tgl3, Tgl4, and Tg15 catalyzes the hydrolysis of TAG [15].

Utilization of CDP-DAG for PI, CL, and PS synthesis: CDP-DAG is partitioned into the production of PI, CL, and PS. Inositol is an essential phospholipid precursor for PI synthesis. Inositol is produced in the cell by converting glucose-6-phosphate to inositol by the sequential enzymatic action of Ino1 and Inm1 [16]. Further, Pis1 catalyzes the synthesis of PI by utilizing CDP-DAG and inositol. Cho1, a PS synthase, catalyzes the conversion of CDP-DAG to PS [17]. PS can be decarboxylated to PE by two PS decarboxylases, Psd1 and Psd2 [5]. For cardiolipin (CL) production, CDP-DAG combines with G3P to synthesize phosphatidylglycerol phosphate (PGP). PGP undergoes dephosphorylation to PG by a phosphatase, Gep4 [18]. Finally, PG and CDP-DAG is used in making CL by the catalytic action of CL synthase, Crd1 [18].

Utilization of DAG for PE synthesis: PE is produced via two major routes: the PS decarboxylation (as described above) and CDP-ethanolamine pathways. In the CDP-ethanolamine pathway, ethanolamine is phosphorylated by Eki1 kinase to ethanolamine-phosphate, which is subsequently activated to CDP-ethanolamine by a cytidyltransferase, Ect1 [5]. Eventually, Ept1 catalyzes the final conversion of CDP-ethanolamine and DAG to PE [5].

Utilization of DAG for PC synthesis: Like PE synthesis, PC can be made via two major pathways, PE methylation and CDP-choline or Kennedy pathway. In the PE methylation pathway, PE undergoes three sequential methylation reactions in the ER by two phospholipid methyltransferase enzymes, Cho2 and Opi3. Cho2 catalyzes the conversion of PE to phosphatidylmonomethylethanolamine (PMME), while Opi3 catalyzes the conversion of PMME to phosphatidyldimethylethanolamine (PDME) and PDME to PE [5, 19]. In the CDP-choline or Kennedy pathway, exogenous choline can be transported into the cell by the Hnm1 transporter [17]. The intracellular choline undergoes phosphorylation to choline-P in the cytosol by Cki1. Choline-P is then activated to CDP-choline by a cytidyltransferase enzyme, Pct1 [5]. Finally, a choline phosphotransferase, Cpt1, catalyzes the conversion of CDP-choline and DAG to form PC [5].

As mentioned previously, supplementation of inositol and choline have a significant impact on the lipid profile in yeast. Susan A. Henry and colleagues have characterized the effects of inositol and choline supplementation on the lipid profile. Inositol decreases the level of PA, that in-turn results in increased levels of PI (Fig 1.4). The Henry regulatory circuit is the mechanism by which inositol controls the levels of PA and PI in the cell (further discussion is included in section 1.4).

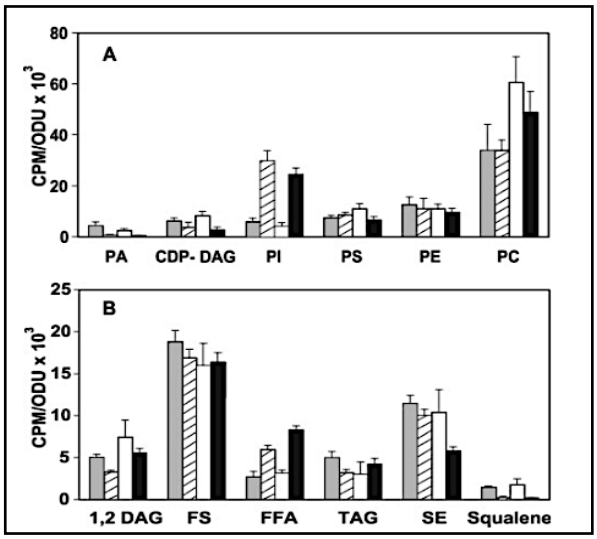

Figure 1. 4. Effect of inositol and choline on phospholipid and neutral lipids (NL) profile in WT yeast cell.

A. Phospholipid profile with and without inositol supplementation. **B.** NL profile with and without supplementation. Grey bars: medium lacking both inositol and choline, Stripped bars: medium containing Inositol, white bars: medium containing choline, black bars: medium containing inositol and choline. Abbreviations: SE, steryl esters; FFA, free fatty acids; FS, free sterols. This figure was obtained from reference [20].

The metabolism of all the major phospholipids described so far can be regulated at various stages in a pathway. Inositol is involved in the regulation of several genes that are involved in phospholipid metabolism. Many of these genes contain an UAS_{INO} element region in their promoters, which is involved in the regulation of the gene through the Henry regulatory circuit [5].

1.4. Regulation of UAS_{INO}-containing genes by the Henry regulatory circuit and other regulatory factors

Inositol availability has far-reaching transcriptional and physiological effects in yeast. As discussed before, inositol is vital for PI biosynthesis. Inositol can either be transported into the cell or can be produced by conversion of glucose-6-phosphate [20]. PI is a precursor for several molecules including the phosphoinositides, polyphosphates, inositol sphingolipids, and GPI

anchors [21]. These inositol containing molecules play an essential role in cell signaling and as structural components of the cell membrane [21].

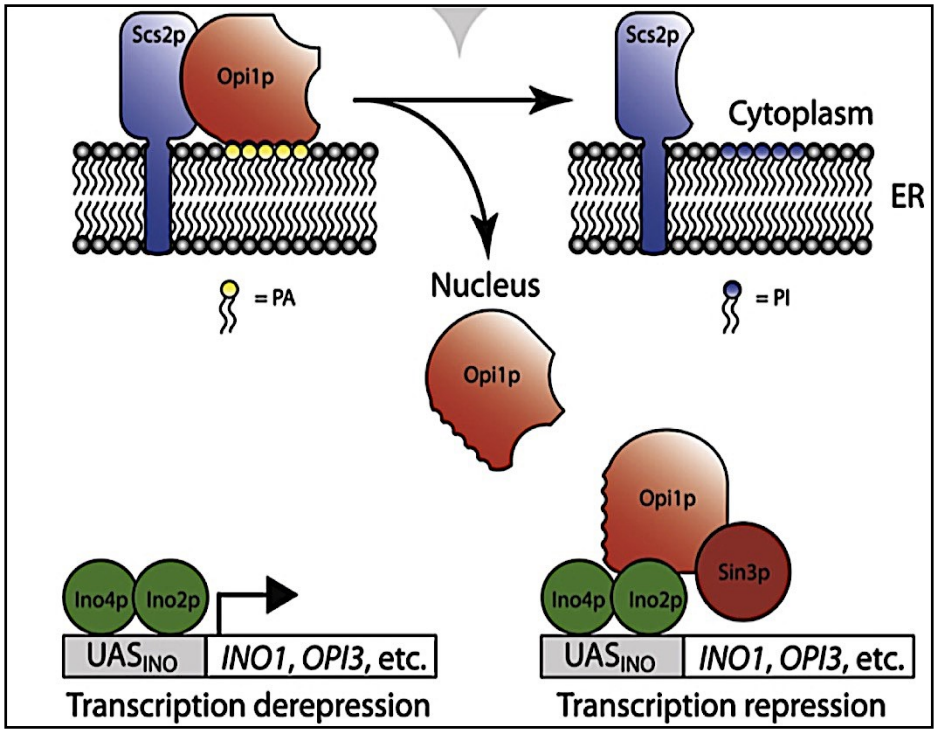

Figure 1. 5. Model for Henry regulatory circuit for regulation of UAS_{ino}-containing genes.

In the absence of inositol, PI levels are low and PA levels are high. The high levels of PA allow Opi1 to interact with the PA and Scs2, allowing the transcription of UAS_{ino}-containing gene by the Ino2-Ino4 complex. Upon supplementation of inositol to the medium, PI level increases, which releases the Opi1 and allows its translocation to the nucleus. Opi1 along with Sin3 results in transcription repression of UAS_{ino}-containing gene. This figure was obtained from reference [5].

Henry regulatory circuit: Most genes responsive to inositol have been found to be regulated by the Henry regulatory circuit involving transcription factors Ino2, Ino4, and Opi1. This complex mechanism involves the modulation of PA levels at the ER membrane surface, which in turn impacts the transit of the Opi1 repressor protein into the nucleus (Fig 1.5.) [5]. Cells grown in the absence of inositol displays low levels of PI and high levels of PA. Under this limiting

condition, the repressor Opi1 interacts with Scs2 and PA at the cytoplasmic face of the ER. The heterodimer Ino4-Ino2 complex bound to a UAS_{INO} consensus sequence-containing gene continues to activate transcription [22]. Conversely, in the presence of inositol, PI levels increase, and PA levels drop, releasing Opi1. Opi1 migrates to the nucleus and binds the heterodimer Ino4-Ino2 bound to the UAS_{INO} consensus sequence-containing gene, resulting in repression [5, 22].

Zinc mediated gene regulation: Zinc is an important nutrient required for growth of *S. cerevisiae.* It is a crucial cofactor for synthesis of numerous metabolic enzymes, chaperones, lipid-binding proteins, and transcription factors. The regulation of a gene by zinc involves the interaction of Zap1, a zinc-inducible transcriptional activator with a zinc response element (UAS_{zre})-containing gene [5]. This mechanism of regulation requires inositol deprivation in the medium that increases intracellular level of PA in the cell. Conversely, reduction in the cytosolic levels of zinc induces PI synthase to increase synthesis of PI. This increased level of PI consecutively regulates gene via the Henry regulatory circuit [5, 23].

Regulation via phosphorylation: The enzymes involved in lipid metabolism can also be regulated by post-translational modification through phosphorylation. There are several kinases such as protein kinase A and C, cyclic-dependent kinase and AMP-activated protein kinase that are known to regulate enzymes involved in phospholipid metabolism [5].

Along with these major regulatory mechanisms, mRNA degradation also contribute in regulating genes involved in lipid metabolism [5]. The next two sections discuss the different classes of lipid-modifying enzymes that are involved in the metabolism of lipids.

1.5. Role of phospholipases, permeases, and glycerophosphodiesterases in phospholipid metabolism

Lipid homeostasis can be achieved by regulating synthesis, transport, breakdown and remodeling of membrane lipids [6]. Phospholipases, permeases and glycerophosphodiesterases are responsible for production, transportation and metabolism of the glycerophosphodiesters (GPXs) in the cell.

Phospholipases are enzymes that hydrolyze phospholipids to various metabolites. These free metabolites are involved in vital cellular processes such as signaling, nutrient acquisition, remodeling and membrane homeostasis [24]. Phospholipases are classified into A, B, C, and D types, depending on the nature of the hydrolysis action carried out by these enzymes. The B-type phospholipases can perform hydrolysis at both *sn-1* and *sn-2* position of phospholipid to produce glycerophosphodiesters (GPXs) and free fatty acids (Fig 1. 6. B, C). Yeast has four genes *PLB1, PLB2, PLB3* and *NTE1* that encode B-type phospholipase enzymes. Plb1 is primarily responsible for deacylation of PC to GPC [25] [26]. Plb2 is responsible for deacylation of exogenous phospholipids [27]. Plb3 primarily acts on PI and PS to produce GPI and GPS [27], respectively, while Nte1 deacylates PC to GPC at the ER [28].

GPXs are hydrophilic molecules that are unable to pass the PM without the aid of permeases. The permease Git1facilitates the uptake and transport of GPI and GPC into the cell (Fig 1. 6. A). Git1 is phosphate regulated, i.e., low levels of phosphate in the medium increases the expression of *GIT1,* and high levels of phosphate decreases the expression [29, 30].

Gde1 is a glycerophosphodiesterase that is found in *S. cerevisiae*, *Candida albicans,* mammals and plants. Gde1 hydrolyzes GPC to G3P and free choline (Fig 1.6. D) [31, 32]. Like Git1, Gde1 is regulated by the levels of phosphate in the medium. The free choline that is produced via the action of Gde1 is recycled through the CDP-choline pathway for PC synthesis.

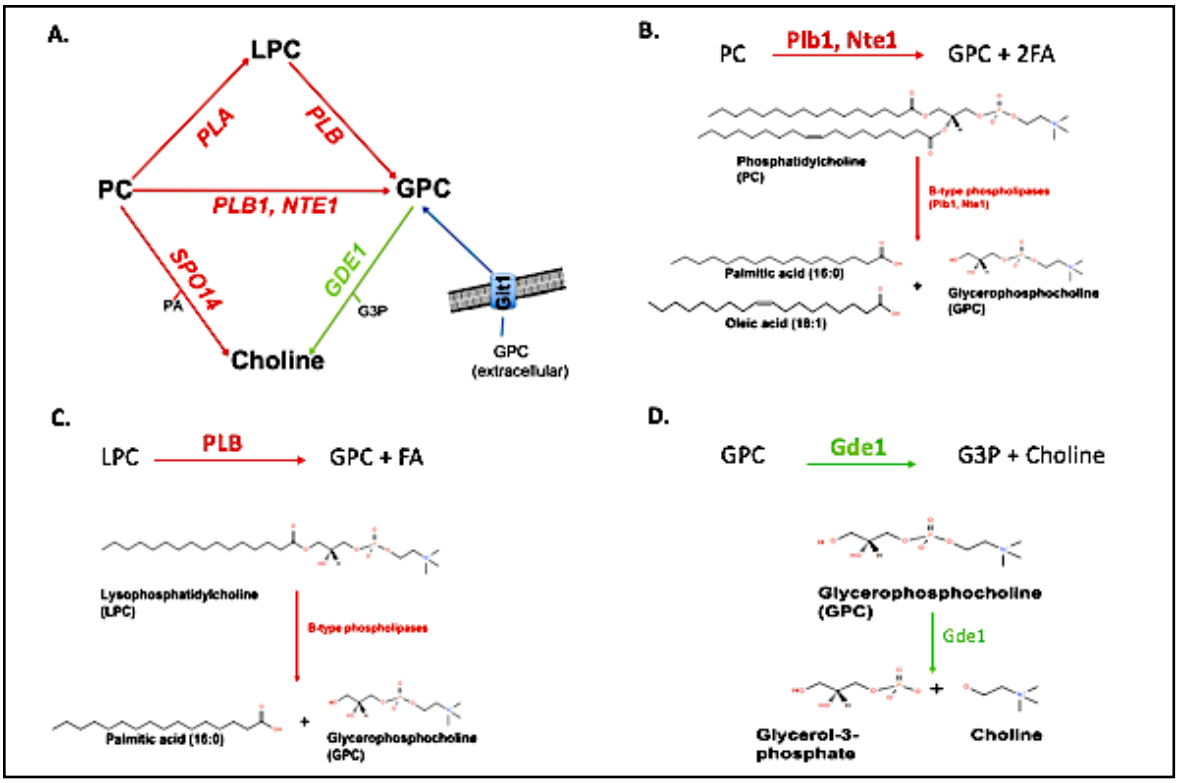

Figure 1. 6. Role of phospholipases, permeases, and glycerophosphodiesterase in the metabolism of GPC.

A. Schematic representation of the enzymes involved in the metabolism of GPC in the cell. Lipases are in red; phosphodiesterase is in green and permease in blue. B. Deacylation of PC to GPC by B-type phospholipase. C. Deacylation of LPC to GPC by PLB. D. Hydrolysis of GPC by phosphodiesterase, Gde1. Structures were obtained from LIPID maps database (https://www.lipidmaps.org/) to make this figure.

1.6. Classification of acyltransferases and transacylases involved in the metabolism of phospholipid

Acyltransferases are a group of enzymes founds in fungi, plants and animals [33]. They catalyze the transfer of an acyl chain from an acyl donor to an acyl acceptor [33], and in the most cases, acyltransferases utilize acyl-Coenzyme A as an acyl donor. Acyltransferases are broadly classified into glycerophosphate acyltransferase (GPATs), dihydroxyacetonephosphate acyltransferases (DHAPATs), acylglycerophosphate acyltransferases (AGPATs) and membrane-bound O-acyltransferases (MBOATs).

The GPATs catalyze the first step in *de novo* synthesis of PA (Fig 1.7) i.e., the conversion of G3P to LPA and the DHAPATs catalyze the conversion of DHAP to form 1-acyl-DHAP (Fig 1.7) [33]. *S. cerevisiae* has two genes, *SCT1/ GAT2* and *GPT2/ GAT1,* that encode enzymes with dual substrate specificity [34], i.e., these enzymes can use both G3P and DHAP molecules as an acyl acceptor (Fig 1.6). The acyltransferases also show different degrees of specificity towards the acyl chains they incorporate in the acceptor molecule. Palmitic acid (C16:0), palmitoleic acid (C16:1), stearic acid (C18:0) and oleic acid (C 18:1) are the major FAs that are esterified on *sn-1* and *sn-2* positions of the glycerol backbone to produce phospholipids [5, 35]. For example, Sct1 prefers incorporation of palmitate (16:0) as an acyl chain, while Gpt2 prefers incorporation of oleate (18:1) at the *sn-1* position of either G3P or DHAP [34, 36].

AGPAT catalyzes the second step in *de novo* synthesis of PA (Fig 1.7), i.e. the conversion of LPA to PA by incorporating an acyl chain at an *sn-2* position of an LPA molecule. In yeast, *SLC1* has been characterized as the AGPAT having the highest activity towards LPA [33, 37]. Some acyltransferases are associated with membranes and belong to membrane-bound *O*-acyltransferases that prefer incorporation of a monounsaturated acyl chain (C16:1 or C18:1) at an *sn-2* of LPL [38]. In yeast, *ALE1* (Alternative published names: *SCL4, LPT1,* and *LCA1*) has been characterized to have LPL acyltransferase activity, including, LPC and LPE acyltransferase activity (Fig 1.8.) [37-42]. Conversely, Cst26/Psi1 that has been characterized as an acyltransferase that prefers incorporation of a saturated acyl chain (18:0) at th*e sn-1* position of LPI to produce PI [43].

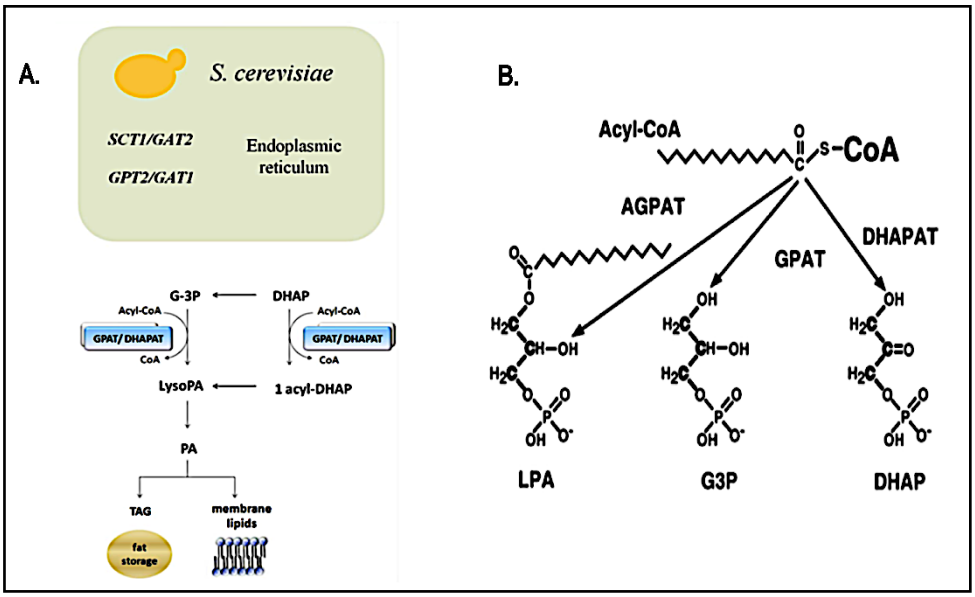

Figure 1.7. Acyltransferases in yeast.

A. Schematic representation of DHAP acyltransferase and G3P acyltransferases in yeast. **B.** Illustration of the substrate specificity for different acyltransferases. Abbreviations: Gro-3-P, glycerol-3-phosphate; LPA, lysophosphatidic acid; DHAP, Dihydroxyacetone phosphate; acyl-DHAP, acyl dihydroxyacetone phosphate; PA, phosphatidic acid; TAG, triacylglycerol. This figure is obtained from reference [34].

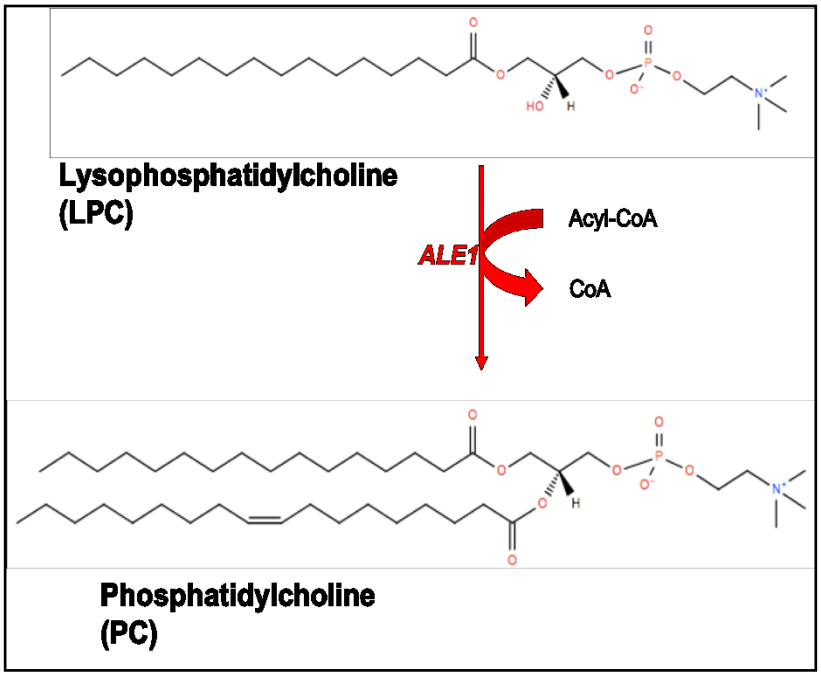

Figure 1. 8. LPLAT acyltransferases in yeast.

Lysophosphatidylcholine acyltransferases (LPLAT), *ALE1* (Alternative published names: *SCL4, LPT1,* and *LCA1*), utilizes monounsaturated acyl-CoA to acylate LPC to PC. The structures were obtained from the LIPID MAPS database (https://www.lipidmaps.org/).

Cardiolipin (CL) is a specialized phospholipid containing four acyl chains. CL is produced and localized to the inner membrane of the mitochondria [6, 44]. Defects in CL remodeling due to the protein Tafazzin are seen associated with the Barth syndrome in mammals [45]. Taz1, the yeast homolog of Tafazzin, is a transacylase that is involved in the remodeling of CL in yeast [18]. Taz1 converts monolysocardiolipid (MLCL) to CL, using phospholipid as an acyl donor and MLCL as the substrate [38]. Lro1 is another transacylase that converts substrates PE or PC and DAG to LPE or LPC and TAG, respectively [46-48].

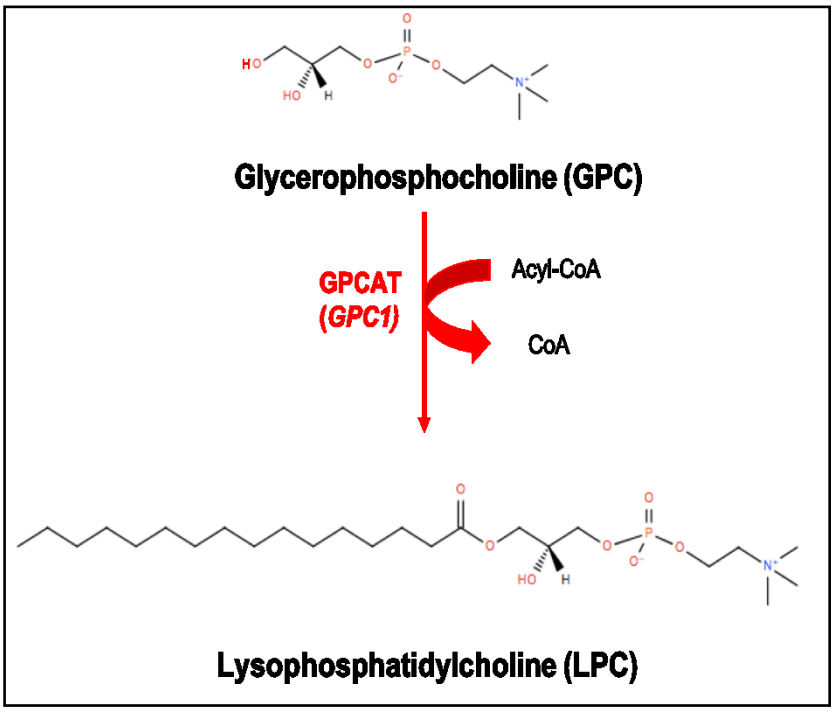

Figure 1. 9. GPCAT acyltransferases in yeast
GPC1 encodes a novel glycerophosphocholine acyltransferase acylating GPC to LPC. The structures were obtained from the LIPID MAPS database (https://www.lipidmaps.org/).

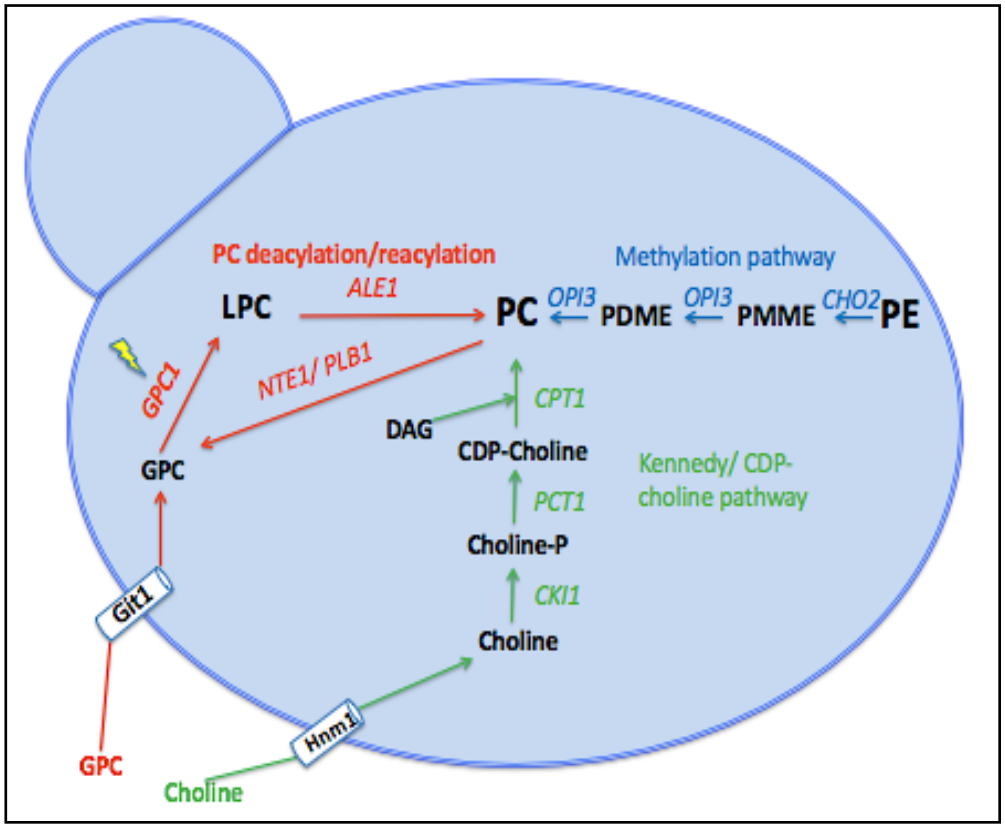

Figure 1. 10. *GPC1* defines a novel PC deacylation/reacylation pathway (PC-DRP) for PC biosynthesis.
GPC can either be transported into the cell or can be produced through PC deacylation by PLBs. GPC can be reacylated to LPC by Gpc1, and LPC can then be subsequently converted to PC by Ale1. The PC-DRP pathway is denoted in red. The methylation and Kennedy pathway are denoted in blue and green respectively. Abbreviation: GPC, glycerophosphocholine; LPC, lysophosphatidylcholine; PDME, phoshodimethylethanolamine; PMME, phosphomonomethylethanolamine.

1.7. A novel pathway for PC biosynthesis in bacterium, yeast and plants

Glycerophosphocholine acyltransferase (GPCAT) activity was first identified in yeast in 2008 by Stalberg and colleagues [49]. The activity was later identified in *Xanthomonas campestris* and plants [49-51]. Stalberg and colleagues attempted to identify the GPCAT encoding gene by performing genetic and biochemical analysis on the known acyltransferases, transacylases and lipases [49]. Still, the gene that encoded the activity remained undiscovered. Our collaborators,

Ida Lager and colleagues, identified YGR149w as the ORF encoding the GPCAT activity by screening cell extracts derived from the *S. cerevisiae* knock-out collection. Using *in vivo* metabolic labeling studies, we have identified the role of YGR149w in a novel pathway for PC biosynthesis in *S. cerevisiae.* The gene was named *GPC1.* The details of these studies are in Chapter two. I have further characterized the physiological function and regulatory features of this pathway. The details of these studies are in Chapter three.

The novel pathway for PC biosynthesis begins with the utilization of glycerophosphocholine (GPC). GPC can either be produced by the complete deacylation of PC by the action of the PLBs, Plb1 or Nte1 (Fig 1.10), or it can be internalized into the cell from the medium through Git1 (Fig 1.6) [26, 28]. The endogenous GPC can be acylated to lysophosphatidylcholine (LPC) by the GPC acyltransferase, Gpc1 (Fig 1.9) [52]. Subsequently, LPC can be converted to PC by the LPCAT, Ale1 [39].

Gpc1 is predicted to be an integral membrane protein with eight transmembrane spanning segments [53], and has a molecular weight of 52 kDa [52]. The predicted topology model of Gpc1 is shown in Fig 1.11. There are five post-translation modification sites present on Gpc1 that was identified by genome wide MS analysis studies (SGD; http://www.yeastgenome.org). Four out of five of these modifications are phosphorylations produced at amino acid (aa) positions 76, 78, 403 and 406, and the final modification is ubiquitination at position 86 (Fig. 1.11). These modifications suggest that both N and C-terminal of the Gpc1 are in the cytoplasmic region. Gpc1 belongs to a new family of acyltransferases having one domain with no known function (DUF2838) [52]. It lacks the know lipases or acyl binding motifs present in other studied acyltransferases and transacylases [49, 52]. Analysis of the *GPC1* homologs reveals a wide distribution in eukaryotes including fungi, animal, plants, algae, and most protist clades. No significant homologs were

present in animal subclades or prokaryotes [52]. The homologs of *GPC1* were found using sequence similarity in three plant species *Arabidopsis thaliana, Brassica napus*, and *Ricinus communis* (Chapter two). The next two sections (1.8. and 1.9.) of the introduction focus on the importance of the acyl chain remodeling that impacts physio-chemical properties of biomembranes.

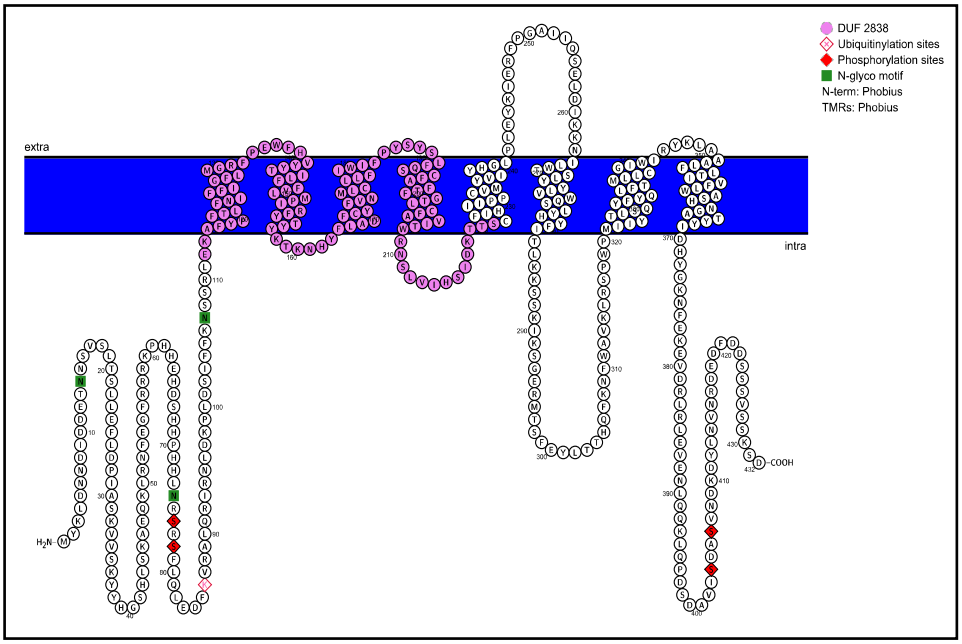

Figure 1.11. Predicted Gpc1 topology model.
Gpc1 is 432 amino acid long containing five sites for post-translational modification present at N and C-terminal of the Gpc1 that are predicted to be in the cytoplasmic region. The model is generated using Protter- open source tool (http://wlab.ethz.ch/protter/start/). Phosphorylation sites are in solid red diamond and ubiquitination site in pink diamond. The region marked by pink circles is a domain of unknow function (DUF2838).

1.8. Acyl chain remodeling affects the phospholipid molecular species that impact physical properties of the membrane

Phospholipids are classified depending upon the nature of the polar head group at the *sn-3* position of the glycerol backbone. However, within each of these classes, phospholipids are present in multiple molecular species depending upon the length and saturation of the acyl chains esterified to the glycerol backbone. The ensemble of these phospholipids with variations in the

acyl chain composition can affect the physicochemical properties of the membrane. Acyl chain remodeling of phospholipid is a post-synthetic process where one or both the acyl chains undergo exchanges. For the reason of simplicity, I am describing the known evidence of the PC remodeling, but remodeling has been studied and shown to occur in other phospholipids [10, 18, 38, 54].

Major evidence of PC remodeling: Remodeling was first reported as the Land's cycle in 1960. This two-step process involves deacylation of PC to LPC by the action of phospholipase A (PLA) and subsequent reacylation to PC [55]. Yamada and colleagues were the next to demonstrate an acyl-CoA dependent acyltransferase activity for both isoforms of LPC *in vitro* in rats [56]. The phospholipid profile in yeast is simple when compared to higher eukaryotes. This made Wagner and colleagues investigate remodeling in yeast. They used a radiolabeling approach, where ^{14}C-palmitate and ^{3}H-oleate FAs were supplied to the medium. They reported selective incorporation of these radiolabeled FAs into both *sn-1* and *sn-2* position of PC within 2 minutes of uptake [57]. Tanaka and colleagues showed PC remodeling by supplementing short eight carbon chain (methyl-^{13}C)$_3$ in medium. The results indicated the exchange of these radiolabeled short acyl chains with the natural C16 and C18 acyl chains [58]. Recently, PC remodeling was shown using deuterium-labeled (methyl-D_3)-methionine followed by ESI-MS/ MS analysis to examine the PC molecular species [10, 59]. The results revealed an increase in monounsaturated PC species (32:1, 34:1) at the expense of diunsaturated PC species (32:2, 34:2) [60]. This evidence suggests that remodeling leads to an alteration in phospholipid molecular species which could potentially affect membrane properties. The following are key attributes of the membrane that could be impacted by the acyl chain remodeling.

Membrane fluidity: Lipid bilayer exists in two phases, the liquid crystalline phase and gel phase [61]. The liquid crystalline phase is a fluidic and disordered state, while the gel phase is a

rigid and ordered state. The length of the acyl chain and the introduction of a *cis*-double bond are the significant characteristics that affect the membrane fluidity (Fig 1.12) [61]. Fluidity is maintained at an altered temperature by modifying both the length and saturation of acyl chains. The classes and *sn*-isomers of phospholipid species play an essential role in achieving the desired membrane fluidity. For instance, PE molecular species have a smaller head group as compared to the PC molecular species, that allows for tighter packing of PE. The phospholipid molecular species with a saturated or longer acyl chain at the *sn-1* position have a lower melting temperature as compared to phospholipid molecular species with similar acyl chain at the *sn-2* position [61, 62]

Membrane thickness: Membrane thickness is influenced by the length and saturation in the acyl chains of the lipids (Fig 1.12). The unsaturated lipids decrease the membrane thickness when compared to the corresponding saturated lipids. Whereas, an increase in the length of the acyl chain would result in an increase in membrane thickness [61, 62].

Membrane intrinsic curvature: Upon hydration phospholipids spontaneously assemble into bilayers, but few lipids prefer to assemble into a non-bilayer phase. This difference in the behavior depends upon the "shape structure" concept [61, 62]. The ratio of the cross-section area of head group to that of the acyl chains determines the phase preferred by the lipid. If the cross-section areas of the head group to that of the acyl chains is similar (example PC), then the molecule would possess a cylindrical shape and would favor forming a bilayer (Fig 1.12). Lipids such as LPC have a larger head group cross-section area compared to its acyl chain. This makes LPC prefer forming micelles in an aqueous environment. These lipids would give a positive intrinsic curvature to the membrane. Lipids such as PE and PA, have a smaller head group cross-section area and a larger acyl chain cross-section area, which gives them the inverted hexagonal shape (Fig 1.12). These lipids would contribute to a negative curvature in the membrane [61, 62].

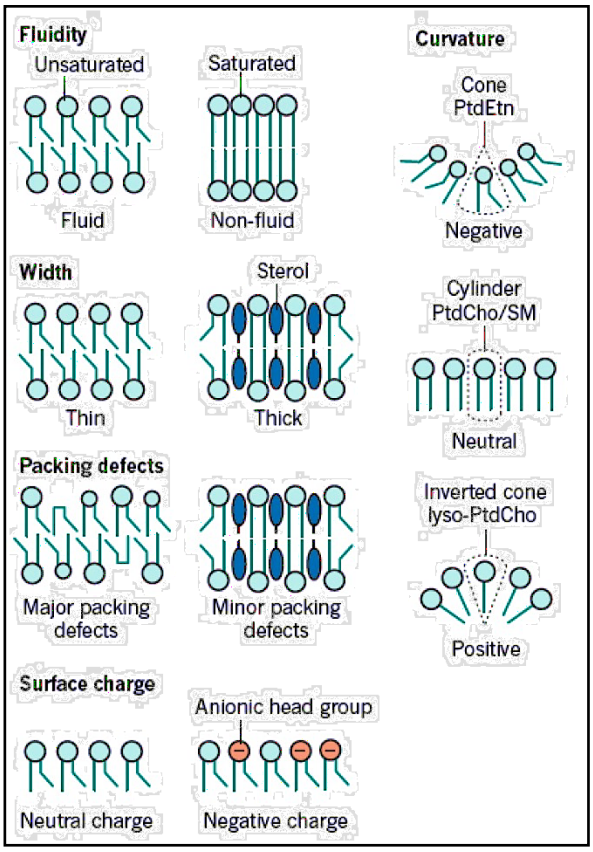

Figure 1. 12. Acyl chain composition affects the physical properties of membrane.
Fluidity increases with short and unsaturated fatty acid. The kinks caused by double bond lower the packing density and inhibit the transition to a solid gel phase. The length of the acyl chain and sterol packaging influence the thickness of a membrane. Lipid shape decides the curvature of the membrane. This figure was obtained from reference [61].

1.9. Significance of phospholipid remodeling for physiological functions in the higher eukaryotes

Phospholipid remodeling is important for preserving the differences in the acyl chain content present in the secretory pathway [63]. These differences are believed to be critical in organelle functioning and identity [10]. Organelles of the secretory pathways show a steady increase in saturated phospholipids at an expense of monounsaturated phospholipids as the location of organelles moves closer to plasma membrane. Alveolar type-II cells produce and

secrete pulmonary surfactant complex that primarily contains dipalmitoylphosphatidylcholine (DPPC). DPPC was shown to be synthesized by a lysophosphatidylcholine acyltransferase (LPCAT) through PC remodeling [64]. Defects in LPCAT activity are known to result in diseases states. The hepatic inflammation of liver results by an increase in the levels of LPC in a Lpcat3 knockout mouse [65]. Lpact3 was also shown to be vital for incorporation of arachidonic acid (C20: 4) into PC for TAG secretion in the intestine and liver [66].

1.10. Membrane lipids in Bacteria and Archaea

Bacterial species exhibit a vast degree of diversity in their membrane lipid composition. This diversity is influenced by the harsh environmental factors to which these organisms are exposed. Most bacterial membranes contain phospholipids, such as PE, PG, CL, Lysine-PG (LPG), PI, PA, and PS [67]. Bacteria can additionally produce phosphate-free lipids such as ornithine lipids (OLs), sulfolipids, diacylglyceryl-N,N,N trimethylhomoserine (DGTS), glycolipids (GLs), DAG, hopanoids (HOPs) and others [67]. *Escherichia coli (E. coli)* is the most common bacterial model organism used for studying the membrane lipids. The three major phospholipid classes in *E. coli* are PE (accounting for 75% of total membrane lipids), PG (accounting for 20% of total membrane lipids) and CL [67]. Bacterial species such as actinomycetes and δ-proteobacteria are known to produce PI, which is typically a eukaryotic lipid [67]. Some of the gram-positive bacterial species can add amino acids like lysine, alanine or arginine to PG to form lysine-PG, alanine-PG and, arginyl-PG, respectively. Bacteria from Cytophaga Flavobacterium-Bacteroides (CFB) group and actinomycetes are known to produce phosphate free lipids, OLs [67]. Eukaryotes and archaea lack OLs [67]. HOPs are present in some groups of bacteria such as cyanobacteria,

methylotrophic bacteria, actinomycetes, β-proteobacteria and δ-proteobacteria [67]. This lipid class is required for improving the stability and permeability of the bacterial membrane [67].

Archaea have a distinctive membrane lipid composition as compared to bacteria or eukaryotes. In bacteria and eukaryote, the fatty acid side chains present in phospholipid are ester-linked to the glycerol backbone. However, in archaea the fatty acid chains are ether-linked to the glycerol backbone [68]. Archaeal membrane lipids have a characteristic feature of containing isoprenoid moieties in its fatty acid chains [68]. The polar head group that classifies the phospholipids are similar to those found in bacteria and eukaryotes. The membrane lipids in archaea show several variations in the length of the isoprenoid chains, cyclization of the isoprenoid chains and numerous other adaptations [68]. However, the synthesis and regulation of these lipids in archaea are not well characterized [68].

1.11. Summary of background and significance

GPCAT activity was previously identified in bacteria, yeast, and plants, but the genes encoding the activities had remained unknown [49-51]. Our collaborators, Ida Lager and colleagues from the Swedish University of Agricultural Sciences, identified the GPCAT-encoding gene using *S. cerevisiae* as the model organism. The objective of this dissertation was to perform a thorough examination of the gene product to determine its role in PC metabolism *in vivo* in *S. cerevisiae*.

S. cerevisiae has two major pathways for bulk synthesis of PC. My research focused on examining the significance of having a third alternative route for PC biosynthesis. The central hypothesis was that the *GPC1* was nonessential for the bulk synthesis but was vital for the post-

synthetic acyl chain remodeling of PC that could have a potential effect on the physical properties of the membrane.

The specific objectives of the project were: 1) Examining the *in vivo* role of Gpc1 in PC biosynthesis, 2) Investigating the role of *GPC1* in post-synthetic PC remodeling and 3) identifying the regulatory mechanisms controlling its expression. These objectives are discussed in detail in Chapter two and three, respectively. These studies have defined a novel PC deacylation/reacylation remodeling pathway (PC-DRP) that has increased our understanding of PC metabolism.

Chapter 2: Cloning of Glycerophosphocholine Acyltransferase (GPCAT) from Fungi and Plants; A Novel Enzyme in Phosphatidylcholine Synthesis

Running title: Cloning and characterization of GPCATs

Reprinted from The Journal of Biological Chemistry, Vol 291, No 48, pages 25066-25076, Accepted November 25, 2016

Bartosz Głąb[a], Mirela Beganovic[b], **Sanket Anaokar[c],** Meng-Shu Hao[d], Allan Rasmusson[d], Jana Patton-Vogt[c], Antoni Banaś[a], Sten Stymne[b], Ida Lager[b]

From the [a]Intercollegiate Faculty of Biotechnology of University of Gdańsk and Medical University of Gdansk, 80-822 Gdansk, Poland. [b]Department of Plant Breeding, Swedish University of Agricultural Sciences, 230 53, Alnarp, Sweden. [c]Department of Biological Sciences, Duquesne University, 600 Forbes Ave, Pittsburgh, PA 15282, USA. [d]Department of Biology, Lund University, Biology building A, Sölvegatan 35, 223 62 Lund, Sweden.

Attributions:

Sanket Anaokar, I performed the Western blot analysis to identify the molecular weight of Gpc1, including constructing a vector plasmid containing *GPC1* with a C-terminal V5-His_6 epitope tag. I performed the *in vivo* studies and analysis of water-soluble metabolites. I was also involved in writing, proofreading and editing the manuscript. Additional experiments done for this project that were not part of manuscript are included in the appendix.

Bartosz Głąb, Mirela Beganovic, Ida Lager, and Sten Stymne characterized the *GPC1* gene by screening yeast deletion collections.

Meng-Shu Hao and Allan Rasmusson, completed the phylogenic tree analysis.

Bartosz Głąb, Jana Patton-Vogt, Ida Lager and Sten Stymne, designed the Research.

2.1. ABSTRACT

Glycero-3-phosphocholine (GPC), the product of the complete deacylation of phosphatidylcholine (PC), was long thought to not be a substrate for reacylation. However, it was recently shown that cell-free extracts from yeast and plants could acylate GPC with acyl groups from acyl-CoA. By screening enzyme activities of extracts derived from a yeast knock-out collection, we were able to identify and clone the yeast gene (*GPC1*) encoding the enzyme, named glycerophosphocholine acyltransferase (GPCAT). By homology search we also identified and cloned GPCAT genes from three plant species. All enzymes utilize acyl-CoA to acylate GPC forming LPC, and they show broad acyl specificities in both yeast and plants. In addition to acyl-CoA, GPCAT efficiently utilizes LPC and lyso-phosphatidylethanolamine as acyl donors in the acylation of GPC. GPCAT homologues were found in the major eukaryotic organism groups but not in prokaryotes or chordates. The enzyme forms its own protein family and does not contain any of the acyl binding or lipase motifs that are present in other studied acyltransferases and transacylases. In vivo labeling studies confirm a role for Gpc1p in PC biosynthesis in yeast. It is postulated that GPCATs contribute to the maintenance of PC homeostasis and have specific functions in acyl editing of PC, *e.g*. in transferring acyl groups modified at *sn*-2 position of PC to the *sn*-1 position of this molecule in plant cells.

2.2. Introduction

Phosphatidylcholine (PC) is the most abundant membrane lipid in all non-photosynthetic eukaryotes and in extraplastidic membranes in photosynthetic eukaryotes. It also has a central role in membrane homeostasis through the remodeling of its acyl groups in response to changing

environmental and metabolic conditions [69]. In plants, PC acyl chain modifications produce multiple polyunsaturated and unusual fatty acids which are delivered from PC, through various pathways, to other lipids, including the storage lipid triacylglycerol [70]. In yeast and other eukaryotic cells, the established pathways for PC biosynthesis are the CDP-choline pathway and the phosphatidylethanolamine (PE) methylation pathways. Once formed, the common pathway for PC turnover is the hydrolysis of acyl groups by phospholipases of the A or B type. Hydrolysis by an A type enzyme results in free fatty acid and lysophosphatidylcholine (LPC). The remaining acyl group of LPC can be hydrolysed by phospholipases of the A or B type to yield free fatty acids and glycerol-3-phosphocholine (GPC).

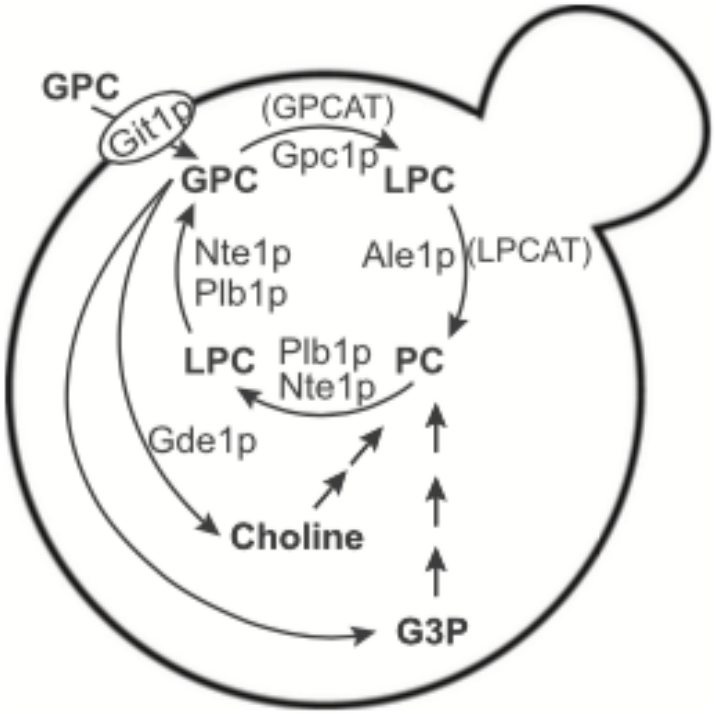

Figure 2. 1. Schematic outline of glycerophosphocholine (GPC) metabolism in yeast.
Yeast gene products are indicated. Generic terms for some enzymatic steps that apply to yeast and plants are shown in parenthesis: GPCAT, glycerophosphocholine acyltransferase; LPCAT, lysophosphatidylcholine acyltransferase. LPC, lysophosphatidylcholine; PC, phosphatidylcholine;

G3P, glycerol-3-phosphate. For simplicity sake, the PE methylation and Kennedy pathways for PC biosynthesis are not shown.

GPC is known to be catabolized to free choline and glycerol-3-phosphate (G3P) [31, 71, 72] and the resulting choline is used in the *de novo* synthesis of PC via the CDP-choline pathway [73]. Importantly, direct acylation of GPC by an acyl-CoA-dependent activity was recently demonstrated in *Saccharomyces cerevisiae* cell free extracts and microsomal preparations [49]. The putative enzyme carrying out the acylation of GPC was named GPC acyltransferase (GPCAT) (see Fig. 2. 1). Recently, GPCAT activities were also demonstrated in microsomal preparations from developing seeds from different plant species, as well as in *Arabidopsis* roots and shoots [50]. To a varying extent, the different microsomal preparations incorporated radioactive [^{14}C]GPC into both LPC and PC even in the absence of acyl-CoA [50].

In this work we screened a yeast deletion library to identify the yeast gene encoding GPCAT, which we have termed *GPC1*. By homology search we have also identified GPCAT encoding genes from plant species. In addition, we report that not only can GPCAT enzymes utilize acyl-CoA to acylate GPC but can also catalyze the transacylation of acyl groups from LPC to GPC. The latter reaction explains the earlier reported incorporation of GPC into lipids in the absence of added acyl-CoA in assays with microsomal preparation from developing oil seeds [50]. The GPCAT does not show any significant homology to other known acyl transferases and constitutes an enzyme family on its own with homologues represented in major eukaryotic organism groups but absent in prokaryotes.

2.3. Results and Discussion

2.3.1. Identification of the yeast GPCAT-encoding gene

A subset of the yeast knock-out collection was used to screen for the GPCAT-encoding gene. Only strains carrying deletions in genes with no known or putative function and with a size of at least 500bp were included. This group contained approximately 600 strains. Yeast extracts from the deletion strains were incubated with [^{14}C]choline labelled GPC, acyl-CoA and, as a control, [^{14}C]G3P; the lipids were separated by thin layer chromatography and visualized on an Instant Imager electronic autoradiograph.

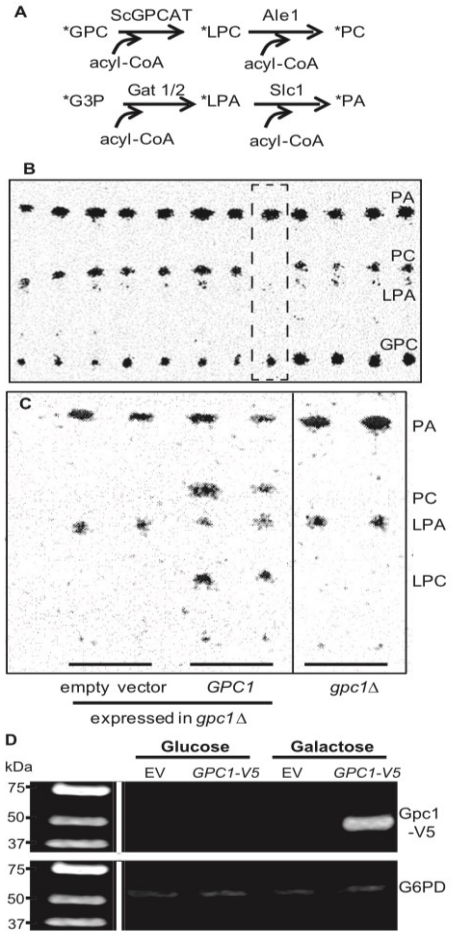

Figure 2. 2. Identification of ScGPCAT (*GPC1*).

Yeast extracts of strains from the yeast deletion collection were incubated with [^{14}C]GPC and 18:1-CoA. [^{14}C]G3P was added to the incubation as an internal control of enzymatic activities. A. The enzyme reactions in yeast from the substrates [^{14}C]GPC and [^{14}C]G3P. The yeast acylating enzymes are indicated in the figure. B. An autoradiogram of the screening on thin layer chromatography plates showing the deletion strain lacking GPCAT activity (within the hatched square). C. Complementation of *YGR149W* (*GPC1*) in the *gpc1*Δ deletion strain. Empty vector as well as the deletion strain (*gpc1*Δ) are also included. Irrelevant lanes from the plate have been removed from the picture (marked by a vertical line). D. Western blot of Gpc1p. Wild type strain bearing empty vector (EV) or a plasmid *(GPC1-V5)* harboring *GPC1* under the control of the galactose-inducible *GAL1* promoter and containing a C-terminal V5 epitope. Cells were grown on either glucose or galactose. Equivalent amounts of protein (75 μg) were loaded onto each lane. Anti Gpc1p-V5 primary antibody and goat anti-mouse secondary antibody were employed. Blot visualized using an Odyssey FC imaging system. Glucose-6-phosphate dehydrogenase (G6PD) was used as the loading control.

In the reaction, the putative GPCAT utilized acyl-CoA to convert GPC to LPC, which was further acylated to PC by the endogenous Ale1p. G3P was added to the assay as an internal control to validate the quality of the yeast extract and to provide a ratio of G3P to GPC acylation activity for detecting decreased GPCAT activity. G3P is acylated to lysophosphatidic acid (LPA) by the enzymes Gat1p and Gat2p and the formed LPA is converted to phosphatidic acid (PA) by Slc1p (Fig. 2.2.A). We identified a deletion strain lacking GPCAT activity, but exhibiting G3P acylation after approximately 200 screened strains, and the remaining strains were not screened. (Fig. 2.2.B). The identified strain bears a deletion in ORF *YGR149W*, here named *GPC1*, which is annotated as a putative protein of unknown function in the *Saccharomyces* Genome Database. The gene was amplified, cloned into a PYES-based yeast vector, and expressed in the identified deletion strain. As can be seen in Fig. 2. 2C, *GPC1* complemented the deletion strain. *GPC1* contains only one defined domain of no known function (DUF2838) and has no known acyl binding domains. The *S. cerevisiae* GPCAT (ScGPCAT) or Gpc1p is a protein of 52 kDa that is predicted to be an integral membrane protein with 8 transmembrane helices by the TMHMM server [74]. Western analysis (Fig. 2.2.D) of a V5-epitope tagged version of Gpc1p under the control of the *GAL1* promoter

(GAL1-GPC1-V5) reveals a protein of the expected molecular weight in cells grown in the presence of galactose.

2.3.2. Evolutionary analysis

Database searches revealed a wide distribution of GPCAT homologues in eukaryotes with generally singletons or dual paralogs being present in each species analyzed (Fig. 2.3.). No significant protein hits were found in prokaryotes, but homologues were found in major eukaryotic organism groups like fungi, animals, plants, algae and several protist clades. However, homologues were not found in for example alveolates or heterokonts nor in animal subclades like chordates and arthropods. In the maximum likelihood tree (Fig. 2.3.), proteins from animals, fungi and Streptophyta (plants and Charophyta) grouped separately as supported by significant bootstrap values. For other eukaryotes basal resolution was not observed. Chlorophyta (green algae) separated into two groups, one of which being associated (bootstrap value of 90%) with *Bodo saltans* (a euglenozoa belonging to Excavata). Significant groups were also observed for some Amobozoa proteins.

GPCAT was found present in all analyzed major groups of plants. However, the plant clade was characterized by displaying a very small sequence divergence as compared to other organisms groups. The plant group revealed a significant group containing seed plants, separate from the moss *Physcomitrella patens* and the lycopod *Selaginella moellendorffii*. The monocot proteins were weakly associated (bootstrap value of 64%), but the major groups of other plants were not resolved.

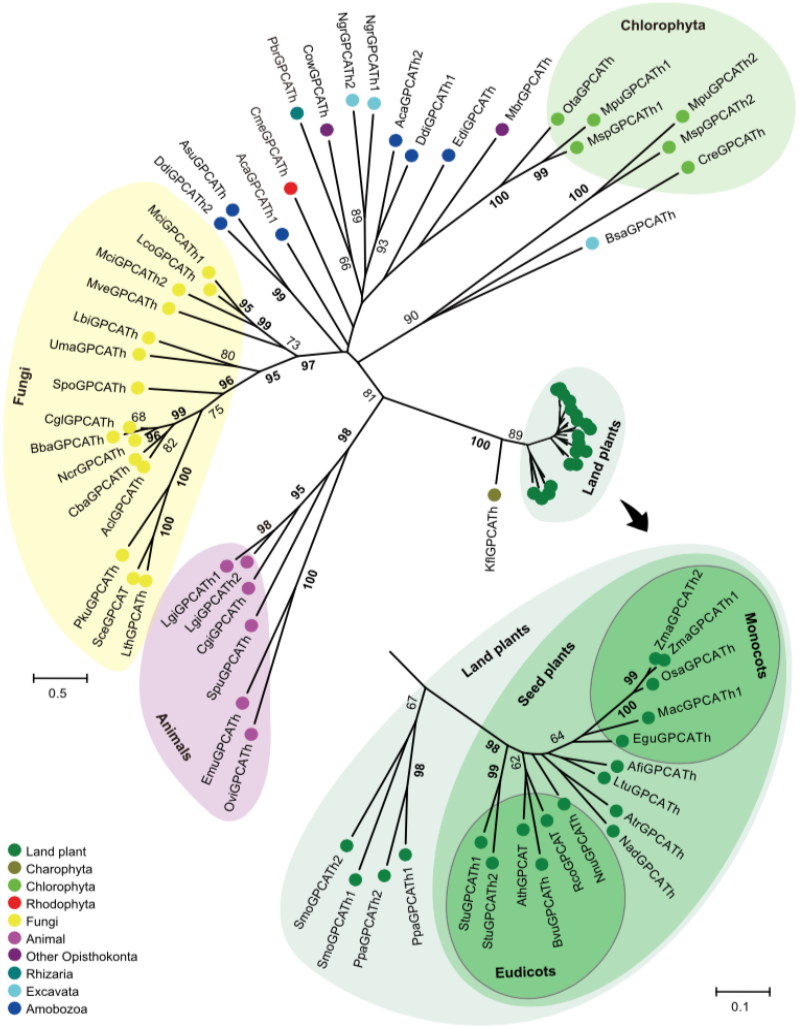

Figure 2. 3. Evolution of the GPCAT family in eukaryotes.
GPCAT homologues from selected species across the eukaryotic clade were aligned and a radial unrooted tree built by maximum likelihood analysis using an LG+G model. The tree is drawn to scale and branch lengths measured in substitutions per site. Bootstrap values above 60 are shown (in %). Values of at least 95 are bolded. Inset, an expanded subtree for the land plant clade is

shown. Abbreviations: *Aca, Acanthamoeba castellanii str. Neff; Acl, Aspergillus clavatus NRRL 1; Afi, Aristolochia fimbriata; Asu, Acytostelium subglobosum LB1; Ath, Arabidopsis thaliana; Atr, Amborella trichopoda; Bba, Beauveria bassiana D1-5; Bsa, Bodo saltans; Bvu, Beta vulgaris subsp. Vulgaris; Cba, Cladophialophora bantiana CBS 173.52; Cgi, Crassostrea gigas; Cgl, Chaetomium globosum CBS 148.51; Cme, Cyanidioschyzon merolae strain 10D; Cow, Capsaspora owczarzaki ATCC 30864; Cre, Chlamydomonas reinhardtii; Ddi, Dictyostelium discoideum AX4; Edi, Entamoeba dispar SAW760; Egu, Elaeis guineensis; Emu, Echinococcus multilocularis; Kfl, Klebsormidium flaccidum; Lbi, Laccaria bicolor S238N-H82; Lco, Lichtheimia corymbifera JMRC:FSU:9682; Lgi, Lottia gigantea; Lth, Lachancea thermotolerans CBS 6340; Ltu, Liriodendron tulipifera; Mac, Musa acuminata subsp. Malaccensis; Mbr, Monosiga brevicollis MX1; Mci, Mucorcircinelloides f. circinelloides 1006PhL; Mpu, Micromonas pusilla CCMP1545; Msp, Micromonas sp. RCC299; Mve, Mortierella verticillata NRRL 6337; Nad, Nuphar advena; Ncr, Neurospora crassa OR74A; Ngr, Naegleria gruberi strain NEG-M; Nnu, Nelumbo nucifera; Osa, Oryza sativa Indica Group; Ota, Ostreococcus tauri; Ovi, Opisthorchis viverrini; Pbr, Plasmodiophora brassicae; Pku, Pichia kudriavzevii; Ppa, Physcomitrella patens; Rco, Ricinus communis; Sce, Saccharomyces cerevisiae S288c; Smo, Selaginella moellendorffii; Spo, Schizosaccharomyces pombe 972h; Spu, Strongylocentrotus purpuratus; Stu, Solanum tuberosum; Uma, Ustilago maydis 521; Zma, Zea mays.* See supplemental Figure S1 for protein alignment and sequence IDs.

2.3.3 ScGPCAT (Gpc1p) catalyzes the acyl-CoA-dependent acylation of GPC

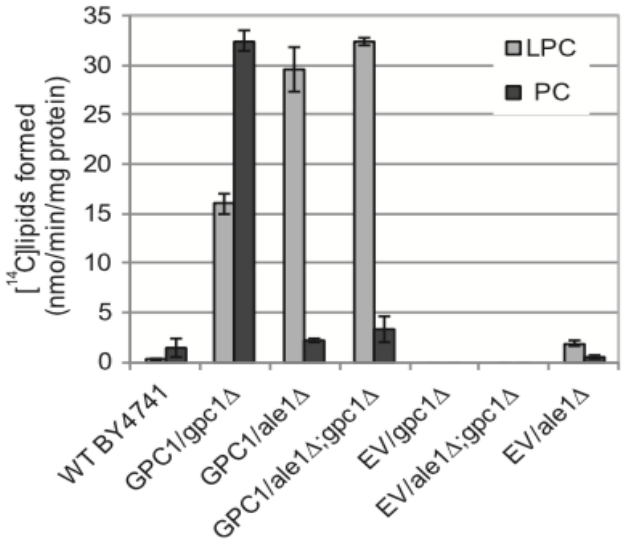

Figure 2. 4. Radioactive lipids formed by microsomes from the indicated strains.
Microsomes were prepared from the indicated yeast strains bearing empty vector (EV) or expressing *GPC1* under the *GAL1* promoter (*GPC1)*. The WT yeast was grown in YPD, yeast strains carrying a plasmid were grown in YNB medium containing galactose. Microsomes (2 µg of protein) were incubated with [^{14}C]choline labelled GPC (0.24 mM) and 18:1-CoA (0.2 mM) for 30 min at 30^{o}C. The results shown are from triplicate assays ± SD. LPC, lysophosphatidylcholine; PC, phosphatidylcholine.

The ScGPCAT activities were assayed with [^{14}C]GPC and non-radioactive 18:1-CoA in microsomal preparations from wild type (WT;BY4741), *gpc1Δ, ale1Δ and ale1Δ gpc1Δ* yeast strains expressing either *GPC1* under the control of the *GAL1* promoter or transformed with empty vector (Fig. 2.4.). In WT, the main radioactivity in lipids was found in PC (85%) and the remaining radioactivity in LPC. Membranes from *ale1Δ* transformed with empty vector incorporated about the same amount of total radioactivity into lipid as WT but only 21% of the radioactivity was found in PC with the remaining activity in LPC, indicating that Ale1p is primarily responsible for LPC acylation.

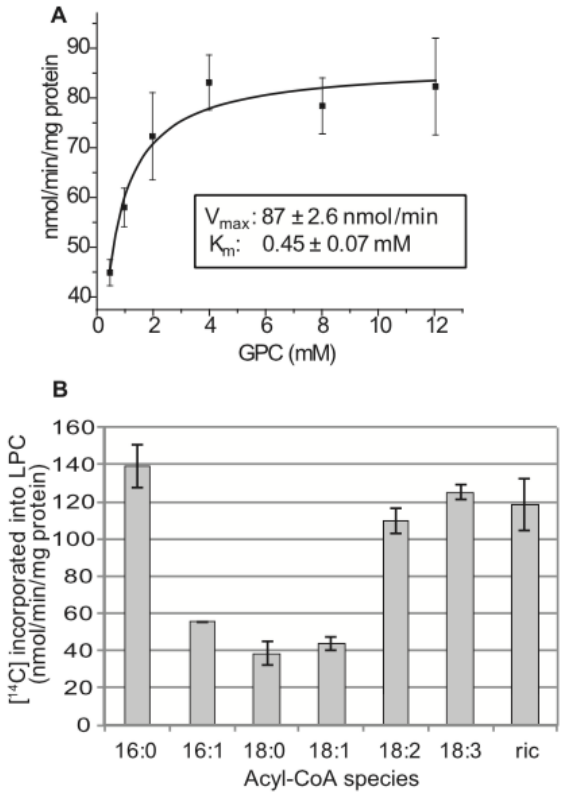

Figure 2. 5. Biochemical characterization of Gpc1p
A. The dependence of Gpc1p activity on GPC concentration in the presence of 18:1-CoA. B. The acyl-specificity of Gpc1p at optimal GPC concentration (4 mM). The activity was measured as incorporation of ^{14}C-activity from [^{14}C]choline labelled GPC into chloroform soluble lipids in the presence of acyl-CoA (0.2 mM). Microsomal preparations (2 µg protein) prepared from *ale1Δ gpc1Δ* expressing *GAL1-GPC1* were incubated for 4 min at 30°C. ric, ricinoleoyl-CoA. Data is given for triplicate assays ± SD.

Membranes from *gpc1Δ* bearing empty vector did not incorporate radioactivity into lipids, whereas membranes from *gpc1Δ* cells expressing *GPC1* incorporated about 30 times more radioactivity into lipids than WT. When GPCAT activity was measured in membranes from *ale1Δ gpc1Δ* harboring *GPC1*, the total radioactivity incorporated into lipid was reduced approximately 25% as compared to the *gpc1Δ* background and the activity now accumulated primarily in LPC (93%), demonstrating again that Ale1p is the main enzyme responsible for the formation of radioactive PC from LPC in these assays. The dependence of GPCAT activity on GPC concentration was determined in microsomal membranes prepared from *ale1Δ gpc1Δ* transformed with *GAL1-GPC1* using 18:1-CoA as the acyl donor (Fig. 2.5A). The K_m for GPC was found to be 0.45 mM with a V_{max} of 87 nmol/min. The linearity of the reaction was tested with 18:1-CoA at optimal GPC concentration and was found to be essentially linear during 16 min of incubation under the incubation condition used (data not shown). The ScGPCAT accepted all the acyl-CoA species tested with a preference for 16:0-CoA, polyunsaturated acyl-CoA and the hydroxylated ricinoleoyl-CoA (Fig. 2.5B).

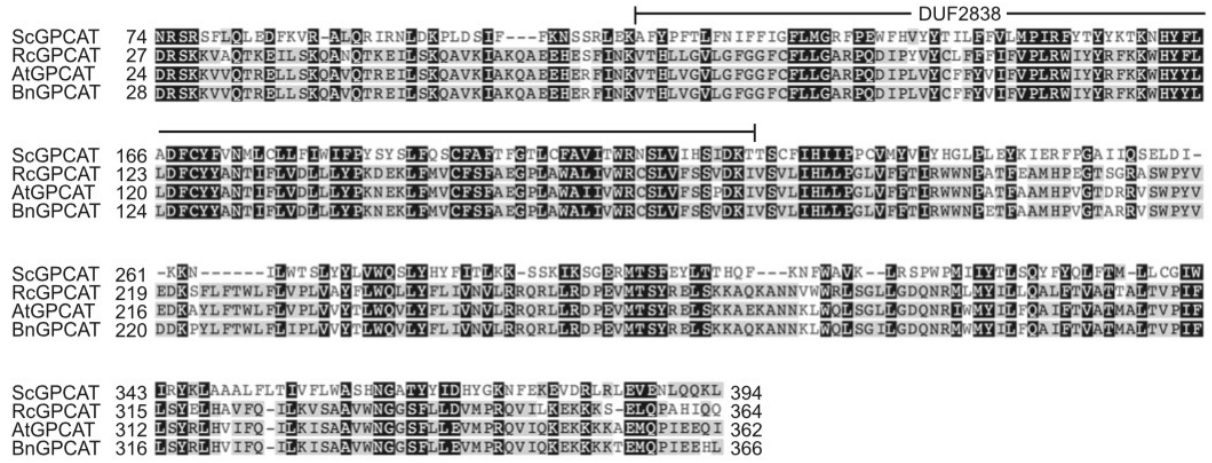

Figure 2. 6. Partial alignment of ScGPCAT

(*Saccharomyces cerevisiae*; NP_011665.1), RcGPCAT (*Ricinus communis*; XP_002514086.1), AtGPCAT (*Arabidopsis thaliana*; NP_198396.1) and BnGPCAT (*Brassica napus*; XP_013682687.1). Sequence numbering is according to the full-length protein sequences. The

conserved DUF2838 domain is marked above the sequence (V_{68} to I_{174} in the *A. thaliana* sequence). Proteins were aligned using Clustal Omega (http://www.ebi.ac.uk) and Geneious (http://www.geneious.com) was used for shading background according to conservation.

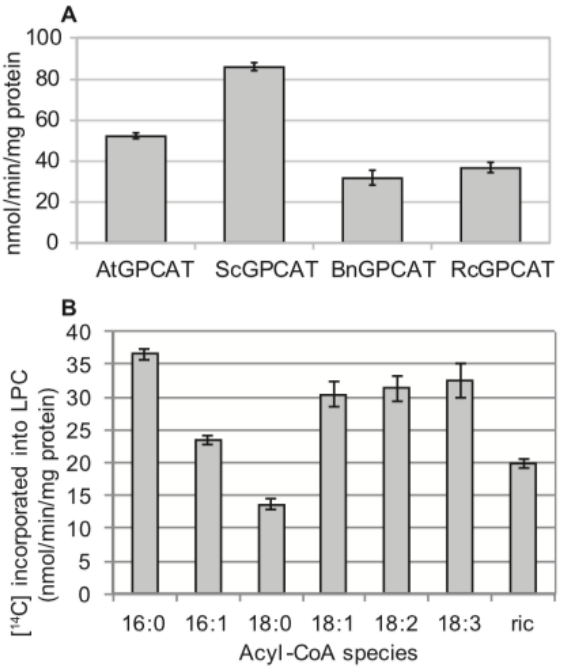

Figure 2. 7. Enzyme activities of plant GPCATs.
A. Specific activity of *Arabidopsis thaliana* GPCAT (AtGPCAT), *S. cerevisiae* GPCAT (ScGPCAT), *Brassica napus* GPCAT (BnGPCAT) and *Ricinus communis* GPCAT (RcGPCAT). B. Acyl-CoA specificity of the RcGPCAT. The activity was measured as incorporation of ^{14}C-activity from [^{14}C]choline labelled glycerophosphocholine (GPC, 4 mM) into chloroform soluble lipids in presence of 18:1-CoA (0.2 mM) by microsomal preparations (in A, 2 µg protein; in B. 4 µg) prepared from *ale1*Δ gpc1Δ yeast cells expressing the different GPCATs. Incubations with microsomes prepared from *gpc1*Δ transformed with empty vector gave no incorporation of radioactivity into the chloroform phase. Incubation time was in A, 8 min, in B, 4 min. Data is given for triplicate assays ± SD. Of the ^{14}C-activity incorporated in lipids, 98-99% was recovered as lysophosphatidylcholine and 1-2% as phosphatidylcholine.

2.3.4 Plant homologues of *GPC1* catalyze acyl-CoA dependent acylation of GPC when expressed in yeast

Sequence similarity was used to identify homologues in *Arabidopsis*, castor bean (*Ricinus communis*) and oilseed rape (*Brassica napus*). The Arabidopsis GPCAT shows 25%

protein sequence identity to the yeast GPCAT in a 340 residues conserved part from D24 to I362 in the *A. thaliana* sequence (Fig. 2.6.). The three different plant GPCATs were expressed in the yeast *gpc1Δale1Δ* strain under the *GAL1*-promoter and the results compared to those obtained for ScGPCAT. The specific activity was highest with ScGPCAT (86 nmol/min/mg protein) whereas the plant GPCAT activities ranged from 32 to 52 nmol/min/mg protein (Fig. 2.7.A). Microsomal preparations from castor bean seeds have high GPCAT activity [50] and the plant accumulates seed triacylglycerols with about 90% of the fatty acid being the hydroxy acid, ricinoleic acid. This fatty acid is synthesized by hydroxylation of oleoyl groups esterified to the *sn*-2 position of PC [75]. It was therefore of interest to investigate the acyl-CoA specificity of the castor GPCAT. Like yeast GPCAT, the castor GPCAT accepted all the acyl-CoAs tested, including ricinoleoyl-CoA (Fig. 2.7.B), although with somewhat different acyl specificities as compared to the yeast enzyme.

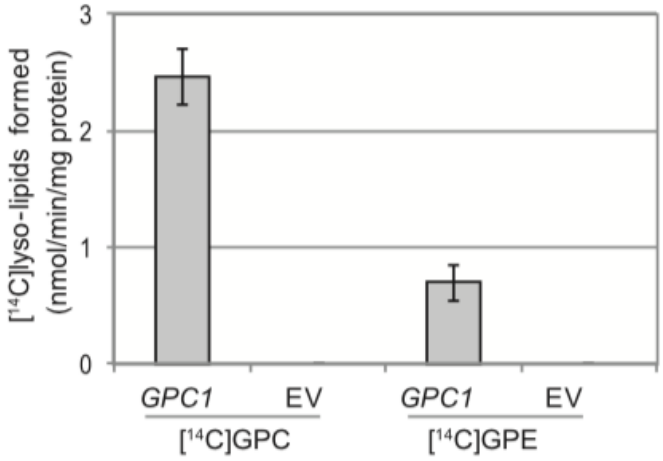

Figure 2. 8. Acylation of glycerophosphoethanolamine

Incorporation of ^{14}C-activity from [^{14}C]choline labelled glycerophosphocholine (GPC, 0.5 mM)) or [^{14}C]ethanolamine labelled glycerophosphoethanolamine (GPE, 0.5mM) into chloroform soluble lipids in the presence of 18:1-CoA (0.4mM). Microsomal preparations (40 µg of protein) of *ale1*Δ *gpc1*Δ yeast cells with overexpressed *GPC1* or empty vector (EV). The radioactivity resided in LPC in assays with added [^{14}C]GPC and in lysophosphatidylethanolamine in case of

added [^{14}C]GPE. Incubation time was 20 min and the temperature was 30°C. Data is given for triplicate assays ± SD.

2.3.5. Gpc1p catalyzes acylation of glycerophosphoethanolamine (GPE) with acyl-CoA

Stålberg et al. [49] reported that yeast also possessed acyl-CoA:GPE acyltransferase activity. In order to test if this activity was catalyzed by ScGPCAT, we performed assays with [^{14}C]GPE and 18:1 acyl-CoA in microsomal preparations of *ale1*Δ *gpc1*Δ strain transformed with *GPC1* or empty vector (Fig. 2.8.). No incorporation of radioactivity into lipids was seen with empty vector, but upon expression of *GPC1* radioactive lysophosphatidylethanolamine (LPE) accumulated, albeit at about 25% of the amount of LPC formed when [^{14}C]GPC was provided. Thus, Gpc1p also catalyzes the acylation of GPE with acyl-CoA.

2.3.6. GPCATs from yeast and plants catalyze transacylation reactions

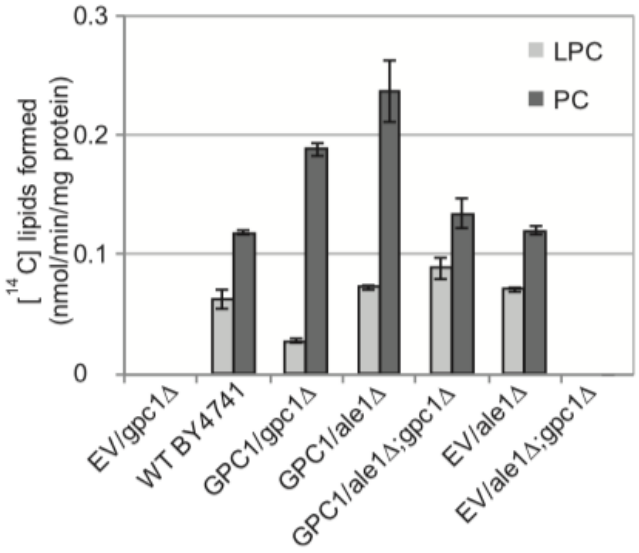

Figure 2. 9. Transacylation activity of GPCAT.
Radioactive lipids formed in incubations of microsomes (40 µg of protein) prepared from yeast lacking or expressing the indicated genes. Incubations contained [^{14}C]glycerophosphocholine (0.24 mM) in the absence of added acyl-CoA and were performed for 90 min at 30°C. The results shown are from triplicate assays ± SD. LPC, lysophosphatidylcholine; PC, phosphatidylcholine. Strains contained empty vector (EV) or expressed *GPC1* from *GAL1* promoter (*GPC1*).Yeast of

WT that was used for microsomal preparation was grown in YPD, yeast strains containing plasmids were grown in YNB medium containing galactose.

The incorporation of [^{14}C]choline labelled GPC into lipid in the absence of exogenous acyl-CoA was assayed in yeast membranes (Fig. 2.9.). Membranes from *gpc1Δ* did not incorporate any radioactivity into lipids whereas the WT and the *gpc1Δ* transformed with *pGAL-GPC1* incorporated similar amount of radioactivity into both LPC and PC. The lack of Ale1p had little or no effect on the incorporation of radioactivity into LPC or PC (Fig. 2.9.).

These experiments indicate that GPCAT is responsible for the production of radioactive LPC from [^{14}C]GPC in the absence of exogenous acyl-CoA and that the second acylation step, the acylation of LPC to PC, is independent of Ale1p activity in the absence of exogenous acyl-CoA. Although GPCAT activity was essential for incorporation of radioactivity from [^{14}C]GPC into lipids in absence of acyl-CoA, its activity did not appear to be a rate limiting factor in WT since the WT and *GPC1* overexpressing strain incorporated similar amount of radioactivity into lipids. A time-course of incorporation of [^{14}C]GPC into lipids in the absence of added acyl-CoA was performed

with membranes from *ale1*Δ *gpc1*Δ cells transformed with ScGPCAT or RcGPCAT. The two enzymes gave similar incorporation patterns (Fig. 2.10).

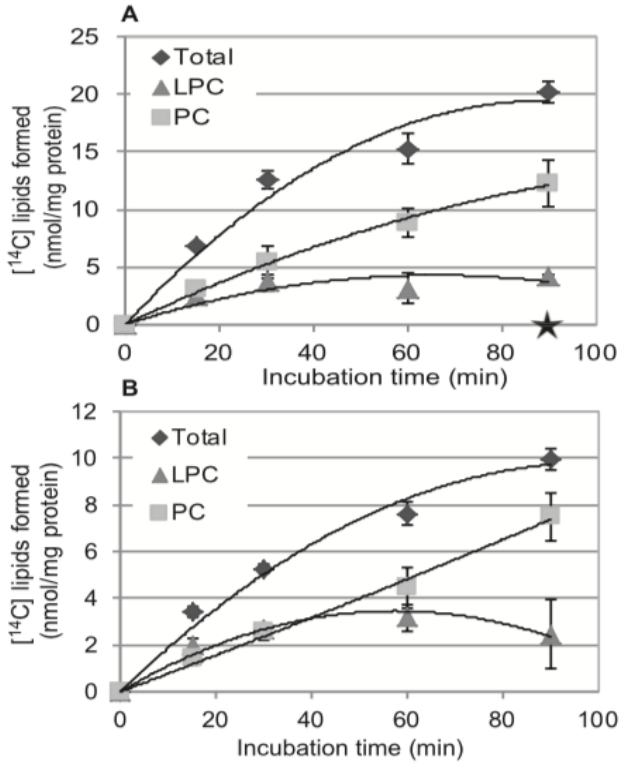

Figure 2. 10. Transacylation activity of GPCAT over time.
Time-course incorporation of ^{14}C-activity from [^{14}C]choline labelled glycero-3-phosphocholine (GPC, 4 mM)) into LPC in incubations in the absence of added acyl-CoA by microsomal preparations (40 µg of protein) prepared from yeast *ale1*Δ *gpc1*Δ cells overexpressing ScGPCAT *(GPC1)* (A) or castor bean GPCAT (RcGPCAT) (B). The enzyme rates for ScGPCAT and RcGPCAT in the absence of acyl-CoA was 0.45 and 0.23 nmol/min/mg, respectively, during the first 15 min. Corresponding incubations with microsomes prepared from the *gpc1*Δ*ale1*Δ strain transformed with empty vector gave no incorporation of radioactivity into the chloroform phase, indicated with a star at 90 min incubation in the graph (A). Data is given for triplicate assays ± SD.

Alternative mechanisms could explain the observed incorporation of radioactivity from [^{14}C]choline- GPC into LPC and PC. The simplest explanation is transfer of an acyl groups from membrane lipids to the added GPC. Among possible acyl donors for such acylation, we tested non-radioactive LPC in combination with [^{14}C]choline-labelled GPC and found that membranes derived from *ale1*Δ*gpc1*Δ bearing *GAL1-GPC1* rapidly formed radioactive LPC, whereas membranes from cells transformed with empty vector totally lacked this capacity (Fig.2.11). When

corresponding incubations were performed with membranes prepared from *ale1*Δ cells (containing an endogenous *GPC1* gene), radioactive LPC accumulated at about 10% of the rate which occurs when *GPC1* is overexpressed with the *GAL1-GPC1* plasmid (Fig. 2.11).

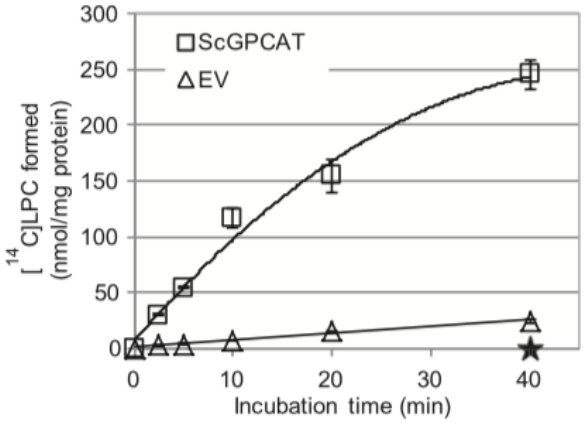

Figure 2. 11. Time course for transacylation activity of ScGPCAT in the presence of added LPC.

Incorporation of ^{14}C-activity from [^{14}C]choline labelled GPC (1 mM) into lipids in the presence of non-radioactive 18:1-LPC (0.5 mM) and microsomal fractions (40 µg of protein). Microsomal fractions were from an *ale1*Δ *gpc1*Δ strain overexpressing *GPC1(scGPCAT)* or from an *ale1*Δ strain expressing empty vector (EV). LPC constituted 98-99% and PC 1-2% of the radioactive chloroform soluble lipids after 40 min. The activity of ScGPCAT during the first 10 min, calculated on the formed radiolabelled LPC, was 9.5nmol/min/mg protein. Corresponding incubations with microsomes prepared from *ale1*Δ *gpc1*Δ transformed with empty vector gave no incorporation of radioactivity into the chloroform phase, indicated with a star at 40 min incubation in the graph. Data is given for triplicate assays ± SD.

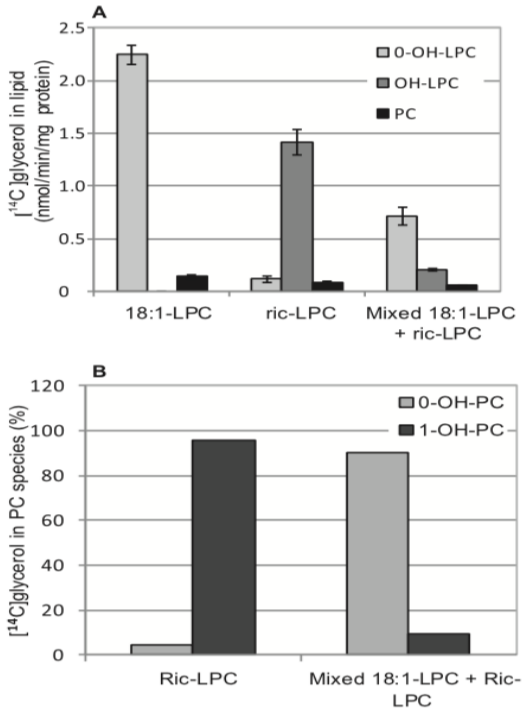

Figure 2. 12. LPC as donor in transacylation activity.
Radioactive lipids formed in incubations of microsomes (40 µg of protein) prepared from *ale1*Δ *gpc1*Δ expressing ScGPCAT. [^{14}C]Glycerol labeled GPC (0.2 mM) and non-radioactive 18:1-LPC or ricinoleoyl-LPC (ric-LPC) (0.1 mM) or an equimolar mixture of both (0.05+0.05 mM) for 30 min. Incubations with microsomes prepared from *ale1*Δ *gpc1*Δ strain transformed with empty vector gave no incorporation of radioactivity into the chloroform phase. Panel A. The results shown are from triplicate assays (± SD). Panel B. Relative distribution of molecular species of PC formed. PC from triplicate assays (Panel A) were pooled before phospholipase C treatment to obtained DAG for separation of molecular species (see Materials and Method section). 0-OH-X, 1-OH-X and designates lipids with no and one ricinoleoyl groups, respectively.

This demonstrates that the transacylation rate is a function of the level of GPCAT activity when the LPC concentration is not rate limiting, as it was in experiment presented in Fig. 2.9. and 2.10. The rate of radioactivity appearing in LPC during the first 10 min with *GAL1-GPC1* was as high as 9.5 nmol/min/mg protein, which is 11% of the acylation rate with 18:1-CoA at optimal GPC concentration with the same membranes. Apart from direct acyl transfer from added LPC, there could be other explanations for the formation of radioactive LPC in assays in which unlabelled LPC but no acyl-CoA had been provided. By adding non-radioactive ricinoleoyl-LPC,

which could be separated from LPC with non-hydroxylated acyl groups by TLC, we demonstrated that the added [^{14}C]glycerol labelled GPC received 90% of its acyl groups from the added LPC (Fig. 2. 12A). This experiment gave conclusively evidence that GPCAT catalysed the transfer of acyl groups from added non-radioactive LPC to [^{14}C]GPC, and thus forming non-radioactive GPC and [^{14}C]-labelled LPC molecules.

Some radioactive PC was also formed in these assays (Fig. 2. 12). When the radioactivity in the different PC molecular species was analyzed in incubations with added ricinoleoyl-LPC , species with one ricinoleoyl group had 96 % of the activity with the remainder being [^{14}C]PC with no ricinoleoyl groups (Fig. 2. 12B). These results show that the second acylation step is not using added ricinoleoyl-LPC in a LPC:LPC transacylase reaction but receive acyl groups from some other lipid(s).

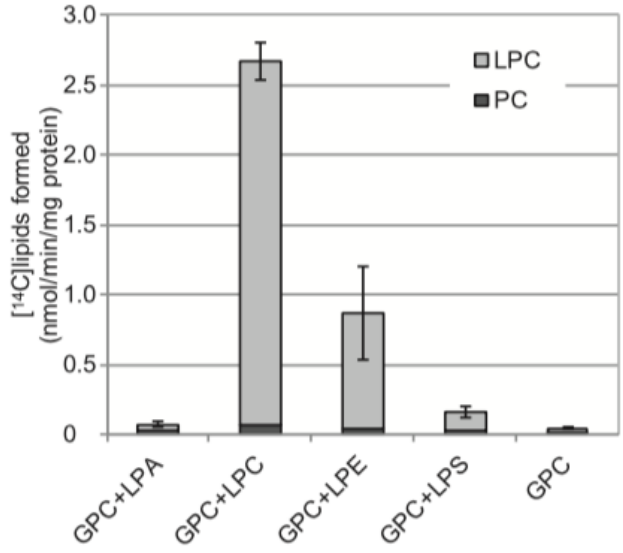

Figure 2. 13. Lysolipids as acyl donors for ScGPCAT (Gpc1p) activity.
Incorporation of ^{14}C-activity from [^{14}C]choline labelled GPC (1 mM)) into chloroform soluble lipids in presence or absence of added (0.4 mM) 18:1-lysophsophatidic acid (LPA), 18:1-

lysophosphatidylcholine (LPC), 18:1-lysophosphatidylethanolamine (LPE) and 18:1-lysophosphatidylserine (LPS) by microsomal preparations (60 µg of protein) prepared from yeast *ale1*Δ *gpc1*Δ cells with overexpressed *GPC1*. Corresponding incubations with empty vector gave no incorporation of radioactivity into the chloroform phase (data not shown). Incubation time was 60 min and temperature was 30°C. Data is given for triplicate assays ± SD. PC, phosphatidylcholine.

2.3.7. Gpc1 catalyzes the transacylation of acylgroups from lysophospholipids other than LPC

We investigated if lysophospholipids other than LPC could serve as acyl donors for the acylation of GPC by Gpc1p (Fig. 2. 13). LPE could donate acyl groups at about 25% of the efficiency with LPC. Incorporation of radioactivity into LPC from added lysophosphatidylserine was low, but significantly higher than in absence of added lysolipids, whereas no increase was seen with added lysophosphatidic acid (Fig. 2. 13).

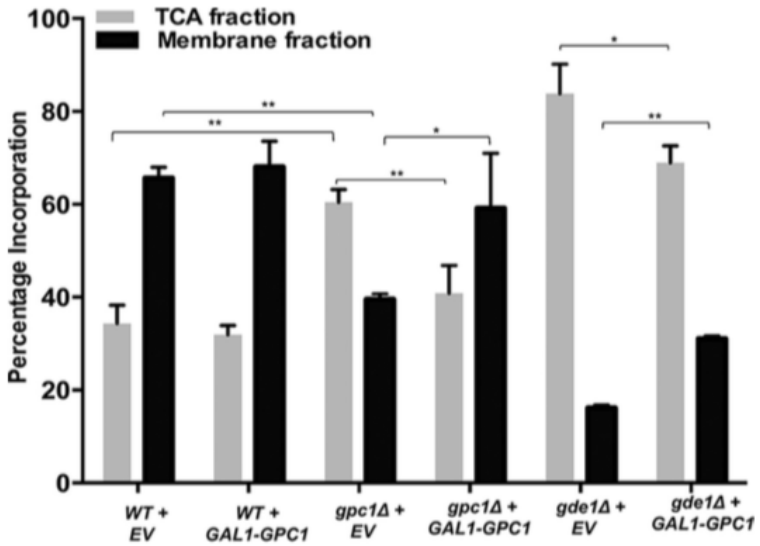

Figure 2. 14. In vivo incorporation of [^{3}H]GPC.
The indicated strains were grown to logarithmic phase in galactose medium and the distribution of the radioactivity between the TCA and membrane extracts was determined. Strains contained either empty vector (EV) or *GPC1* under the control of the *GAL1* promoter (*GAL1-GPC1)*. Data represent average of 3 independent cultures ±SD. A t-test was performed to determine significance as indicated by brackets (*$P \leq 0.05$; **$P \leq 0.0008$).

2.3.8. In vivo labeling indicates a physiological role for Gpc1p in PC biosynthesis

In vivo radiolabeling experiments were performed to examine the role of Gpc1p-mediated GPC acylation in cellular PC biosynthesis. For these studies, the medium contained [^{3}H]GPC and a low concentration of phosphate in order to induce transcription of the *GIT1* encoded permease [76] responsible for the uptake of GPC into the cell [31]. Following growth to logarithmic phase, cells were separated into membrane and TCA-extractable fractions and the percentage of radioactivity in each fraction determined. As shown in figure 2.14, loss of *GPC1* (compare WT +EV to *gpc1Δ* + EV) resulted in less incorporation of [^{3}H]GPC radioactivity into the membrane fraction and a concomitant increase in the intracellular fraction. Importantly, the *gpc1Δ* strain containing the *GAL1-GPC1* plasmid

TABLE 2. 1.

Values for intracellular percentages are derived from Fig 2. 13

Strain	Choline	GPC	Intracellular percentage
	%	%	%
WT + EV	14	21	35
WT + GAL1-GPC1	11	21	32
gpc1Δ + EV	23 ± 3.2	37 ± 2.1	60
gpc1Δ + GAL1-GPC1	16 ± 4	25 ± 5.6	41
gde1Δ + EV	2 ± 0.2	82 ± 8.8	84
gde1Δ + GAL1-GPC1'	2 ± 0.3	67 ± 9.7	69

displayed a distribution of radioactivity similar to WT. When *GPC1* was overexpressed in the WT strain, there was no change in the distribution of counts as compared to WT containing empty vector. This suggests that expression of *GPC1* from its single genomic copy, as occurs in the WT strain, is not rate-limiting for radioactive flux into the membrane fraction under these conditions. As expected, a *gde1Δ* mutant lacking the glycerophosphodiesterase responsible for GPC

hydrolysis (see Fig. 1) [31] exhibited a greater proportion of counts in the internal fraction as labelled GPC (Table 1) as compared to WT (compare WT + EV to *gde1Δ* + EV). In contrast to the WT strain, overexpression of *GPC1* in *gde1Δ* did result in an increase in membrane counts and a decrease in intracellular counts as compared to the empty vector control. This suggests that in the presence of high intracellular levels of substrate (as engendered by loss of Gde1p), *GPC1* expression from the single genomic copy is rate-limiting for incorporation of [^{14}]GPC into membrane. In all cases, the radioactivity in the membrane fraction was found only in PC, suggesting that the LPC produced under these conditions is either rapidly converted to PC or deacylated back to GPC. The TCA-extractable fractions consisted of GPC and free choline (Table 1). These results confirm a cellular role for Gpc1p in the synthesis of PC via acylation of GPC.

Stålberg et al. [49] demonstrated that the generally accepted assumption that GPC cannot be acylated and thus could not be a substrate for the synthesis of PC was incorrect. These authors [49] demonstrated acyl-CoA-dependent GPC acylation (GPCAT reaction) in microsomal fractions from yeast and later Lager et al. [50] showed the same enzyme reaction in microsomal fraction from plants. Here we report on the cloning and characterization of the GPCAT-encoding genes from yeast and plants. The GPCAT genes have not been annotated for any function in yeast or plant databases and do not fall into MBOAT or acyl-CoA:glycerol-3-phosphate acyl transferase GPAT (PhospholipidsB type) families of acyltransferases. GPCAT is also unique in that it has, in addition to acyl-CoA acyltransferase activity, LPC:GPC transacylase activity. Our labeling studies employing intact yeast cells demonstrate the *in vivo* relevance of these enzymatic activities. It is remarkable that despite having acyl-CoA acyltransfer and transacylation activity, the GPCAT enzymes lack any recognizable domain present in other such enzymes where the catalytic activity has been established.

As is the case with any enzyme, the gene/enzyme relationship cannot be unequivocally established until the enzyme is purified to homogeneity. None-the-less, the preponderance of evidence indicates that Gpc1p harbors catalytic activity and is not a regulatory protein or a non-catalytic subunit of a larger complex. First of all, plant GPCAT proteins are functional in yeast, despite having only 25% amino acid identity (see Fig. 2. 6) with Gpc1p. Secondly, when *GPC1* is overexpressed, the transacylation and acylation activities are ten to forty times higher as compared to the wild type condition. These findings argue against a regulatory function or being a subunit of an enzyme for the gene product.

Homologues of GPCAT are widely distributed among eukaryotic organisms but no homologues were found in prokaryote clade. Interestingly, the plant clade showed a very low sequence divergence as compared to other eukaryotic groups. A common reason for low sequence divergence is a low substitution rate being a consequence of protein-protein interactions [77]. Therefore, we investigated the Membrane-based Interactome Network Database (M.I.N.D.) which contains high-confidence data of protein-protein interaction for *Arabidopsis* membrane proteins, based on the split-ubiquitin system in yeast [78]. Four proteins, out of 151 hits, were related to acyl lipid metabolism and found to interact with AtGPCAT, when excluding interactions tested positive in only one out of two assays in the primary screen. Three of these hits are associated with sphingolipids (At2g31360; At3g06470; At1g69640), whereas the fourth hit belongs to the family of oleosin proteins (At2g25890). Further studies are needed to resolve if plant-specific protein-protein interactions are a reason for the low sequence divergence in plants.

The physiological function of GPCAT in yeast and plants remains to be explored. At face value, GPCAT activity may be part of a recycling pathway to restore PC levels following PC turnover via deacylating phospholipases. On a more complex level GPCAT has been suggested to

be involved in various aspects of acyl editing and phospholipid remodeling in yeast and plants [60, 79, 80]. Overall, it can be assumed that PC homeostasis is maintained by the concerted action of GPCAT, lyso-phospholipid lipases and lysophosphatidylcholine acyltransferases (LPCATs), in addition to the major pathways of PC biosynthesis (the CDP-choline and methylation pathways). It should be noted that GPC is believed to only be formed via deacylation of PC and if so, GPCAT cannot contribute to any net synthesis of PC if it is not provided to the cell from outside. Since plasma membrane GPC transporters are found in yeast [30, 31] and fungi [81] exogenous GPC could however under certain environmental conditions contribute to net synthesis of PC via GPCAT in these cells. In all cells, GPCATs would contribute to an acyl editing whereby acyl groups from the acyl-CoA pool can be inserted into the s*n-1* position of PC via LPC formation from GPC. Since we show that GPCAT also can acylate GPE with acyl-CoA at about the 25% of the rate of GPC, it could also be involved in acyl editing of PE, similar to what we proposed for PC editing.

Thus, GPCAT catalyzed acylation of GPC by acyl-CoA can be predicted to have a role in maintaining PC homoeostasis and in acyl editing of this phospholipid. We have now shown that the incorporation of [^{14}C]GPC into lipids observed in plant microsomal membranes in absence of acyl-CoA [50] is due to GPCAT-catalyzed transacylation of acyl groups from LPC to GPC. Since this reaction does not form any new lipid molecular species it might function as a GPC transporter across intracellular membrane and compartments and/or catalyzing the movement of LPC from one leaflet of the membrane to the other. GPCAT can also transfer acyl groups from LPE to GPC in forming GPE and LPC, albeit at a lower rate than if LPC and GPC were substrates. Thus, GPCAT could also be involved in exchanging acyl groups between PC and PE.

We show here that the [^{14}C]LPC formed from [^{14}C]GPC by transacylation from added LPC was to some extent further converted to [^{14}C]PC and that this transfer did not involve LPC:LPC transacylation (LPCT), at least not with LPC containing ricinoleoyl moiety. LPCT reactions were demonstrated in microsomal preparations from developing safflower seeds [50]. The enzyme(s) responsible for the formation of PC from LPC in the yeast microsomes remains to be established.

The strategy we used for identifying the GPCAT gene is an example of how the function of a non-annotated gene can be established. Our approach differs from most current methods for identifying the function of genes, which primarily rely on forward and reverse genetics and require an observable phenotype or extrapolation by homology to genes with a priori known function. More than 20% of all genes encoding putative proteins in any eukaryote are still not reliably annotated with experimentally defined functions and their functions are not accessible via forward or reverse genetics because silencing or overexpression do not yield obvious phenotypes. We predict that discovery of many new functions and novel enzyme reactions will require renewed emphasis on classical biochemical methods coupled with the increasingly powerful molecular biology and high through-put technologies.

The identification of the GPCAT genes now allows for determining their physiological functions by forward and reverse genetics in the plethora of eukaryotic clades where homologues are present and such work is now in progress in our laboratories.

2.4. EXPERIMENTAL PROCEDURES

2.4.1. Chemicals - [1-^{14}C]Radioactive fatty acids, [^{14}C]choline, [^{14}C]glycerol-3-phosphate were purchased from Perkin-Elmer and [^{14}C]ethanolamine from American Radiochemicals. Non-

radioactive fatty acids and CoA were obtained from Larodan (Malmö, Sweden). Di-ricinoleoyl-PC was kindly provided by ENI/Metapontum Agrobios, Metaponto, Italy. Ricinoleoyl-LPC was produced by phospholipase A_2 (from *Naja naja*, Sigma) treatment of di-ricinoleoyl-PC. All other non-radioactive fine chemicals were obtained from Sigma Chemical Company. Acyl-CoAs were prepared according to the method described by Sanchez et al. [82]. [^{14}C]Choline-labelled GPC and [^{14}C]ethanolamine labelled GPE were obtained by growing WT yeast cells (SCY62) with [^{14}C]choline or [^{14}C]ethanolamine and purifying the labelled PC or PE and deacylating it according to [50]. The specific activity of the [^{14}C]GPC and varied between 40 000 dpm/nmol to 86 000 dpm/ nmol whereas [^{14}C]GPE only had about 200 dpm/nmol. [^{14}C]Glycerol labelled GPC was prepared by incubating microsomal preparations from developing safflower seeds with 18:1-CoA and [^{14}C]G3P according to Guan et al. [83]. After extracting the lipids from the assay into chloroform [84] the formed [^{14}C]glycerol labelled PC was separated by TLC and de-acylated as above. The specific activity of the [^{14}C]glycerol labelled GPC varied between 26 000 dpm/nmol and 53 000 dpm/nmol.

TABLE 2

Yeast strains used in this study

Strain	Genotype
BY4741	*Mat a, his3Δ1, leu2Δ0, met15Δ0, ura3Δ0*
gpc1Δ	*Mat a, his3Δ1, leu2Δ0, met15Δ0, ura3Δ0, gpc1::KANMX*
ale1Δ	*Mat a, his3Δ1, leu2Δ0, met15Δ0, ura3Δ0, ale1::KANMX*
ale1Δ gpc1Δ	*Mat a, his3Δ1, met15Δ0, ura3Δ0, ale1::LEU2, gpc1::KANMX*
gde1Δ	*Mat a, his3Δ1 leu2Δ0 met15Δ0 ura3Δ0, gde1::KANMX*

2.4.2.Yeast Strains, Plasmids and Microsomal Preparations - The yeast strains used are from the yeast knock out *Mat a* collection (Thermo Scientific) in the background BY4741 (see Table 2). The double yeast mutant (*ale1*Δ *gpc1*Δ*)* was obtained by one-step PCR-mediated gene disruption using the *gpc1*Δ strain as background. The *ALE1* gene was replaced by the LEU marker (primers used:

5'ATGTACAATCCTGTGGACGCTGTTTTAACAAAGATAATTACTGTGCGGTATTTCACAC

CG3',

5'CTACTCTTCCTTTTTTGAAATAGGCTTTGGTGAGTAACCAGATTGTACTGAGAGTGC

AC3').

BY4741 was used as WT in GPCAT assays. The genes encoding GPCAT from yeast (*YGR149W*) and *Arabidopsis* (At5g35460) were amplified by PCR, whereas the genes from castor bean (XM_002514040) and oilseed rape (BnaA04g07370D) were ordered synthetically (GenScript) by using known sequence information. The Gateway® system was used to clone into the yeast expression vector pYes-DEST52, which places genes under control of the *GAL1* promoter (referred to as *GAL1-GPC1* in text and figures). For Western analysis, *GPC1* was cloned into pYES2.1 which contains a C-terminal V5-6xHIS epitope tag (referred to as *GAL1-GPC1-V5* in text and figures). The vector pYES2 was used as the empty vector control (EV in figures). Microsomal membranes were prepared according to the method described in [50].

2.4.3. Yeast-based screen for identifying GPCAT-encoding gene - The yeast knock-out *Mat a* collection from Thermo Scientific was used for the screen. The deletion strains were transferred from the glycerol stock to a microplate containing solid YPD and grown for 2-3 days at 30°C then plated on YPD plates and grown for additional 2-3 days. Individual yeast strains were transferred to 2 ml tubes together with with 0.5 mm zirconia/silica beads and 0.1M phosphate buffer, pH 7.2 and disrupted (8x30s) using a Mini Beadbeater-8 (Biospec Products). After centrifugation 20µl of the yeast extract was incubated with 100nmol [^{14}C]GPC, 100nmol [^{14}C]G3P, 1mg BSA, 20mM EDTA and 20nmol 18:1-CoA for 20 min at 30°C. The reactions were terminated by 110µl MeOH:$CHCl_3$: HAc (50:50:1v/v/v), vortexed and centrifuged. The chloroform phase was applied to a TLC plate (Silica 60, Merck) and the lipids were separated in $CHCl_3$: MeOH:HAc:H_2O

(90:20:20:3v/v/v/v). The radiolabeled lipids were visualized with Instant Imager (Packard Instrument Co.) electronic autoradiograph.

2.4.4. Sequence alignment and phylogenetic tree - Database searches were carried out with the Arabidopsis and yeast GPCAT protein as queries using BLASTp and tBLASTn against the Genbank database at the National Center for Biotechnology Information (http://www.ncbi.nlm.nih.gov). Proteins were selected for inclusion based on phylogenetic distribution of the species. Complementary searches were carried out in genome databases for *Klebsormidium flaccidum* (http://www.plantmorphogenesis.bio.titech.ac.jp/~algae_genome_project/klebsormidium/) and *Liriodendron tulipifera, Aristolochia fimbriata* and *Nuphar advena* (http://ancangio.uga.edu/). All hits used had e-values $<10^{-11}$. Back-searches by BLASTp against *A. thaliana* and yeast GPCAT were carried out to verify homology. The selected sequences were also analysed by BLink (NCBI) to exclude contaminants. Alignments were made using the T-Coffee PSI/TM-Coffee [85] web-service (http://tcoffee.crg.cat/apps/tcoffee/do:tmcoffee), unless otherwise indicated in the figure legend. Alignments were subjected to maximum likelihood analysis in MEGA 6.0.6 [86], using an 85% limit for partial gaps. Bootstrap testing was conducted with 1000 replicates.

2.5.5. Microsomal enzyme assay - The enzyme assays were performed with microsomal membranes prepared from recombinant yeast cells and yeast transformed with empty vector as indicated in the figure legends. Microsomal membranes, radioactive and non-radioactive substrates were incubated in mixtures at concentration and times stated in the figure legends in 0.1M phosphate buffer, pH 7.2 with 1% of BSA (essentially fatty acid free) in a final volume of

50 µl at 30°C with shaking (250 rpm). LPC were added to the assay mixture dissolved in phosphate buffer, pH 7.2.

2.5. 6. Lipid Extraction, Separation, and Analysis - The microsomal assays were terminated by addition of 170 µl of 0.15M acetic acid and 500 µl of $CHCl_3$:MeOH (1:1, v/v) and vortexed. After centrifugation, the chloroform phase was removed, and an aliquot was taken to liquid scintillation counting of the radioactivity. The remaining chloroform phase from the extraction of the assays, after removal of an aliquot to liquid scintillation, was applied on TLC plate (Silica 60, Merck), and the plate was developed in $CHCl_3$:MeOH:HAc:H_2O (85:15:10:3.5 v/v/v/v.). Radioactive spots were visualized and identified by R_f values of authentic standards, and the relative amount of radioactivity in each spot was determined by Instant Imager (Canberra Packard Instrument Co.) electronic autoradiograph. Absolute amounts of radioactivity in each spot were calculated from the total amount of radioactivity in the chloroform phase as determined by liquid scintillation. In the experiments where the molecular species of radioactive LPC and PC were determined, the lipid extract from the assays were separated on TLC twice with $CHCl_3$:MeOH:HAc:H_2O (85:15:10:3.5 v/v/v/v). This separated ricinoleoyl-LPC from LPC with non-hydroxylated acyl groups and the relative proportions of radioactivity between these LPC species were determined by autoradiography. The PC species with hydroxylated acyl groups and no hydroxylated acyl groups were not clearly separated and these PC species were eluted together from the gel and treated with PLC (from *Clostridium perfringens*, Sigma). The resulting diacylglyerols species were then separated on TLC developed with hexane/diethyl ether/acetic acid (70:140:3 v/v/v). The relative radioactivity between diacylglycerols with no, one and two ricinoleoyl groups were then determined by autoradiography.

2.5.7. In vivo labeling and fraction isolation - *WT* (BY4741), *gpc1Δ* and *gde1Δ* strains contained either empty vector (pYES 2.1) or *GAL1-GPC1 (*pYES 2.1-*YGR149w).* Cultures were maintained aerobically at 30°C in yeast nitrogen base (YNB) medium containing 2% galactose and altered to lack inositol and contain a low level of KH_2PO_4 (200 μM) to induce expression of the Git1 transporter for GPC uptake. Amino acid concentrations were as described [87], but uracil was removed to maintain the plasmids. For labeling experiments, the medium was supplemented with 5 μM of ^{3}H-choline-GPC and grown to log phase before harvesting. A membrane fraction and TCA-extractable intracellular fraction were isolated as described previously [88]. The percentages of radioactive counts in each fraction were determined using a liquid scintillation counter.

2.5.8. Analysis of choline-containing metabolites and lipids following in vivo labeling - The water-soluble choline-containing metabolites were separated using anion exchange chromatography as described in [88]. Standards were used to verify the separation procedure and label incorporated into each metabolite was quantified using liquid scintillation counting. Lipids were extracted from the membrane fraction as described previously [88] and separated by TLC as described for the in vitro assays.

2.5.9. Western blotting- Protein extraction and quantification were performed as described in [76]. Protein (75 μg) was loaded into each lane of a Mini-PROTEIN 4-15% gel (BIO-RAD). The semi-dry transfer was performed onto a PVDF membrane using TRANS-BLOT SD (BIO-RAD). Membrane was blocked in blocking buffer (5% milk in tris buffer saline- 0.1% Tween 20 solution (TBST) for 60 min at room temperature. Primary antibody was used against V5 epitope

(Monoclonal V5 Epitope Tag Antibody (Invitrogen, catalog no. R960-25) at a dilution of 1:1000 in TBST containing 5% BSA and incubated at 4°C for overnight. The primary antibody was then removed and membrane was washed trice with TBST for 10 min each. The goat anti-Mouse secondary antibody (Li-Cor Biosciences, catalog no. 926-322-10) was used at a dilution of 1:10,000 in TBST containing 5% milk. Membranes were incubated in secondary for 60 min at room temperature. Secondary was removed, and the membrane was washed trice with TBST for 10 min each. Finally, membrane was visualized using Odyssey FC imaging system. Glucose-6-phosphate dehydrogenase (G6PD) was used as the loading control. The same procedure as above was employed for G6PD; primary antibody was anti-G6PD (Sigma-Aldrich, catalog no. HPA000-834) and secondary antibody was goat anti-rabbit (Li-Cor Biosciences, catalog no. 926-68071).

Chapter 3: The glycerophosphocholine acyltransferase Gpc1 is part of a phosphatidylcholine (PC)-remodeling pathway that alters PC species in yeast

Accepted on December 7, 2018 by Journal of Biological Chemistry

Sanket Anaokar[1], Ravindra Kodali[1a], Benjamin Jonik[1], Mike F. Renne[2], Jos F.H.M. Brouwers[3], Ida Lager[4], Anton I.P.M de Kroon[2], Jana Patton-Vogt[1*]

From the [1]Department of Biological Sciences, Duquesne University, Pittsburgh, PA, USA;
[1a] Department of Chemistry and Biochemistry, Duquesne University, Pittsburgh, PA, USA;
[2]Membrane Biochemistry & Biophysics, Bijvoet Center and Institute of Biomembranes, Utrecht University, Utrecht, The Netherlands;
[3]Department of Biochemistry and Cell Biology, Institute of Biomembranes, Utrecht University, Utrecht, The Netherlands;
[4]Department of Plant Breeding, Swedish University of Agricultural Sciences, Alnarp, Sweden

Chapter 3 Attributions:

I completed all the work in this chapter except noted here.

Ravindra Kodali, helped optimize and analyze lipid samples using LC-MS.

Mike F. Renne, a graduate student in Dr. de Kroon lab, completed the gas chromatography study Fig 3.5.D.

Running title: PC remodeling in *Saccharomyces cerevisiae*

* To whom correspondence should be addressed: Jana Patton-Vogt: Department of Biological Sciences, Duquesne University, Pittsburgh, PA 15282; pattonvogt@duq.edu. Tel. (412) 396-1053; Fax: (412)-396-5907

Keywords: Gpc1, Ale1, phosphatidylcholine, glycerophosphocholine, lipid remodeling, acyltransferase, membrane fluidity, lipid saturation

3.1. ABSTRACT

Phospholipase B–mediated hydrolysis of phosphatidylcholine (PC) results in the formation of free fatty acids and glycerophosphocholine (GPC) in the yeast *Saccharomyces cerevisiae.* GPC can be reacylated by the glycerophosphocholine acyltransferase Gpc1, which produces lysophosphatidylcholine (LPC), and LPC can be converted to PC by the lysophospholipid acyltransferase Ale1. Here, we further characterized the regulation and function of this distinct PC deacylation/reacylation pathway in yeast. Through *in vitro* and *in vivo* experiments, we show that Gpc1 and Ale1 are the major cellular GPC and LPC acyltransferases, respectively. Importantly, we report that Gpc1 activity affects the PC species profile. Loss of Gpc1 decreased the levels of mono-unsaturated PC species and increased those of di-unsaturated PC species, while Gpc1 overexpression had the opposite effects. Of note, Gpc1 loss did not significantly affect phosphatidylethanolamine, phosphatidylinositol, and phosphatidylserine profiles. Our results indicate that Gpc1 is involved in post-synthetic PC remodeling that produces more saturated PC species. qRT-PCR analyses revealed that *GPC1* mRNA abundance is regulated coordinately with PC biosynthetic pathways. Inositol availability, which regulates several phospholipid biosynthetic genes, down-regulated *GPC1* expression at the mRNA and protein levels and, as expected, decreased levels of monounsaturated PC species. Finally, loss of *GPC1* decreased stationary phase viability in inositol-free medium. These results indicate that Gpc1 is part of a post-synthetic PC deacylation/reacylation remodeling pathway (PC-DRP) that alters the PC species profile, is regulated in coordination with other major lipid biosynthetic pathways and affects yeast growth.

3.2. Introduction

Cellular membranes must adjust their lipid composition in response to internal and external cues. These adjustments occur through the coordinated control of multiple metabolic activities, including biosynthetic enzymes involved in lipid synthesis, phospholipases involved in lipid turnover, and acyltransferases involved in lipid remodeling. Because lipid composition affects the biophysical properties of the membrane, these alterations are crucial to cellular function [61, 89]. Defects in lipid metabolism are associated with multiple disease states and cellular dysfunctions [54, 90-94].

Phosphatidylcholine (PC) is the major glycerophospholipid in most eukaryotic membranes. In *Saccharomyces cerevisiae*, bulk synthesis of phosphatidylcholine (PC) occurs primarily via the PE methylation pathway and the CDP-choline (Kennedy) pathway (Fig. 3.1). In the absence of exogenous choline, the CDP-choline pathway does not contribute to net PC synthesis, but is important for recycling choline derived from turnover pathways. Characterized turnover pathways include the production of phosphatidic acid (PA) and free choline via phospholipase D activity (Spo14/Pld1) [5, 95] and the production of free fatty acids and GPC via phospholipases of the B type encoded by *NTE1* and *PLB1* [25, 26, 28]. GPC can subsequently be degraded to free choline and glycerol-3-phosphate by the glycerophosphodiesterase, Gde1 [31, 96]. Based on *in vitro* experiments with yeast extracts, another route for GPC conversion, namely its acylation to LPC, was described [49]. Recently, a gene encoding such a GPC acyltransferase activity, *GPC1*, was identified [52]. After LPC formation by Gpc1, the lysophospholipid acyltransferase, Ale1, can act to form PC [39]. Overall, the degradation of PC to form GPC, followed by its stepwise reacylation to PC, defines a novel PC deacylation/reacylation remodeling pathway (PC-DRP) for PC biosynthesis [25, 52, 97].

PC, like other phospholipids, consists of multiple molecular species based on acyl chain differences at the *sn-1* and *sn-2* position of the glycerol backbone. The repertoire of fatty acids in yeast is relatively simple as compared to the higher eukaryotes, consisting primarily of C16 and C18 fatty acids with either one or no double bond [57]. Thus, the four major PC species observed through mass spectrometry have the following acyl chain combinations: 32:1PC (mono-unsaturated) consists of C16:0 and C16:1, 32:2PC (di-unsaturated) consists of C16:1 and C16:1, 34:2PC (di-unsaturated) consists of C16:1 and C18:1, 34:1PC (mono-unsaturated) consists of either C16:0 and C18:1 (this being the predominant acyl chain combination) or C16:1 and C18:0 [38, 60, 98].

The steady state PC molecular species profile is the result of the molecular specificity of the PC biosynthetic routes combined with post synthetic acyl chain exchange [38]. The PE methylation pathway produces predominantly di-unsaturated PC species, whereas the CDP-choline pathway produces a more mixed profile [38, 99]. Furthermore, a number of studies have provided evidence for the post-synthetic remodeling of PC species [57, 58]. Indeed, PC remodeling was clearly demonstrated by pulse-chase studies using deuterium labeled (*methyl*-D_3)-methionine followed by ESI-MS/MS analysis. Those studies revealed a post-synthetic increase in mono-unsaturated PC species (32:1, 34:1) at an expense of di-unsaturated PC species (32:2, 34:2) [99]. Prior to this work, an acyltransferase responsible for remodeling PC to more saturated species in *S. cerevisiae* had not been identified.

Here we undertook a more thorough examination of PC remodeling via PC-DRP and the role of the GPC acyltransferase, Gpc1. Importantly, we report that Gpc1 is a key player in post-synthetic PC remodeling events that result in more saturated PC species. In addition, we find that

Gpc1 is regulated with respect to other aspects of lipid metabolism and that loss of Gpc1 impacts stationary phase viability.

3.3. EXPERIMENTAL PROCEDURES

3.3.1. Strains, Plasmid, Media and Growth Conditions

The *S. cerevisiae* strains used in this study are presented in Table 1. Strains were maintained aerobically at 30°C with shaking or on a roller drum. Growth was monitored by measuring optical densities at 600 nm (A_{600}) using BioMate3 Thermo Spectronic spectrophotometer. Media used in this study were yeast peptone dextrose (YPD) or yeast nitrogen base (YNB) with 2% glucose and amino acid composition as described in [87]. The YNB medium was made according to DIFCO manual, but lacking inositol. For studies requiring inositol, 75 μM of inositol was provided. Transformations of autonomously replicating plasmids were performed using the lazy bones plasmid transformation protocol as described [100]. For integrating DNA into the genome, the high efficiency transformation procedure was used [101]. The empty vector, pRS426 and vector overexpressing *GIT1* gene*, ADH-GIT1* were from [102].

3.3.2. Construction of Deletion Strains

The wild type (BY4742) *S. cerevisiae* strain was purchased from Open Biosystems (Thermo Scientific, Huntsville, AL). The deletion strains used in this study were made using PCR-based homologous recombination technique as described in [88, 103]. Nutritional markers, *LEU2* and *URA3,* were amplified from pRS415 and pRS416, respectively, using primers listed in Table 2.

3.3.3. Construction of Chromosomal C-terminal 3xHA Tag for *GPC1*

The *3xHA-URA3* cassette was amplified from plasmid pPMY-3xHA [104] using the primer set shown in Table 2. The PCR product was transformed into *WT* strain, and transformants were selected on YNB plates lacking uracil. Control PCR was performed on genomic DNA extracted from transformants to verify the integration of the entire cassette into the genome. To counter-select against the *URA3* gene, the verified colonies were then reselected on a YNB plate containing 1mg/ml of 5-fluoroorotic acid (5-FOA). Genomic DNA was extracted from colonies that grew on 5-FOA plates and were used as template to check for the insertion of 3xHA at C-terminal end. Colonies producing the correct amplicon are JPV846 (*WT+GPC1-3xHA),* used in the western blot analyses.

3.3.4. In vivo Labeling and Lipid Isolation

For the long-term labelling experiment represented in Fig 2A, strains were grown in YNB inositol-free medium containing 5 μM of ^{14}C-GPC (≅200,000 cpm/ml) (ARC 3880) and a low concentration of KH_2PO_4 (200 μM) to induce expression of the Git1 transporter for GPC uptake. Cultures were allowed to grow to logarithmic phase, harvested and the cell pellets were treated with 5% trichloroacetic acid (TCA) for 20 min on ice. Following centrifugation, the supernatant was discarded and cell pellets were incubated at 60°C for 60 minutes with 1 ml of ESOAK (95% ethanol, diethylether, H_2O, pyridine, NH_4OH (28-30%); 15:5:15:1:0.036 v/v/v/v). The tubes were centrifuged to pellet the debris and 1 ml of lipid-containing supernatant were transferred to fresh tubes containing 2.5 ml of chloroform/methanol (2:1) and 0.25 ml of 0.1 M HCl. Following vortexing and low speed centrifugation, the bottom layers containing glycerophospholipids were dried under N_2. Lipids were then suspended in chloroform/methanol (2:1), spotted onto Silica Gel

TLC Plates (Whatman, Millipore Sigma 105626) and plates were developed in chloroform:methanol:acetic acid:water; (85:15:10:3.5 v/v/v/v) [50]. The TLC plates were imaged using a Typhoon 8200 phosphor imager. For Fig. 2B, image quant software was used to quantitate the PC and LPC spots. For Fig 2A, no LPC was detected, allowing the radioactivity (CPM) in the lipid fraction to be converted to pmole PC/ODU based on the specific activity of the exogenous label.

For the experiments aimed at detecting LPC (Fig 2B), strains containing either empty vector or *ADH-GIT1* [102] were grown in YNB inositol-free medium containing 5 μM of ^{14}C-GPC (≅200,000 cpm/ml) and a standard level of KH_2PO_4. Cultures were inoculated at an A_{600} of ~ 0.2 from startup cultures. Cultures were allowed to grow for 4 h before harvesting ~ 3.2 ODU's of cells for each strain. Lipid extraction, separation and quantitation were as described in previous paragraph. LPC and PC standards (Avanti Polar lipids) were used to verify lipid migration on the TLC plates. Radiolabeled GPC was purchased from ARC, unlabeled GPC from Sigma Scientific.

3.3.5. Analysis of PC and PE molecular species profiles by mass spectrometry

The indicated strains were grown to logarithmic phase and 30 ODUs of each were harvested. The cell pellets were suspended in 2 ml of 5% TCA, followed by a 15 min incubation on ice. After centrifugation, the cell pellets were washed with 20 ml of Nano-pure H_2O. Phospholipids were extracted from the pellet as described above and were finally resuspended in 500 μL of $CHCl_3$: MeOH (1:1, v/v). A 5 μL lipid sample was injected into an Agilent 1200 HPLC system coupled to an Agilent 6460 triple quadrupole LC/MS system. Lipid separations were performed on a Varian PLRP-S (150 X 2.1 mm, 5 μm) column at a flow rate of 0.35 ml/min and the column was maintained at 50°C. Samples were eluted with a linear gradient using of 75%

methanol in water (A) and 100% methanol (B). Both solvents contained 10 mM ammonium acetate and 0.1% formic acid. Electrospray ionization-MS was performed with scanning mode set to multiple reaction monitoring set at *m/z* 184.1 product ion to detect PC molecules. PE species were detected by neutral loss scanning at 141 amu in positive ion mode. The MS parameters were optimized at: collision energy, 25 eV for PC and 15 eV for PE; capillary voltage 3500 V; fragmentor voltage, 100 V; dwell time, 200 ms; drying gas temperature, 320^{o}C; sheath gas temperature, 350 ^{o}C; sheath gas flow, 11 liters/min and drying gas flow, 10 liters/min. Data were acquired and analyzed using Agilent Mass Hunter Work Station software. Reported values for various PC and PE species were corrected for isotope effect [105].

3.3.6. Analysis of PI and PS molecular species profiles by mass spectrometry

Total lipid extracts were dissolved in $CHCl_3$: MeOH 1:1 and injected in a UHPLC system equipped with a Kinetex HILIC column (50x4.60mm, 2.6 µm; Phenomenex, Utrecht, NL) with a SecurityGuard ULTRA HILIC precolumn. Lipids were eluted using a binary gradient of acetonitrile:acetone 9:1 (v/v) (with 0.1% formic acid; Eluent A) and 50 mM ammonium formate in acetonitrile:H_2O 7:3 (v/v) (with 0.1% formic acid; Eluent B). The linear gradient was from 100% A to 50% A in 1 min, followed by isocratic elution at the latter composition for an additional 2 min before a 1 min cleaning of the column with 100% B. Flowrate throughout the analysis was 1 ml/min. MS analysis was performed on an LTQ-XL mass spectrometer (Thermo Scientific) using electrospray ionization (ESI) and detection in the negative mode (source voltage -4.2 kV). Full-scan mass spectra were recorded over a range of 450-950 m/z. Data were converted to mzML format and analyzed using XCMS version 1.52.0 [106] running under R version 3.4.3, including isotope correction.

3.3.7. Analysis of acyl chain composition

Total cellular acyl chain composition was analyzed as described previously [36]. Briefly, total lipid extracts corresponding to 100 nmol phospholipid phosphorus were dried, and transesterified in methanolic H_2SO_4 (40:1 v/v) at 70°C. Fatty acid methyl esters (FAME) were extracted with hexane and separated on a Trace GC (Interscience, Breda, NL) equipped with a biscyanopropyl-polysiloxane column (Restek, Bellefonte, PA). FAME were identified, and signal intensity was calibrated using a commercially available standard (Nu-Chek, Elysian, MN). Acyl chain compositions are presented as mol% of total FAME recovered.

3.3.8. RNA Extraction and Real-Time Quantitative RT-PCR (qRT-PCR)

RNA was extracted from logarithmic phase cells using the hot phenolic RNA extraction protocol [107]. The extracted RNA sample was quantified using Thermo Scientific NanoDrop UV-visible spectrophotometry. Dnase treatment was performed on 7 μg of RNA using the TURBO DNA-free™ kit (Applied Biosystems) as per the manufacturer's protocol. The Verso™ SYBR Green 1-step QRT-PCR ROX kit (Thermo Scientific) was used to determine the message levels on an Applied Biosystems StepOne-Plus™ real-time PCR thermocycler. The primer nucleotide sequence sets used in these studies are shown in Table 3. The optimal primer concentration (70-100 nM) and template concentration (100 ng/25 μL reaction) were determined by performing a standard curve on each primer set. Reverse transcription was performed at 50°C for 15 min followed by 95°C for 15 min for RT inactivation and polymerase activation. The thermal profile for amplification were: 40 cycles at 95°C for 15 s, 54.5°C for 30 s and 72°C for 40 s [88]. Primer set specificity was determined by melting curve analysis. A no template control and a no RT

control were used to validate the absence of contaminants in RNA samples. Experiments were performed using 3 independent biological replicates and each replicate was analyzed in experimental triplicates. The data were normalized to the endogenous control gene, *SNR17,* and analyzed by the $\Delta\Delta C_t$ method and [108, 109].

3.3.9. Protein Extraction and Western Blot Analysis

For figure 7a, cells were grown in YNB medium containing or lacking 75 μM of inositol. Cultures corresponding to 25 ODU's of cells were harvested at log phase. The cell pellet was resuspended in ice cold extraction buffer (120mM NaCl, 50mM Tris-HCL (pH 7.5), 2mM EDTA, 1mM PMSF, 1% NP-40, 0.1% SDS and 1% Triton X-100) containing 1x Yeast/ Fungal Protease Arrest ^{TM} mixture (G-Biosciences catalog no. 786-333). Lysis was performed using glass bead for 8 cycles of the following: 30 seconds of vortexing and 30 seconds of incubation on ice. The cell debris was pelleted by centrifugation at 2000X *g* for 5 min.

For figure 3. 9, cells were grown in YNB medium lacking inositol. Equivalent ODU's of cells were harvested at log and stationary (24 hours) and late stationary phase (48 hours). Cell were lysed for 10 min on ice with 50 µL extraction buffer (0.2 M NaOH, 0.2 % mercaptaethanol) containing 1x Yeast/ Fungal Protease Arrest ^{TM} mixture (G-Biosciences catalog no. 786-333). Proteins were precipitated with 50 µL of 50% TCA and pelleted at 12,000 x g for 5 min. The pellets were suspended in 120 µL of dissolving buffer (4% SDS, 0.1 M Tris hydrochloride pH6.8, 4mM EDTA, 20% glycerol, 2% 2-mercaptaethanol, 0.02% bromophenol blue)[110].

Samples were heated at 37°C for 15 min. Protein in the supernatant was quantified using the Bradford assay kit (Thermo Fisher). An equivalent amount of protein was added to each lane. Western blot analysis was performed as described in [52]. Mouse monoclonal anti-HA (Sigma-

Aldrich, Cat no. H3663) was used as primary antibody, and goat anti-mouse antibody (LI-COR, cat no. 925-32210) was used for detection. The G6PD was used as the loading control [52].

3.3.10. Re-cultivation from a Stationary Phase Culture

Indicated strains were grown in YNB medium lacking inositol. Cultures were restarted at an A_{600} ~0.005 and growth curves were determined by measuring optical density at 600 nm (A_{600}) as described previously for 4 days (all data points not shown). The ability to grow following re-cultivate was examined by restarting the cultures at A_{600} ~0.005 from day 3 and day 4 of the cultures used in the growth curve. The stationary phase was confirmed by microscopy, where most cells were in the unbudded G_0 phase. Growth of the re-cultivated cultures was monitored at three different time points.

3.3.11. Statistical analysis

Paired t-test analysis or 2-way anova was performed to establish significances using GraphPad Prism 6.

3.4. Results

3.4.1. GPC can be hydrolyzed by Gde1 or acylated by Gpc1

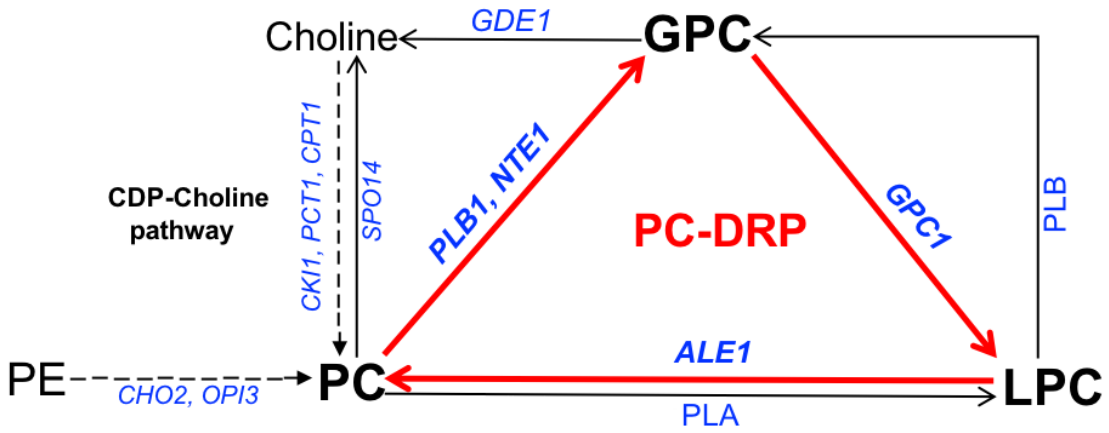

Figure 3. 1. Schematic outline of PC metabolism in yeast.
PC remodeling through PC-DRP is indicated by red arrows. PC-DRP includes deacylation of PC to GPC by *PLB1* or *NTE1* followed by step-wise reacylation of GPC to LPC by *GPC1* and LPC to PC by *ALE1*. The *de novo* PC synthesis routes are indicated by dotted arrows. Abbreviations: FA, fatty acid; G3P, glycerol 3-phosphate; DAG, diacylglycerol. *Gpc1* starts by acylating GPC.

Cellular GPC has two potential metabolic fates. The glycerophosphodiesterase encoded by *GDE1* can hydrolyze GPC to produce glycerol-3-phosphate and choline [31, 97]. Additionally, GPC can be acylated (likely at the *sn-1* position) to LPC by Gpc1, a recently described acyltransferase [52]. LPC can be converted to PC by Ale1, consistent with its role as a lysophospholipid acyltransferase [39, 40]. To gain further insight into the relative flux of GPC towards hydrolysis versus acylation, *in vivo* metabolic labelling was employed in strains lacking *GPC1* and/or *GDE1* (Fig. 3.2). Cells were grown in the presence of [^{14}C] -GPC, which enters through the Git1 transporter [29, 30, 111], and label incorporation in the lipid fraction was determined.

The [^{14}C]-LPC intermediate in the acylation of [^{14}C]-GPC to [^{14}C]-PC is virtually undetectable under the uniform labeling conditions employed in Fig 3.2 A, therefore only the label in PC is quantified. As shown in Fig 3.2 A, a *gpc1Δ* mutant incorporates roughly 35% less label into PC as compared to wild type, consistent with its role as a GPC acyltransferase. A *gde1Δ* mutant incorporates 50% less label into PC, indicating that a large portion of the label incorporated into PC in a wild type strain under low phosphate conditions originates from free [^{14}C]-choline released through the action of Gde1. A *gde1Δgpc1Δ* double mutant incorporates even less label, confirming the importance of both metabolic routes in determining the ultimate fate of GPC. The label remaining in the *gde1Δgpc1Δ* double mutant is likely the result of an uncharacterized acyltransferase and/or glycerophosphodiesterase that can act on GPC.

3.4.2. Gpc1 and Ale1 are central players in the step-wise acylation of GPC to lysoPC and then to PC

To demonstrate that Gpc1 produces LPC *in vivo*, and thereby confirm its cellular role, we designed an alternative labeling scheme and employed an *ale1Δ* mutant to block the second acylation step (Fig 3.2 B). In the experiment represented in Fig 3.2 A, cells were grown under low phosphate conditions in order to induce the expression of *GIT1* [111], a condition that also induces the expression of *GDE1* [31, 32]. Here, a plasmid harboring *GIT1* under the control of the constitutive *ADH1* promoter [102] was employed to allow cell growth under normal phosphate level, a condition that represses the expression of *GDE1* and, therefore, reduces the hydrolysis of GPC once it enters the cell [31, 32]. In addition, the labelling time in the presence of [^{14}C]-GPC was reduced to roughly 2 generations. Under these conditions, a 3-fold increase in labeled LPC was detected in an *ale1Δ* mutant as compared to wild type, and that increase was counteracted by

simultaneous deletion of *GPC1* (see the *ale1Δgpc1Δ* double mutant). At the same time, labeled PC levels decreased in an *ale1Δ* mutant and decreased further in an *ale1Δgpc1Δ* double mutant. The fact that PC levels were reduced by only 50% in the *ale1Δ* strain suggests that other enzymes may exist that are capable of converting LPC to PC in the cell. However, an additional possibility is that the increased LPC being produced is hydrolyzed, ultimately releasing free choline that could be incorporated into PC via the Kennedy pathway. These results confirm the formation of the immediate product of Gpc1 activity, LPC, *in vivo*, and the role of Ale1 in converting LPC into PC.

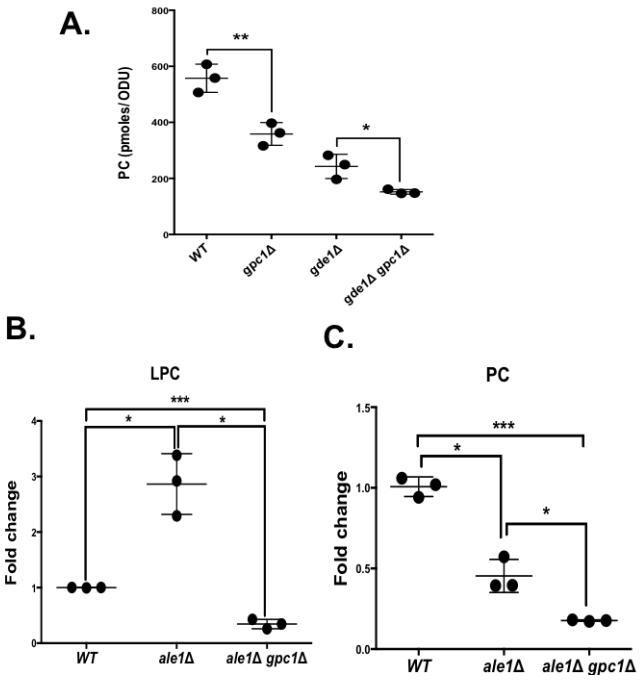

Figure 3. 2. The role of Gpc1 in PC metabolism.

A. The indicated strains were grown to log phase in the presence of 5μM [^{14}C]choline-GPC. Cells were harvested, phospholipids were extracted and separated, and PC was quantified as described in Experimental Procedures. B. Indicated strains contained plasmid in which *GIT1* was constitutively expressed under the control of the *ADH1* promoter. Cells were grown in the presence of [^{14}C]choline-GPC for 4 hours, harvested, and phospholipids were extracted and analyzed as described in Experimental Procedures. The data is normalized to the wild type (*WT)* containing *ADH1-GIT1*. Roughly 100-fold more PC was detected as compared to LPC in the wild type strain. Data represent average of 3 independent cultures ± SD. A t-test was performed to determine significance as indicated. (*p value value ≤ *0.05, **0.005, ***0.0005).

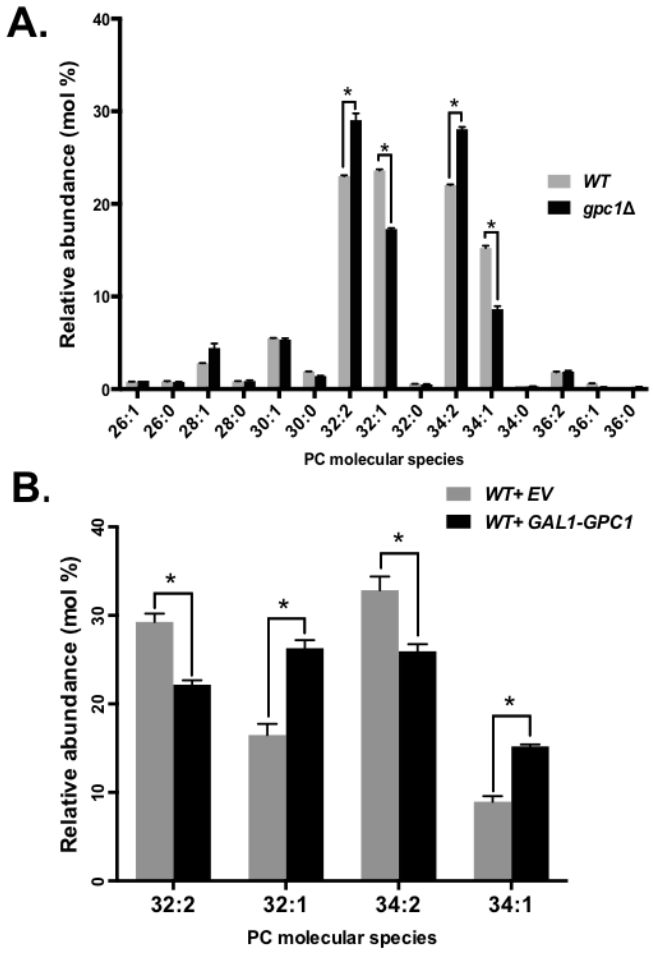

Figure 3. 3. Gpc1 impacts PC molecular species profile.
A, B, The indicated strains were grown to late log phase, cultures were harvested, and lipids were extracted. PC species were separated and analyzed using LC- MS/MS, as described in Experimental Procedures. Data represent average of 3 independent cultures ± SD. A t-test was performed to determine significance as indicated (*p value ≤ 0.05).

3.4.3. Gpc1 impacts the PC molecular species profile

A potential function for the PC-DRP is to modify the acyl chain content. In order to determine if Gpc1 activity affects the PC molecular species profile, LC-MS/MS was performed (parent ion scanning for *m/z* 184). Cells were not supplemented with exogenous GPC for these experiments, so the substrate for Gpc1 activity presumably arose through endogenous phospholipase B activity [97]. Fig. 3.3A includes the range of PC species produced by yeast.

Focusing on the major species, the data indicate that the loss of Gpc1 results in a decrease in mono-unsaturated PC species (32:1, 34:1) and an increase in di-unsaturated PC species (32:2, 34:2) as proportions of the total PC pool. Overexpression, as predicted, has the opposite effect (Fig. 3.3B). When *GPC1* was placed under the control of the *GAL1* promoter and cells were grown on galactose, there was an increase in mono-unsaturated PC species (32:1 and 34:1) and a decrease in di-unsaturated PC species (32:2, 34:2). In total, these results indicate that Gpc1 impacts the PC species profile and suggest that Gpc1 activity favors the utilization of saturated acyl-CoA species when acylating GPC.

3.4.4. Loss of Pct1 and Ale1 have minor effects on the PC species profile

Since Ale1 converts LPC to PC as part of the PC-DRP, we analyzed its impact on the PC molecular species profile. If Ale1 were the only LPC acyltransferase in the cell, and assuming that Ale1 does not affect the species profiles of the lipid precursors of PC (PE and DAG), the profile of the *ale1Δ* mutant should resemble that of the *gpc1Δ* mutant, as the reacylation pathway would stall at LPC, and the LPC produced would likely be rapidly hydrolyzed by phospholipases. In fact, the *ale1Δ* mutant did not resemble the *gpc1Δ* strain in terms of PC species, as a slight decrease in PC32:2 and an increase in PC34:2 were its only significant changes from WT. The *ale1Δ gpc1Δ* mutant, like *gpc1Δ*, exhibited an increase in di-unsaturated species and a decrease in mono-unsaturated species as compared to WT, although the magnitude of the changes was not identical between the two strains (Fig. 3. 4). These results suggest that there may be more acyltransferases capable of acylating lysoPC in the cell [33, 37].

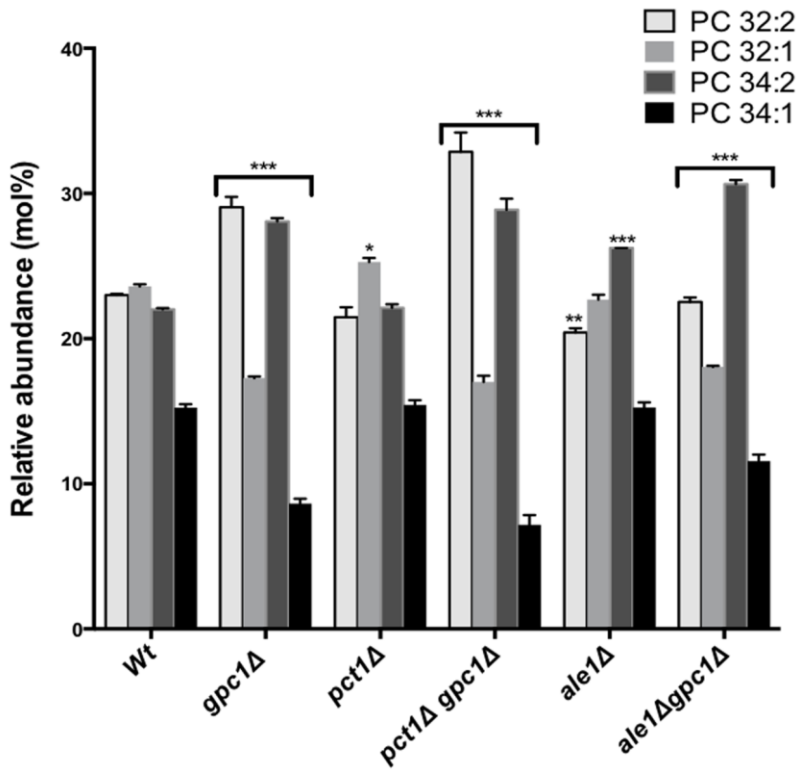

Figure 3. 4 Loss of *PCT1* or *ALE1* has minor effects on PC species profile.
The indicated strains were grown to late log phase, cultures were harvested, and lipids were extracted. PC species were separated and analyzed as described in Experimental Procedures. Data represents average of 3 independent cultures ± SD. A 2-way ANOVA was performed to determine significance for each strain compared to the *WT* (*p value ≤ *0.05, **0.004, ***0.0001).

The steady state PC molecular species profile in a cell represents a combination of PC biosynthesis, PC degradation and PC acyl chain remodeling. In the experiments presented in Fig. 3. 3, cells were grown in the absence of free choline, so the PE methylation pathway, not the Kennedy pathway, was primarily responsible for PC biosynthesis. However, flux through the Kennedy pathway can also occur as a result of free choline released through phospholipase-mediated turnover. In order to examine the extent to which PC turnover resulting in free choline release followed by re-synthesis contributes to the observed PC species profile, we utilized a *pct1Δ* mutant in which flux through the Kennedy pathway is blocked. As shown in Fig 3. 4, the PC species profile in *pct1Δ* was largely unchanged from wild type (in agreement with ref 20), but did result in a small but

significant increase in 32:1 PC. That increase may be the result of the observed uptick in *GPC1* transcript upon *PCT1* deletion (forthcoming Fig. 3. 6), as evidenced by the fact that 32:1 again decreases in a *pct1Δgpc1Δ* double mutant. Overall, these results indicate that the PC species profiles generated under our experimental conditions are primarily the result of PC synthesis via the PE methylation pathway followed by PC remodeling via PC-DRP.

3.4.5. Loss of Gpc1 does not affect PE, PI, PS species profiles and slightly decreases total 16:0 FA content

We reported previously that Gpc1 had limited ability to utilize acyl-CoAs to acylate glycerophosphoethanolamine (GPE) in an *in vitro* system [52]. To probe the possibility that Gpc1 acylates GPE to affect PE *in vivo*, we analyzed the PE molecular species. As shown in Fig. 5A, we did not detect any significant difference in PE molecular species profile when comparing a wild type strain to a *gpc1Δ* strain. Hence, Gpc1 does not play a major role, if at all, in PE remodeling *in vivo* under the conditions employed here.

The effect of *GPC1* deletion on the phosphatidylinositol (PI) and phosphatidylserine (PS) species profiles was also examined. As shown in Figs. 3. 5B and 3. 5C, no significant differences between wild type and *gpc1Δ* were found. In addition, the overall fatty acid composition of all cellular lipids was determined by gas chromatography. As shown in Fig. 3. 5D, WT and *gpc1Δ* fatty acid compositions are largely the same, with the exception of a small but significant decrease in C16:0 in *gpc1Δ*. This change is consistent with the fact that the *gpc1Δ* mutant displays a decrease in monounsaturated PC species and may reflect the loss of a small C16:0 sink resulting from the inability of *gpc1Δ* to add C16:0 to GPC during the PC remodeling process. The results

indicate that loss of *GPC1* does not induce large-scale changes in fatty acid composition, but rather highly specific effects.

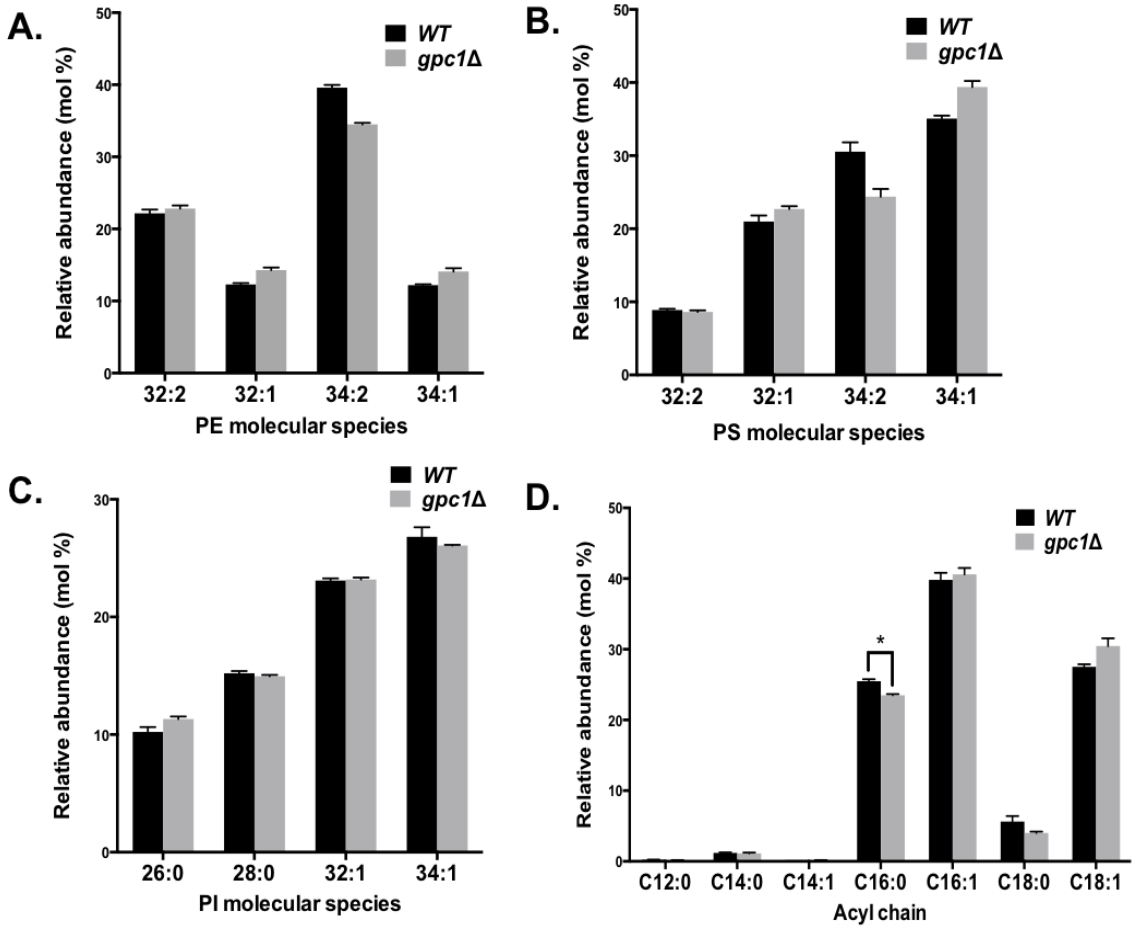

Figure 3. 5. Loss of *GPC1* has no significant effects on PE, PS, PI species profiles and slightly decreases the total C16:0 acyl chain content.

A, B, C, D. The indicated strains were grown to log phase, harvested, and lipids were extracted. A, B, C. PE, PS and PI species were analyzed by MS as detailed in Experimental Procedures. D. Total acyl chain composition was determined using gas chromatography. Data represent average of 4 independent cultures ± SD A t-test was performed to determine significance as indicated (*p value= 0.0008).

3.4.6. *GPC1* expression is upregulated by attenuation of PC biosynthesis and by inositol limitation

To gain further insight into the physiological role of Gpc1, we examined its transcriptional regulation in response to alterations in major lipid biosynthetic pathways. To examine PC biosynthesis, we employed a *cho2Δ* mutant (attenuated PE methylation pathway), *a pct1Δ* mutant (blocked Kennedy pathway), and a *cho2Δ pct1Δ* mutant. The PE methylation pathway for PC biosynthesis is not completely blocked in the *cho2Δ pct1Δ* double mutant, due to a partially redundant function supplied by the methyltransferase, Opi3 [19]. As shown in Fig. 3. 6a, *GPC1* message levels, as measured by qRT-PCR, are increased roughly 3-fold in each single mutant and in the double mutant as compared to wild type. Thus, inhibition of either pathway for PC biosynthesis causes an increase in *GPC1* message, but the effect is not additive.

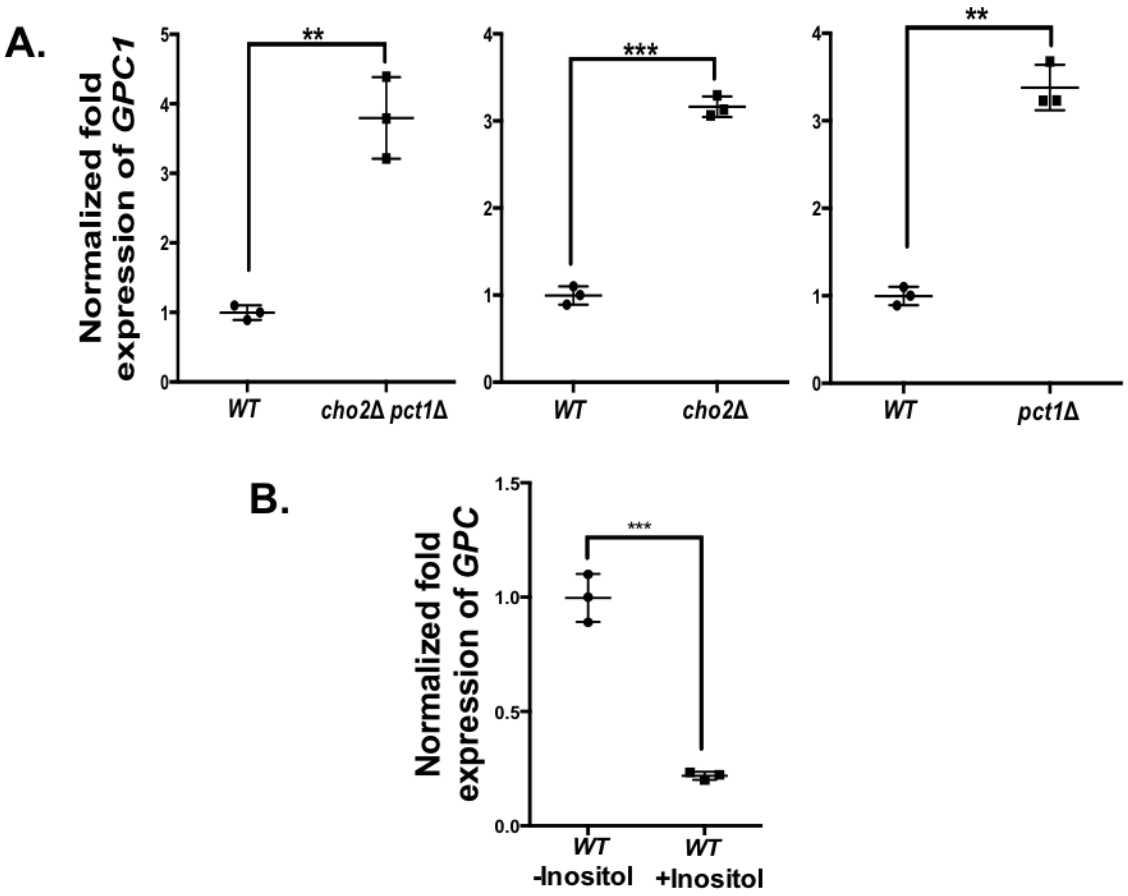

Figure 3. 6. *GPC1* transcript is increased by attenuation of PC and by inositol limitation.
A, B. The indicated strains were grown to log phase, cells were harvested, and RNA was extracted. *GPC1* transcripts were quantified by qRT-PCR. Data was normalized to the amount of the endogenous control mRNA, *SNR17,* and expressed relative to the wild type (WT) strain. *B,* Wild type grown in the presence of 75 μM inositol (WT+Inositol) compared to wild type grown in the absence of inositol (WT-Inositol). Experiments were performed in biological triplicates and assayed in experimental triplicate. A t-test was performed to establish significance (*P ≤ **0.005, ***0.0005).

A number of phospholipid biosynthetic genes are regulated by the presence of inositol in the medium via a complex mechanism involving the modulation of PA levels at the ER, which in turn impacts the transit of the Opi1 repressor protein into the nucleus [22, 112]. Thus, inositol availability has a general impact on phospholipid composition and flux through the various pathways [5, 22]. As shown in Fig 3. 6B, there is a roughly 5-fold decrease in *GPC1* message upon inositol supplementation

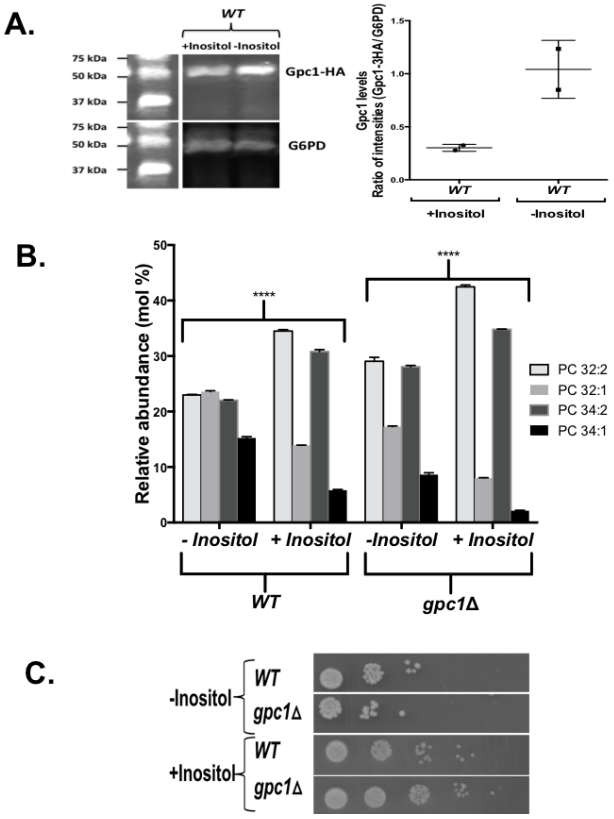

Figure 3. 7. Inositol supplementation affects Gpc1 protein level and PC species profile.
A. *WT* strain was grown in medium containing 75 μM inositol (+Inositol) or lacking Inositol (-Inositol). Western blot analysis was performed using anti-HA Mouse IRdye 680 and Goat antimouse IRdye 800. Glucose-6-phosphate dehydrogenase was used as loading control. Protein bands were quantified using Image Studio™ software. Data represents 2 biological replicates. B. The indicated strains were grown to late log phase before harvesting. Phospholipids were extracted, and PC species were analyzed using LC-MS/MS. Data represent average of 3 independent cultures ± SD. A t-test was performed to establish significance (*P ≤ ****0.0005) C. Strains were cultured in synthetic medium, harvested and resuspended in sterile water. 10-fold serial dilutions (5 μl) were spotted onto plates containing (+Inositol) or lacking (-Inositol) inositol.

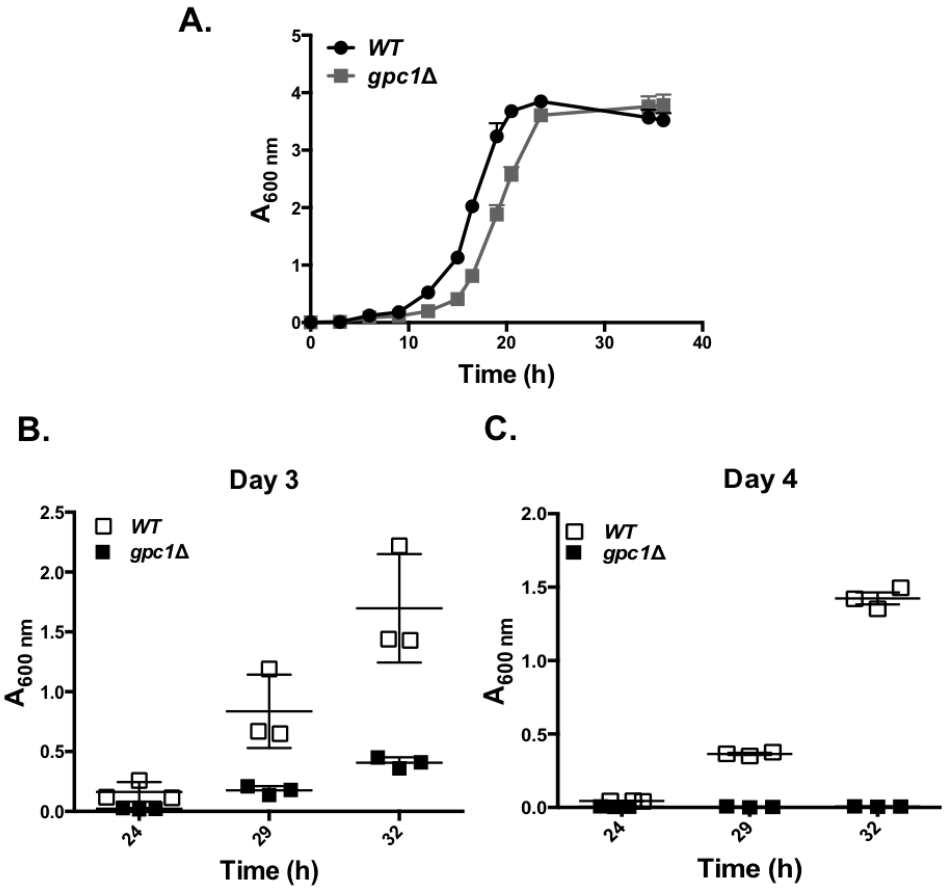

Figure 3. 8. Loss of *GPC1* impacts growth and stationary phase viability in inositol free medium.

A. Indicated strains were grown in synthetic liquid medium lacking inositol and growth was monitored by measuring optical density at OD_{600} over 40 hours. The cultures (A) were allowed to continue shaking at 30°C until day 4 (roughly 96 hours). B. On Day 3 and Day 4, cells were taken from the original cultures and inoculated in fresh YNB I- medium to an A_{600} of 0.005. OD_{600} was determined at 24, 29, 32 hrs. Experiments were performed with 3 biological replicates, all data points not shown.

3.4.7. Inositol supplementation represses *GPC1* expression and increases di-unsaturated PC species

Following the qRT-PCR findings (Fig. 3. 6) the effect of inositol availability was examined more thoroughly, as this perturbation produced the largest transcriptional response, and would not confound the interpretation of the PC species profile by impacting PC biosynthesis (as

would the *cho2Δ* and *cho2Δpct1Δ* mutants). As seen in Fig. 3. 7A, the decrease in *GPC1* transcript upon inositol supplementation, was reflected in a decrease in Gpc1 as measured by Western analysis. It should be noted that the PC species profiles presented in Fig. 3 were performed on cells grown in the absence of inositol (I-) in order to maximize *GPC1* expression. When grown in the presence of inositol (I+), there is a clear increase in diunsaturated PC species and a clear decrease in monounsaturated PC species (Fig. 3. 7B) in a wild type strain, similar to the effect of *GPC1* deletion (Fig. 3. 3A and Fig. 3. 7B) in I- medium. A similar pattern of changes in PC molecular species profile upon inositol limitation was reported previously [20]. Loss of Gpc1 and inositol supplementation together result in an even greater increase in di-unsaturated species, indicating that factors beyond Gpc1 are at play in impacting the PC species profile under these conditions.

3.4.8. Loss of Gpc1 impacts growth and stationary phase viability in inositol free medium

Growth assays were performed to assess the phenotypic consequences of diminished PC remodeling as a function of inositol availability. In the absence of inositol, where *GPC1* expression is upregulated, there is a small but significant growth defect on plates (Fig. 3. 7C), which is not consistently seen in I^+ conditions. To explore this finding further, we monitored growth in liquid culture under I^- conditions. As shown in Fig. 3. 8A, *gpc1Δ* mutants displayed an increase in lag time resulting in slower growth overall, although the rate of doubling during logarithmic phase was comparable to wild type.

To determine if decreased ability of cells to regrow from stationary phase was the reason behind the increased lag time, a re-cultivation experiment was performed. Cells were grown to stationary phase (as in Fig 3. 8A) but the cultures were incubated longer, for a total of 4 days. On days 3 and 4, cells were taken from the original cultures and inoculated in fresh YNB I^- medium.

By day three, *gpc1Δ* lagged well behind wild type in its ability to reinitiate growth as measured at three time points over 32 hours (Fig. 3. 8B; Day 3). In four day old cultures, no growth was detected in the *gpc1Δ* cultures as measured over 32 hours (Fig. 3. 8C; Day 4). These results indicate that loss of Gpc1 results in a loss in stationary phase viability in inositol-free medium. Western blot analysis was performed to examine Gpc1 protein levels as a function of growth phase. While Gpc1 was found to be expressed in logarithmic phase (Fig 3. 9), little or no expression was detected in stationary phase (24 and 48 hours of growth). This finding suggests that no further remodeling of PC via this pathway occurs once the cells reach stationary phase.

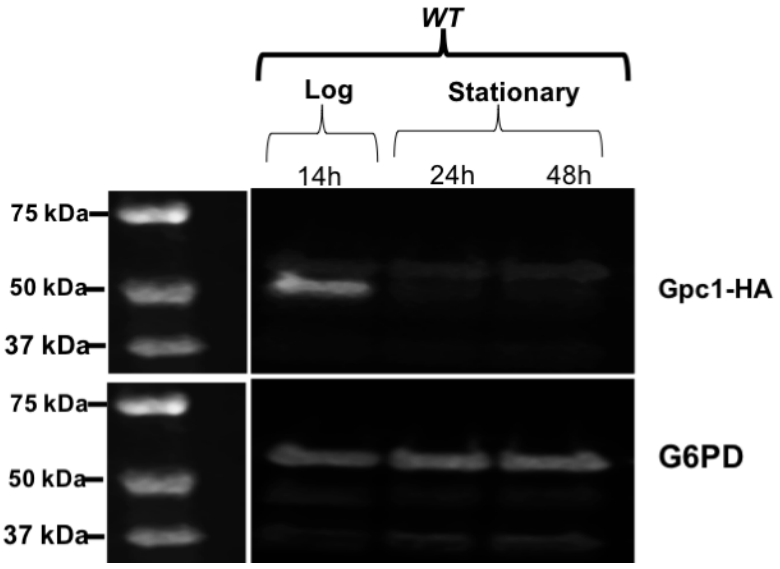

Figure 3. 9. Gpc1 is highly expressed in logarithmic phase.
WT strain was grown in medium lacking Inositol. Cultures were harvested at log (14 h), early stationary (24 h) and late stationary (48 h) phases. Western blot analysis was performed using anti-HA Mouse IRdye 680 and Goat antimouse IRdye 800. Glucose-6-phosphate dehydrogenase was used as loading control.

3.5. Discussion

PC metabolism consists of interconnected pathways of synthesis, degradation, recycling of catabolites, and remodeling (Fig. 3. 2A). Deacylation of PC via phospholipases of the B type

produces GPC. Our previous studies have shown that GPC is found both intracellularly and extracellularly and that it can be transported into the cell via the Git1 permease [30, 31]. A well-characterized pathway for GPC degradation is its hydrolysis to choline and glycerol-3-phosphate by the glycerophosphodiesterase, Gde1 [31, 96]. Prior to the identification of *GPC1*, GPC acyltransferase activity had been detected in *Xanthomonas campestris, S. cerevisiae* and plants [49-51]. Our recent identification of the gene encoding Gpc1 provided a tool for examining the relative flux of GPC between degradation versus acylation. When considering the label incorporated into PC from exogenous GPC, roughly 50% occurs via Gde1 activity producing free choline that is subsequently utilized by the Kennedy pathway. Roughly 30% is acylated by Gpc1, and another 20% is presumably metabolized by unknown enzymes. Thus, reacylation is not a trivial pathway for GPC conversion to PC. Through the use of mutants and radiolabeling (Fig. 3. 2 B) the primary roles of Gpc1 and Ale1 in the stepwise conversion of GPC to PC as part of the PC-DRP were confirmed.

Although the acylation of GPC to PC clearly occurs in the cell, the synthesis of PC at a level that supports growth requires either a functional PE methylation pathway or a functional Kennedy pathway [6] [58]. Hence, we hypothesized that the primary purpose of GPC reacylation may not be bulk synthesis, but rather the synthesis of specific PC species as part of a remodeling pathway. Evidence for post-synthetic PC remodeling in yeast has been described by multiple research groups [55] [57, 58, 113, 114]. Importantly, De Kroon and colleagues have used stable-isotope pulse-chase analysis coupled with MS to prove the post-synthetic formation of more saturated PC species as a function of time, and demonstrated the involvement of Plb1 [60]. Prior to the identification of Gpc1 activity [49, 52], PC remodeling was believed to involve the removal

of a single acyl chain at the *sn-2* position, followed by reacylation by a LPC acyltransferase (LPCAT), a cycle first described by Lands [115]. Once LPC is formed, it can be acylated to PC by Ale1 [39, 40, 116], with some publications indicating that Ale1 prefers incorporation of an unsaturated acyl-CoA species at *sn-2* position of 1-acyl LPC [39, 41, 116-118]. A recent publication has provided evidence that Ale1 may also have limited ability to acylate the *sn*-1 position of the synthetic LPC analog, 2-alkyl-*sn*-glycero-3-phosphocholine [114]. Importantly, we posit that the previous step in the remodeling pathway, the acylation of GPC, is carried out by the glycerophosphocholine acyltransferase (GPCAT) activity of Gpc1, adding another dimension to the process of PC remodeling, namely the potential exchange of both acyl chains. Of course, this finding does not preclude the possibility of PC remodeling occurring via other acyltransferase or transacylase activities [33, 37]. PC molecular species profiling of cells lacking *GPC1* (Fig. 3. 3A) or overexpressing *GPC1* (Fig. 3. 3B) clearly indicates that Gpc1 impacts the PC species profile, producing a higher content of more saturated PC species (32:1 and 34:1) when present. The impact of Gpc1 on phospholipid molecular species is limited to PC, as PI, PE, and PS species profiles are unchanged by loss of Gpc1.

The obvious general question arising from these results is under what circumstances is Gpc1 activity and PC remodeling beneficial? The PC molecular species profile is highly dynamic [119, 120]. Given that changes in PC saturation status may well affect a membrane property such as fluidity, we reasoned that Gpc1 must be co-regulated with regards to other lipid metabolic processes to maintain optimal bilayer function. As a first approach, we utilized qRT-PCR to assess changes in transcript levels by attenuating the methylation pathway (*cho2Δ)* or blocking the Kennedy pathway (*pct1Δ)* either singly or in combination results in an uptick in *GPC1* message

levels. Granted, this experiment does not have a straightforward interpretation, as the inhibition of the major PC biosynthetic pathways may cause an increase in GPC reacylation as an end towards preserving PC, not remodeling PC. By similar reasoning, we did not test the effects of choline supplementation in this study (but will be examined in future studies), as that perturbation would increase biosynthesis through the CDP-choline pathway, potentially obscuring the interpretation of the findings. Nonetheless, our results clearly show that *GPC1* message increases upon inhibition of PC biosynthesis.

Inositol availability has far-reaching transcriptional and physiological effects in yeast. Inositol is required for PI biosynthesis. In turn, PI is a precursor for phosphoinositides, polyphosphates, inositol sphingolipids, and GPI anchors [5, 20, 22]. Inositol can be synthesized by the cell and/or imported into the cell from the medium [121]. In the absence of exogenous inositol, a number of genes involved in phospholipid metabolism are transcriptionally induced [5, 22]. Inositol supplementation results in a 5-fold downregulation of *GPC1* message, and a 3-fold decrease in protein level (Figs. 3. 6B and 3. 7A). Downregulation of *GPC1* transcript and protein levels by inositol supplementation resulted in changes in the PC species profile, providing an explanation for a similar result reported by Henry and colleagues [20] prior to the identification of Gpc1.

Most genes responsive to inositol limitation contain one or more UAS_{INO} elements (consensus sequence 5'CATGTGAAAT3') in their promoters and are regulated by Ino2, Ino4, and Opi1 via the Henry Regulatory Circuit [21, 22, 122]. The transcription factors, Ino2 and Ino4, typically bind to UAS_{INO} as a heterodimer to activate transcription when inositol is limiting, and

the Opi1 repressor binds to Ino2 to block transcriptional activation when inositol is available. The Gpc1 promoter contains a sequence (CTTGTGAATA) that is 3 base pair off from the consensus Ino2:Ino4 binding sequence [123] at -193 to -202. In addition, it contains a site (CATTTG) for Ino4-dependent/Ino2-independent binding [124] at -182bp to -187bp. Further evidence for control by the Henry Regulatory Circuit is provided by microarray studies performed prior to the characterization of Gpc1 in which Opi1 [125] and Ino4 [126] were shown to affect transcription of the *GPC1* ORF, YGR194w. Further studies would be required to unequivocally prove binding of Ino2 and/or Ino4 to the *GPC1* promoter.

In medium lacking inositol, where *GPC1* is upregulated, *gpc1Δ* mutants display decreased stationary phase viability (Fig. 3. 8). However, we did not detect Gpc1 expression in stationary phase, suggesting that the alteration in PC species that occurs via PC-DRP during log phase may prepare the membrane for events that occur in later stages of growth. Gpc1 is predicted to be an integral membrane protein with 8 transmembrane domains [52]. A definitive localization study has not been performed for Gpc1, but will be the focus of future studies and may shed light on its role in cell viability. Of note, the changes in lipid metabolism resulting from I- medium are accompanied by the induction of multiple stress response pathways, including the Unfolded Protein Response (UPR), the PKC-MAPK pathway, and others [22]. Thus, the loss of cell viability observed under I- conditions upon loss of *GPC1* is likely the result of a complex series of events.

In summary, our data indicate that Gpc1 is part of a novel PC deacylation/reacylation remodeling pathway (PC-DRP) that provides the opportunity for post-synthetic alteration of both acyl chains species and, thereby, to impact the biophysical properties of the membrane.

Acknowledgements

This work was supported, in whole or in part, by National Institutes of Health Grant R15 GM 104876 (to J.P.-V.), PlantLink and the Strategic Research Area project "Trees and Crops for the Future (to I.L.) and The Netherlands Organization for Scientific Research (NWO) (to M.R. and A.deK). The purchase of mass spectrometers was supported by National Science Foundation Grant MRIDBI-0821401 to Duquesne University. The authors thank Dr. Amrah Weijn for help with the MS sample preparation.

Table 1
S. cerevisiae strains used in this study

	Strain	Genotype	Reference
JPV 399	WT, BY4742	BY4742; *MATα his3Δ1 leu2Δ0 lys2Δ0 ura3Δ0*	Research Genetics
JPV 788	*gpc1*Δ	BY4742; *gpc1::KanMX*	This study
JPV 125	*gde1*Δ	BY4742; *gde1::KanMX*	This study
JPV 834	*gde1*Δ *gpc1*Δ	JPV 125; *gpc1::URA3*	This study
JPV 272	*cho2*Δ *pct1*Δ	BY4742; *cho2:: KanMX pct1:: LEU2*	This study
JPV 839	*cho2*Δ *pct1*Δ *gpc1*Δ	JPV 272; *gpc1::URA3*	This study
JPV 841	*pct1*Δ *gpc1*Δ	JPV 788; *pct1:: LEU2*	This study
JPV 269	*cho2*Δ	BY4742; *cho2::KanMX*	Research Genetics
JPV 270	*pct1*Δ	BY4742; *pct1:: LEU2*	Research Genetics
JPV 832	*ale1*Δ	*Mat **a**: his3Δ1 leu2Δ0 met15Δ0 ura3Δ0 ale1::KANMX*	[52]
JPV 833	*ale1*Δ *gpc1*Δ	JPV 832; *gpc1::KANMX*	[52]
JPV 846	*WT+GPC1-3xHA*	BY4742; *GPC1-3xHA*	This study

Table 2
Nucleotide primer sequences used for gene deletions
The Bold sequences are homologous to the template plasmid. The deleted gene was replaced with gene name in parentheses.

Gene name	Primer	Sequence (5'-3')
GPC1(URA3)	Forward	ATGTACAAGTTGGACAATAACGACATTGACGATGAAACGAATAACTCTGTTTCACTGACG **AGCGAACAAAAGCTGG**
GPC1(URA3)	Reverse	CTTAATCACTCTTTGAGGATACACTTGAAGAGTCGTCAAAATCTTCGTCACGGTTGACAT **CTGTAGGGCGAATTGGG**
GPC1(LEU2)	Forward	ATGTACAAGTTGGACAATAACGACATTGACGATGAAACGAATAACTCTGTTTCACTGACG **CACATACCTAATATTATTGC**
GPC1(LEU2)	Reverse	CTTAATCACTCTTTGAGGATACACTTGAAGAGTCGTCAAAATCTTCGTCACGGTTGACAT **GAATCTTTTTAAGCAAGGAT**
GPC1-1-3XHA	Forward	TTGAATGTCAACCGTGACGAAGATTTTGACGACTCTTCAAGTGTATCCTCAAAGAGTGAT **AGGGAACAAAAGCTGGAG**
GPC1-1-3XHA	Reverse	GTAAAGCGCCTGTAAATAAAAGCTCTCAAAGTTAACAGATAAATGAAGTGAACTATCTTA **CTGTAGGGCGAATTGGG**

Table 3
Nucleotide primer sequences for qRT-PCR

Gene name	**Primer**	**Sequence (5'-3')**
SNR17	Forward	TTG ACT CTT CAA AAG AGC CAC TGA
SNR17	Reverse	CGG TTT CTC ACT CTG GGG TAC
GPC1	Forward	AAA TTA GCT GCG GCC CTA TT
GPC1	Reverse	TAT CAT TCA CGG AGG CAT CA

Chapter 4: Summary and future directions

4.1. Summary of novel findings

My dissertation work has increased our understanding of PC metabolism through the characteristics of Gpc1. The first major finding focused on identifying and determining the *in vivo* role of Gpc1. GPCAT homolog analysis revealed a wide distribution of homologs in eukaryotes including fungi, animal, plants, algae, and most protist clades. In a second major finding, I have determined the role of Gpc1 in a PC deacylation/reacylation remodeling pathway (PC-DRP). Membrane remodeling involving Gpc1 resulted in an increase in the monounsaturated PC species at the expense of diunsaturated PC species. PC remodeling through PC-DRP occurs by removal of both the acyl chains at the *sn-1* and *sn-2* positions of GPC by a phospholipase of the B-type followed by sequential reacylation by Gpc1 and Ale1. This process results in an increased level of saturated PC species. This process was found to be vital for cell viability at the stationary phase under inositol-free conditions. Also, inositol was found to be involved in downregulating the expression of *GPC1*. PC-DRP signifies a new aspect to PC metabolism. Given that plant homologs of Gpc1 have similar functions collectively, I expect these findings to improve our understanding of PC metabolism across multiple species. The following are some of the open questions and future directions that should be addressed.

4.2. What is the impact of the PC-DRP pathway on the total PC synthesis?

Yeast has two major pathways, i.e., the Kennedy and methylation pathways, for bulk PC synthesis. Either one is sufficient for cell survival upon disruption of the other. The PC-DRP pathway is an alternative route for PC synthesis in yeast, but it is crucial to know the impact of this pathway on total PC synthesis.

This can be approached by performing a ^{32}P-orthophosphate labeling in the WT and *gpc1*Δ strains grown in synthetic medium without the supplementation of GPC. The absence of exogenous GPC would force the cell to utilize the intracellular GPC that is produced by the action of Plb1. The ^{32}P-orthophosphate would be incorporated in all phosphate containing molecules, including the phospholipids, in the cell. Potential changes in the level of PC upon deletion of *gpc1*Δ can be quantified as described in appendix A.5. I had initiated these studies (Figure A. 5) in WT and *gpc1Δ* containing empty vector or *GAL1-GPC1* overexpressor, but it was performed in a single replicate. This experiment can be performed in biological replicates to get publication quality data.

4.3. Is *GPC1* expression regulated through the Henry Regulatory Circuit?

I have documented the effect of inositol supplementation in downregulating *GPC1* expression. This downregulation could be due to the so-called Henry regulatory circuit that is known to regulate a number of phospholipid biosynthetic genes. Opi1, Ino2 and Ino4 are key transcription factors that play a crucial role in regulating the genes responsive to inositol limitation. There is evidence from microarray studies that were performed before the characterization of *GPC1* [120,121] that suggest *GPC1* expression might be controlled by Opi1 and Ino4 transcription factors. This could be verified by measuring *GPC1* message levels in *opi1*Δ and *ino4Δ* strains.

4.4. Does ethanol or reactive oxygen species (ROS) play a role for the decreased cell viability in stationary phase*?*

We have documented that the inability to remodel PC results in loss of cell viability at the stationary phase. A possible reason for this loss could be due to the production of ethanol in stationary phase that may act as a membrane fluidizer. Remodeling the PC by Gpc1 would increase

the level of saturated PC species which could rigidify the membrane. Thus, Gpc1 might be crucial in sustaining viability at the stationary phase. Also, *GPC1* expression is upregulated (Figure A. 10) when ethanol/glycerol was used as the carbon source instead of glucose. Overall, these results suggest that PC remodeling by Gpc1 could help in negating the effect of ethanol as the membrane fluidizer. This effect can be delineated by studying the growth pattern of *WT* and *gpc1Δ* strains upon supplementation of ethanol. I would expect the *gpc1Δ* strain to grow slower than the *WT*. A direct method of measuring fluidity, such as, by using lipophilic probe diphenylhexatriene (DPH) would be informative [127].

Another possible explanation for the decreased cell viability could be due to the lipid peroxidation that is seen during stationary phase [128, 129]. The Remodeling of PC through PC-DRP would increase the saturation state of PC and that could provide resistance against lipid peroxidation. Msn2 and Msn4 are transcription factors that are known to be involved in regulating the oxidative stress [130]. I have identified Msn2 and Msn4 stress response elements (-154bp to -158bp) in *GPC1* promoter that might be involved in regulating *GPC1* [130]. The role of Msn2 and Msn4 in *GPC1* expression can be examined by determining *GPC1* message levels in *msn1*Δ and *msn2*Δ strains. A direct measure of lipid peroxides in WT and *gpc1Δ* by MDA assay [131] would also be informative.

4.5. Is the ortholog of *GPC1* from *Candida albicans* involved in PC biosynthesis?

Candida albicans is an opportunistic fungal pathogen that is known for 1-2 million human deaths each year. We have identified ORF 19.88 (*caGPC1)* as the ortholog of *GPC1* in *C. albicans* and predict that *caGPC1* be involved in a similar novel route for PC biosynthesis. Also, our lab has recently shown that the inability to transport GPC into the cell is associated with decreased

virulence of *Candida albicans*. This suggests that this metabolite is essential for growth during infection [81].

These studies can be initiated by constructing a *gpc1Δ/gpc1Δ* homozygous deletion strain and a heterozygous deletion strain by reintegrating a single copy of *GPC1* into the homozygous mutant. This could be approached either by the traditional PCR-based gene deletion or by use of a CRISPR/ Cas9 system. The WT and the mutants can then be tested by performing *in vivo* metabolic labeling studies as described in chapter two to examine the role of the ortholog in PC biosynthesis.

4.6. Is *GPC1* expression affected by the addition of saturated or unsaturated fatty acids?

Since *GPC1* defines a PC-DRP that increases the saturation state of PC, it is possible that supplementation of saturated (16:0, 18:0) or an unsaturated (16:1, 18:1) fatty acids might have an impact on the *GPC1* transcript, protein, activity or level. The impact on *GPC1* transcript can be tested by growing *WT* in the synthetic medium supplemented with and without these fatty acids. The mRNA levels can then be quantified as described in Chapter three. These findings would provide us with an insight into the adaptation of *GPC1* expression with regards to the changes in the FA content. The most exciting result from expression data can then be pursued by examination of Gpc1 protein levels by Western blot analysis.

4.7. Is PC-DRP regulated with coordination to sphingolipid biosynthesis?

Sphingolipids are the second major class of membrane lipids. Sphingolipid biosynthesis can be inhibited by a drug named myriocin that blocks the serine palmitoyltransferase, Lcb1, to inhibit the *de novo* synthesis [132]. Given that sphingolipids are essential membrane components [133], it is not surprising that inhibition of their synthesis would result in changes to PC

metabolism. Our previous finding indicates that inhibition of sphingolipid biosynthesis results in an increase in the *PLB1* message level and the expected increase in the GPC production [88]. In addition, I have identified that inhibition of sphingolipids synthesis results in upregulation of *GPC1* expression in a *WT* strain (Fig A.8.a). An obvious question to explore is if PC deacylation by Plb1 and GPC reacylation by Gpc1 is regulated in coordination with the sphingolipid biosynthesis. This could be tested by examining the transcript levels of genes involved in PC-DRP (*PLB1, NTE1, GPC1,* and *ALE1)* upon perturbation of sphingolipids biosynthesis.

A. Appendix

The following are notable experiments that were not published, either because they did not fit in the theme of a publication or were not performed with enough biological replicates.

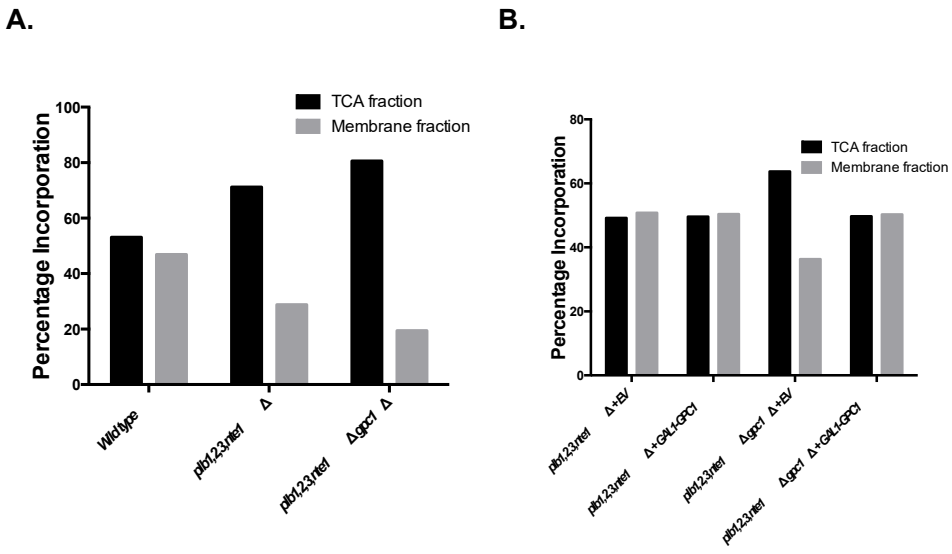

A. 1. Effect of phospholipase-B mutation on radiolabeled ^{3}H-GPC incorporation into metabolities.
A, B. WT, *plb1, 2, 3*Δ *nte1*Δ, and *plb1, 2, 3*Δ *nte1*Δ *gpc1*Δ strains with or without the EV or *Gal1-GPC1* plasmids were used in this study. Cultures were grown to log phase in synthetic medium lacking inositol and containing 200 μM KH_2PO_4 and 5 μM of choline (^{3}H) -GPC. Cells were harvested and separated into the extracellular, intracellular and membrane fractions. The ^{3}H label was quantified in all these fractions as described in chapter 2. A. The *plb1, 2, 3*Δ *nte1*Δ mutant showed an increase in the TCA fraction and a decrease in the membrane fraction when compared to the WT. Similar trends were seen for *plb1, 2, 3*Δ *nte1*Δ *gpc1*Δ. These results suggest that the inabilities in deacylation (*plb1, 2, 3*Δ *nte1*Δ) and deacylation/ reacylation (*plb1, 2, 3*Δ *nte1*Δ *gpc1*Δ) reduces the flux of ^{3}H-GPC to ^{3}H-PC. The experiment was performed in a single replicate. This penta-mutant was constructed for our collaborator, Dr. Ida Lager, for investigating the role of *GPC1* under limited PC deacylation condition.

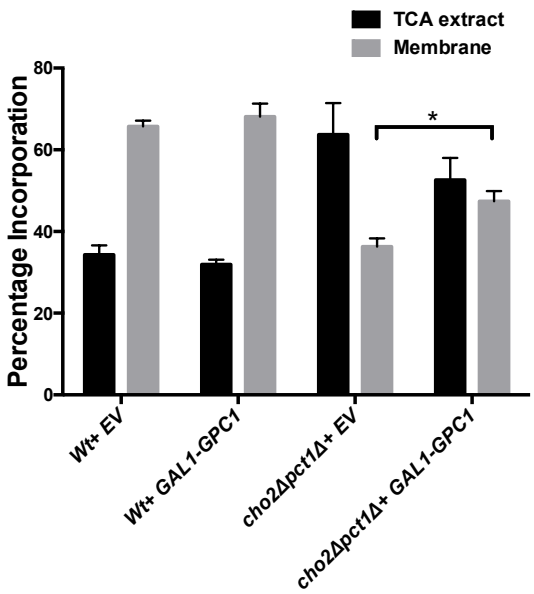

A. 2. Overexpression of *GPC1* in strain attenuated for PC biosynthesis results in increased flux of ^{3}H-GPC into the membrane fraction.

WT and *cho2*Δ *pct1*Δ containing EV or *Gal1-GPC1* plasmid were used in this study. Cultures were grown to log phase in synthetic medium lacking uracil, and containing 2% galactose, 5 μM ^{3}H-GPC and 200 μM KH_2PO_4. Cells were harvested and separated in fractions as described in chapter two. The *cho2*Δ *pct1*Δ has attenuation in two major pathways for PC biosynthesis. The overexpression of *GPC1* in *cho2*Δ *pct1*Δ strain results in an increased flux of ^{3}H-GPC from intracellular fraction into ^{3}H-PC in the membrane fraction. Finally, overexpression of *GPC1* in WT strain did not change the flux of ^{3}H-GPC, as Gpc1 dosage may not be rate-limiting. The experiments were performed in biological triplicates. The experiment was performed in biological triplicate. A t-test was performed to determine significance as indicated (*p-value ≤ 0.05).

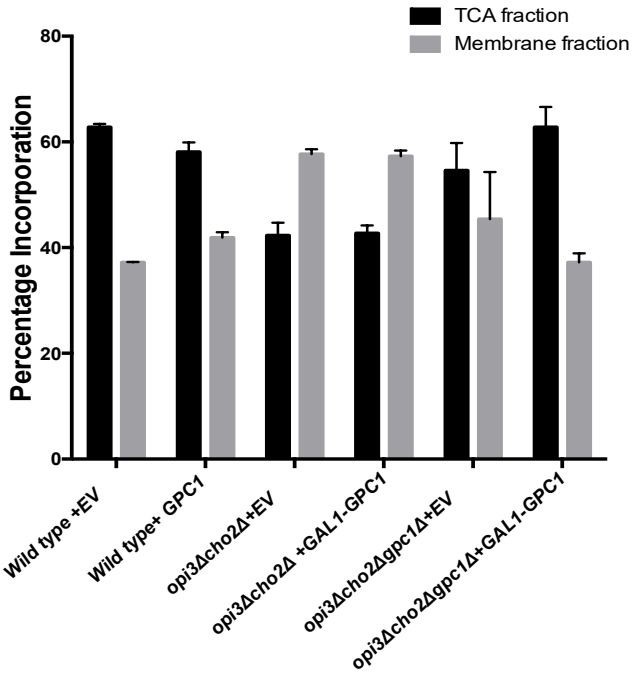

A. 3. Examination of ^{3}H-GPC flux in methylation pathway mutant, *opi3*Δ *cho2*Δ.
WT, *opi3*Δ *cho2*Δ and *opi3*Δ *cho2*Δ *gpc1*Δ containing EV or *Gal1-GPC1* were used in this study. Cultures were pregrown in synthetic medium containing 100 μM choline. Cultures were restarted to log phase in synthetic medium lacking uracil, inositol and choline, and containing 2% galactose, 200 μM ^{3}H-GPC, and 200 μM KH_2PO_4. The experiment was performed similarly to as described in Fig A. 2. The *opi3Δ cho2Δ* resulted in decreased intracellular fraction and an increased membrane fraction when compared to the WT. This result suggests that ^{3}H-GPC was used for PC synthesis either through *GPC1* or through the Kennedy pathway. The fact that loss of *GPC1* in *opi3*Δ *cho2*Δ results in a decreased flux of ^{3}H-GPC to ^{3}H-PC suggest that the *GPC1* was a key player in for PC synthesis upon disruption of methylation pathway. However, the results for *opi3*Δ *cho2*Δ *gpc1*Δ and WT do not look similar, and this suggests that a portion of ^{3}H(choline) -GPC was hydrolyzed to ^{3}H-choline for PC synthesis via the Kennedy pathway. As upon overexpression of *GPC1* in *opi3*Δ *cho2*Δ *gpc1*Δ did not result in in increased membrane incorporation, this strain was not pursued for further metabolic studies. Experiments were performed in 3 biological replicates.

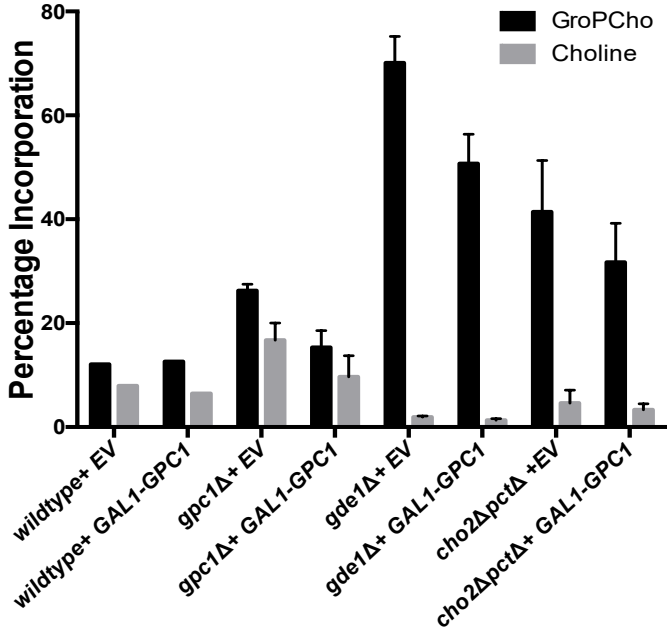

A. 4. Examining the intracellular metabolites in various mutants.
The growth condition, media and the labeling approach were similar as described in Fig A. 2. The water-soluble choline-containing metabolites were separated using anion exchange chromatography as described in [88]. The intracellular fractions were diluted 5-fold in deionized H_2O, applied to a 250 µl Dowex 50Wx8 200-400 cation exchange column. [^{3}H] GPC was eluted with a 1 ml and 2 ml H_2O washes. If present, [^{3}H] choline phosphate was eluted with a subsequent 3 ml H_2O wash. [^{3}H] choline was eluted with 5 ml HCl wash. Standards were used to verify the separation procedure and label incorporated into each metabolite was quantified using liquid scintillation counting. In almost all the strains, most of the water-soluble label was detected as GPC. Upon overexpression of *GPC1* in all strains, there was a significant decrease in GPC fraction, suggesting that it is used in PC synthesis. The experiments were performed in biological triplicate.

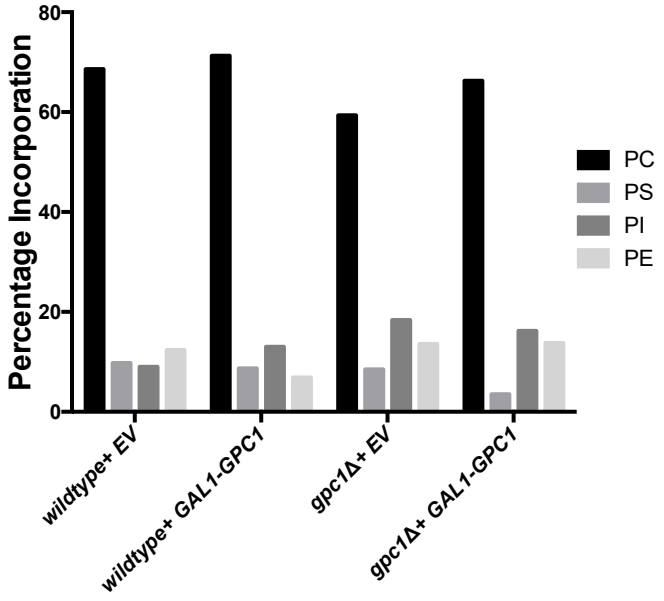

A. 5. A ^{32}P labeling to investigate the impact of Gpc1 on total PC content.

WT (BY4742) and *gpc1Δ* strains containing either empty vector (pYES 2.1) or *GAL1-GPC1 (*pYES 2.1-*YGR149w)* were employed. Cultures were maintained aerobically at 30°C in yeast nitrogen base (YNB) with 2% galactose and amino acids as described in [87], but lacking uracil to maintain the plasmids. The medium lacked inositol and contained a normal KH_2PO_4 level (7 mM). For labeling experiments, the medium was supplemented with 5 μCi/ ml of ^{32}P (inorganic phosphate) and grown to log phase before harvesting. Phospholipids were isolated using the lipid extraction protocol described in [88]. Various control strains were used as markers to identify the four major types of phospholipids pertaining to our study (PC, PS, PI, PE). Normal silica gel TLC plates were used in this study. The mobile phase that was used for the separation of phospholipids is chloroform:ethanol:water:triethylamine (30:35:7:35). The ^{32}P screen was exposed for two hours before imaging in Typhoon scanner 8600. Image Quant software was used to quantify the phospholipid spots. Unlike following radiolabeled [^{3}H]GPC incorporation, P^{32} incorporation adds label to all phospholipids. The preliminary results suggest that the GPC acylation pathway does have a small impact on the total PC level. Overall, this experiment shows that the novel pathway is not responsible for the bulk synthesis of PC. This will need to be repeated with replicates to obtain a statistical significance to the generated data.

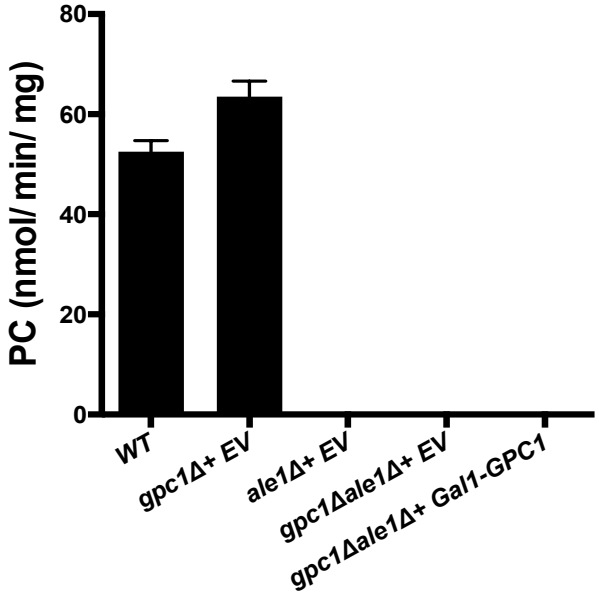

A. 6. Gpc1 lacks LPC acyltransferase activity *in vitro.*

Microsomes from *WT, ale1Δ and ale1Δ gpc1Δ* EV or *GAL1-GPC1* were used in this study. Microsomal membranes were prepared as described in [50]. Microsomal membranes corresponding to 20 µg total protein were incubated together with 10nmol 18:1- LPC, 10 nmol [14C]18:1-CoA and 0.1M phosphate buffer, pH7.2, in a total volume of 50µl at 30°C with shaking. LPC were added to the assay dissolved in phosphate buffer. The microsomal assays were terminated after 4 minutes by addition of 170 µl of 0.15M acetic acid and 500 µl of CHCl3:MeOH (1:1, v/v) and vortexed. After centrifugation the chloroform phase was transferred to a new tube and an aliquot was taken to liquid scintillation counting of the radioactivity. The remaining chloroform was applied on a TLC plate (Silica 60, Merck) and developed in CHCl3:MeOH:HAc:H2O (85:15:10:3.5 v/v/v/v). Radiolabelled lipids were identified by Rf values of authentic standards, and the relative amount of radioactivity in each spot was determined by Instant Imager (Canberra Packard Instrument Co.) electronic autoradiograph. Absolute amounts of radioactivity in each spot were calculated from the total amount of radioactivity in the chloroform phase as determined by liquid scintillation. Microsomes were incubated with LPC and [^{14}C]18:1-CoA . Lipid samples were then separated and detected using TLC and Typoon scanner respectively. Data represent 3 independent cultures +/- SD. This experiment was performed by Dr. Ida Lager.

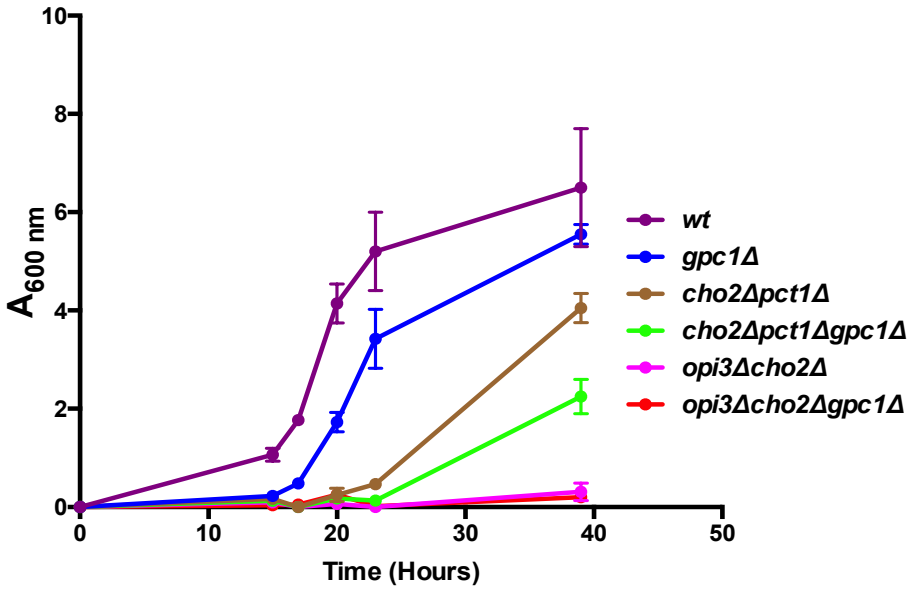

A.7. Loss of *GPC1* affects growth in synthetic medium lacking inositol.
The WT, *gpc1*Δ, *cho2*Δ *pct1*Δ, *cho2*Δ *pct1*Δ *gpc1*Δ, *opi3*Δ *cho2*Δ, and *opi3*Δ *cho2*Δ *gpc1*Δ were used in this study. Start-up cultures were grown in synthetic medium lacking inositol and choline. Cultures were restarted in 350 µl of fresh medium at 0.005 ODU's in a 48 well plate. Growth was monitored at $A_{600\ nm}$ for 40 hours using spectramax plate reader using the end program. Loss of *GPC1* resulted in a slower growth as compared to the WT strain. The *cho2*Δ *pct1*Δ strain grows slower than the WT due to the attenuation in the major pathways for PC synthesis. Also, the triple deletion (*cho2*Δ *pct1*Δ *gpc1*Δ) worsened the growth defeats. Finally, as expected the *opi3*Δ *cho2*Δ and *opi3*Δ *cho2*Δ *gpc1*Δ mutants slowed a severe growth defect in medium lacking inositol and choline.

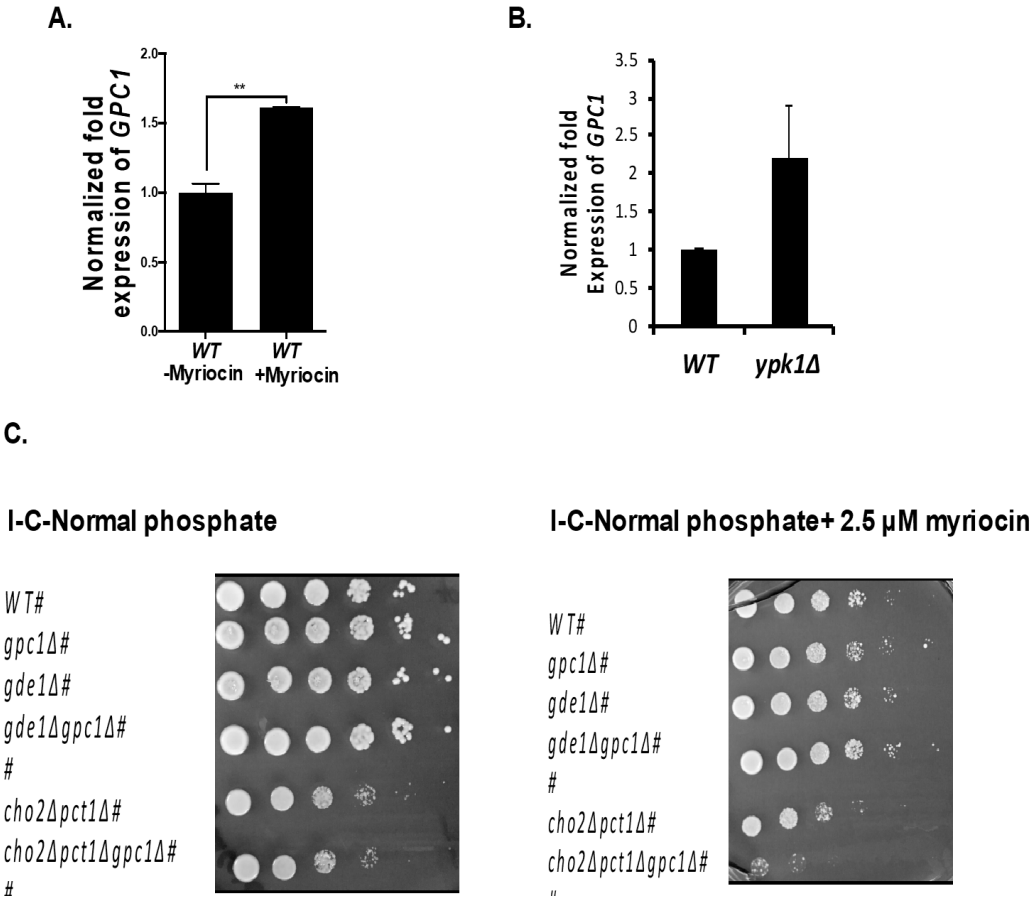

A. 8. Inhibition of sphingolipid biosynthesis affects *GPC1* expression and impacts growth: A, B. The indicated strains were grown to log phase, cells were harvested, and RNA was extracted. The *Gpc1* transcript were quantified using qRT-PCR. To inhibit sphingolipid biosynthesis, we employed myriocin at a concentration of 2.5 µM, which inhibits the serine palmitoyltransferase, Lcb1 [132]. Similarly, treatment of cells with myriocin resulted in a roughly 50% increase in *GPC1* message (Fig. A. 8. A). Similar upregulation of *GPC1* transcript were seen in the *ypk1*Δ mutant that is known to have perturbation with sphingolipid synthesis. C. Strains were cultured in synthetic medium. 10-fold serial dilutions were spotted onto plates containing (2.5 µM) or lacking myriocin. These plates have been repeated twice in biological replicates.

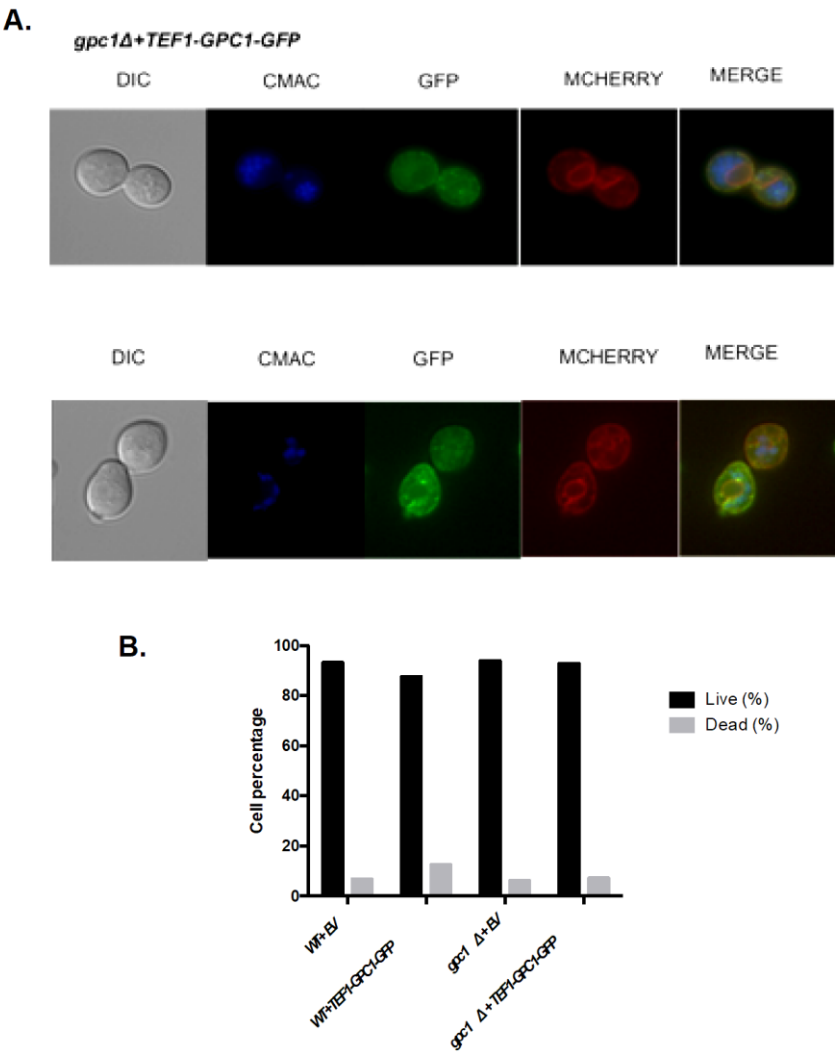

A. 9. Gpc1 is predominantly localized to ER and vacuoles.
A. Cultures were maintained in synthetic medium lacking inositol. Start-up cultures were started in synthetic medium lacking both inositol and choline, next day, cultures were diluted back to 0.2 ODU and allowed to grow for 3 hours before the microscopy. The CMAC dye and Sec61-MCHERRY plasmid were the markers for vacuoles and ER, respectively. I was able to determine the localization of Gpc1 in *gpc1*Δ containing the *TEF1-GPC1-GFP* plasmid but was unable to be determined it in WT strain containing *TEF1-GPC1-GFP*. We found that upon overexpression of *GPC1* there was an increase in cell death in WT strain. Gpc1 was found to be localized predominantly at the ER. B. Cultures were maintained in synthetic medium lacking inositol. Cell viability was determined using trypan blue assay. The WT containing *TEF1-GPC1-GFP* showed a 2-fold increase in cell death when compared to *WT+EV*.

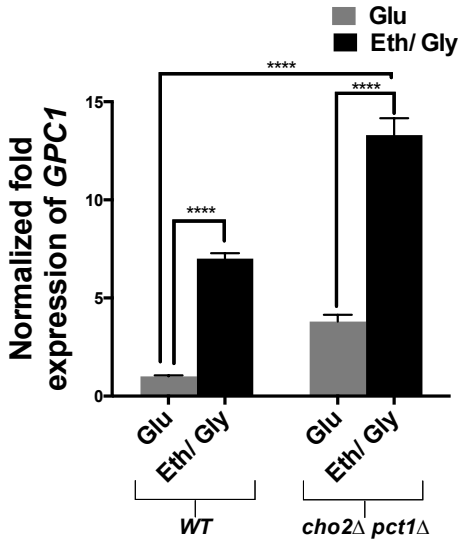

A. 10. *GPC1* expression is upregulated by non-fermentative carbon source and in a *cho2*Δ *pct1*Δ mutant.

The WT and *cho2*Δ *pct1*Δ strains were employed in this study. Cultures were maintained aerobically at 30°C with shaking or on a roller drum. Media used in this study were Yeast nitrogen base (YNB) with 2% ethanol/2% glycerol or 2% glucose and amino acid composition as described in [87]. Cultures were grown to log, harvested and RNA was extracted. *GPC1* transcripts were quantified using qRT-PCR. Upon the utilization of ethanol/ glycerol as the carbon source, the *GPC1* expression increased more than 7-fold in WT strain. The expression for *GPC1* in *cho2*Δ *pct1*Δ is 3-fold higher to the WT when growth in medium containing glucose, but this effect was elevated to 13-folds upon switching the carbon source from glucose to ethanol/ glycerol. Data represent an average of 3 independent cultures ± SD. A t-test was performed to determine significance as indicated (*p-value ≤ 0.0005).

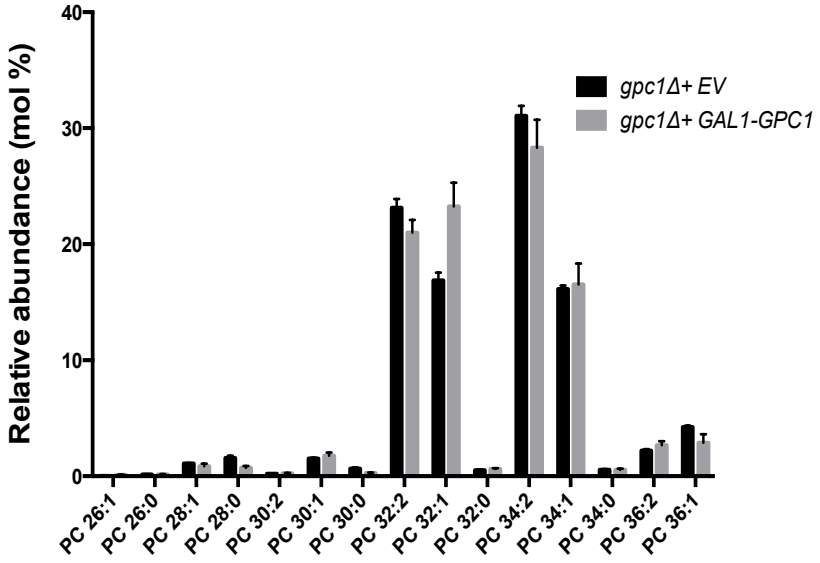

A. 11. Overexpression of *GPC1* increases monounsaturated PC species at the expense of diunsaturated PC species.

The indicated strains were grown to log phase, cultures were harvested, and lipids were extracted. PC species were separated and analyzed as described in methods of chapter 3. Our earlier finding suggested that the loss of *GPC1* resulted in decreased monounsaturated PC species at the expense of diunsaturated PC species. To confirm this finding, we repeated the experiment by overexpressing *GPC1* in *gpc1Δ.* The overexpressing of *GPC1* in *gpc1Δ* strain resulted in increased monounsaturated PC species at the expense of diunsaturated PC species. Similar overexpression data was obtained in a WT strain that was used for the publication (Chapter 3). Data are average of 3 independent cultures ± SD.

Experiments A. 12 and A. 13 were performed as a collaborative project with Dr. Todd Reynolds. This data is also in reference [134]

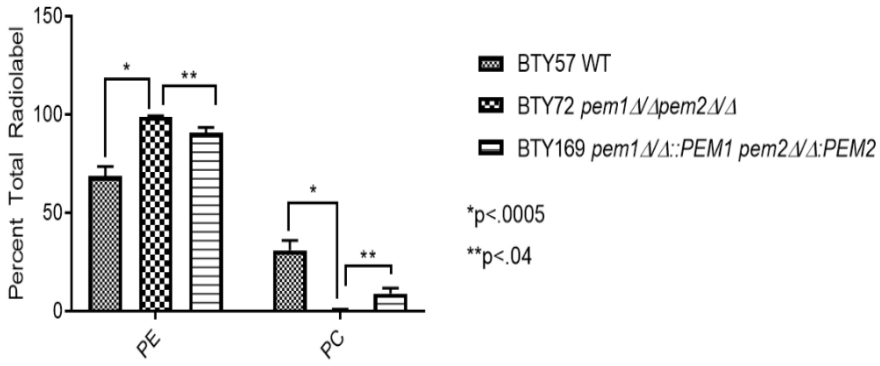

A. 12. The *pem1Δ/Δ pem2Δ/Δ* mutant fails to produce PC via the CDP-DAG pathway.

BTY57 (WT SC5314), PEM1Δ/Δ PEM2Δ/Δ, and *PEM1Δ/Δ::PEM1 PEM2Δ/Δ::PEM2* strains were employed in this study. Cultures were maintained aerobically at 30°C in yeast nitrogen base (YNB) containing 2% glucose and lacking amino acids as strains were prototrophic. For labeling experiments, medium was supplemented with 100 μM of choline, 5 μM of ethanolamine and 0.1μCi/ml of ^{14}C ethanolamine (Cat. no ARC3845). See strain table in publication. Cultures were grown to logarithmic phase, and 20 ODU's of cells were harvested and the cell pellets were treated with 5% trichloroacetic acid (TCA) for 20 min on ice. The supernatant was discarded, and cell pellets were incubated at 60°C for 60 minutes with 1 ml of ESOAK (95% ethanol, diethylether, H_2O, pyridine, NH_4OH (28-30%); 15:5:15:1:0.036 v/v/v/v). The tubes were centrifuged to pellet the debris and 1 ml of lipid-containing supernatant were transferred to fresh tubes containing 1 ml of chloroform/methanol (2:1) and 0.25 ml of 0.1 M HCl. Following vortexing and low speed centrifugation, the bottom layers containing glycerophospholipids were dried under N_2. Lipids were then suspended in chloroform/methanol (2:1). Lipids representing equivalent amounts (approximately 1.5 ODU's) were spotted onto the Silica Gel TLC Plates (Whatman, Millipore Sigma 105626). The mobile phase that was used for the separation of phospholipids was chloroform: ethanol: water: triethylamine (30:35:7:35). TLC plates were imaged using a Typoon scanner 8600. Image Quant software was used to quantify the regions of intensity (ROI) for PE. The experiment was performed in biological triplicates and was repeated to confirm the results. The *pem1Δ/Δ pem2Δ/Δ* mutant shows the expected buildup of radiolabeled ethanolamine in PE, but not in PC. Reintegration of single copy of *PEM1* and *PEM2* in *pem1Δ/Δ pem2Δ/Δ* mutant resulted in an increase in PC synthesis. The [^{14}C] ethanolamine labelling experiment was performed to confirm that the knockout strains, *pem1Δ/Δ pem2Δ/Δ* and *ept1Δ/Δ,* display disrupted PC and PE biosynthesis, respectively. Pem1 and Pem2 have phosphatidylethanolamine methyltransferase activity that are required for conversion of PE to PC via the methylation pathway. Loss of these genes resulted in disruption of the methylation pathway, and in turn resulted in decreased PC synthesis. An unpaired *t*-test was performed. P-values as denoted.

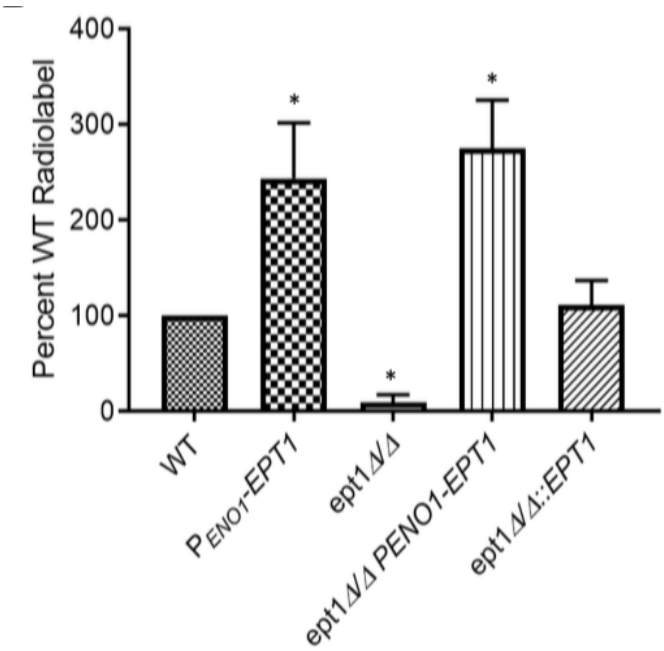

A. 13. Loss of *EPT1* results in diminished PE synthesis.

Cultures were grown to log phase in minimal medium containing [^{14}C] ethanolamine. Phospholipids were extracted and analyzed as described in (A. 12). Incorporation of the radiolabel into PE were quantified. Loss of *EPT1* resulted in no or minimal incorporation of [^{14}C] ethanolamine to PE, and the reintegrated *ept1*Δ/Δ::*EPT1* showed PE incorporation similar to that of *WT.* The overexpresser *ept1*Δ/*ΔPENO1-EPT1* and P_{eno1}-*EPT1* resulted in greater PE synthesis when compared to *WT*. Ept1 has ethanolamine phosphotransferase activity that is crucial in the CDP-ethanolamine pathway for PE synthesis. Loss of *EPT1* resulted in blocked CDP-ethanolamine pathway, and, in turn, resulted in decreased PE synthesis Experiment was performed in biological triplicates. An unpaired *t*-test was performed (*p< 02).

Figure A.14- A.16 represent data for a collaborative project with Dr. Allyson O'Donnell. Some or all the data will be included in a manuscript that is in preparation.

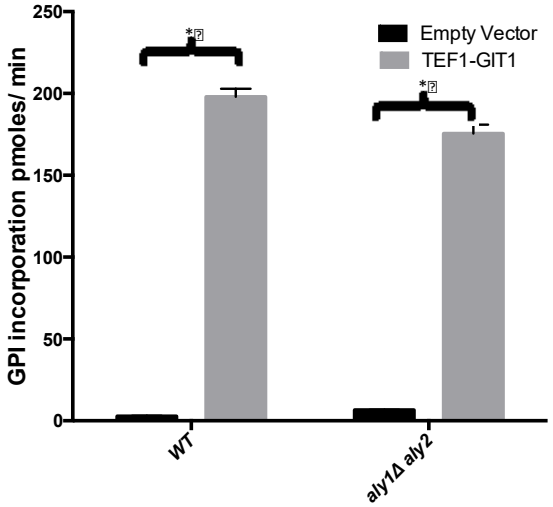

A. 14. [^{3}H]GPI transport assays confirms the function of the overexpression construct.

WT and *aly1Δ aly2Δ* with/ without the empty vector or *TEF1-GIT1-GFP* plasmid were used in this study. Cultures were grown aerobically at 30°C in synthetic medium lacking inositol and choline and containing 10mM inorganic phosphate (high phosphate) to logarithmic phase. In brief, cells were washed with water and resuspended in 100 mM citrate buffer, pH 5 to A_{600} = 5. The assays were initiated by adding 50 µL of 25 µM of [^{3}H]GPI to 200 µL of cell suspension). After 5 minutes of incubation at 30°C, the assays were stopped by the addition of ice-cold DI H_2O. Samples were filtered over Whatman GFC filters (Whatman number 1822-025). Filters were washed with 10 ml of ice cold DI H_2O before suspending in 10 ml of scintillation fluid for counting using liquid scintillation counter [76]. The *TEF1-GIT1* construct resulted in a massive increase in the transport of GPI in both WT and *aly1Δ aly2Δ* strains (grey bars). Experiments were performed in biological triplicate, and a t-test was performed to determine the significance. P-value ≤ 0.0001.

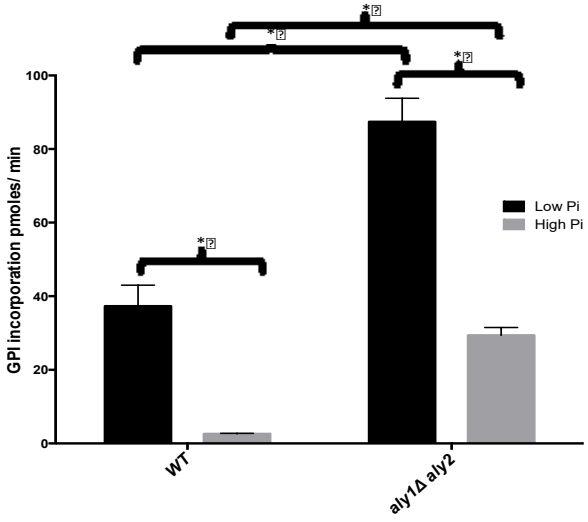

A. 15. Loss of *ALY1* and *ALY2* results in an increase in the GPI transport in both low and high phosphate medium.

Transport assays were performed over 5 min of uptake in *WT* and *aly1Δ aly2Δ* strains. Cultures were grown overnight at 30°C in synthetic medium lacking inositol and choline supplemented and containing 200 µM inorganic phosphate (low phosphate). The following day, single cultures were used to reinoculate two fresh cultures containing either 100 µM (low) or 10 mM (high) levels of inorganic phosphate at an A_{600} of 0.2. All cultures were grown to an A_{600} of 0.5 at which point they were harvested and assayed for transport activity. *WT* (BY4741) and *aly1Δ aly2Δ* cultures (biological triplicates) were grown aerobically overnight at 30°C in yeast nitrogen base (YNB) medium altered to lack inositol, contain a low level of KH_2PO_4 (200 µM), and to contain 2% glucose. Amino acid concentrations were as described [87]. The medium lacked inositol (I-) and contained a low KH_2PO_4 level to induce expression of the *GIT1* transporter for GPI uptake. The overnight cultures were diluted to log phase in fresh medium containing a high level of KH_2PO_4 (10 mM P_i) and allowed to double. To begin labeling, 4 ml cultures normalized to OD_{600} =0.2 were spiked with 5µM [^{3}H]GPI (100,00 cpm/ml). The cultures were harvested following aerobic growth at 30°C for 5 hours (OD_{600} range of 1.3-1.5). A membrane fraction, a TCA-extractable intracellular fraction and an extracellular fraction were isolated as described previously [88]. The percentages of radioactive counts in each fraction were determined using a liquid scintillation counter. Lipids were extracted from the membrane fraction and separated by TLC. Radioactive (American Radiolabeled Chemicals Inc.) and nonradioactive (Avanti Polar Lipid) phosphatidylinositol (PI) standards were used to verify the migration of PI on the TLC plate. Tritium labeled GPI ([^{3}H]inositol-GPI) was produced through the deacylation of phosphatidyl[^{3}H]myo-inositol, as described in chapter 2. *aly1Δ aly2Δ* showed an increase in GPI incorporation in both low and high phosphate condition, when compared to the *WT*. Experiments were performed in biological triplicate, and a t-test was performed to determine the significance. P-value ≤ 0.0001.

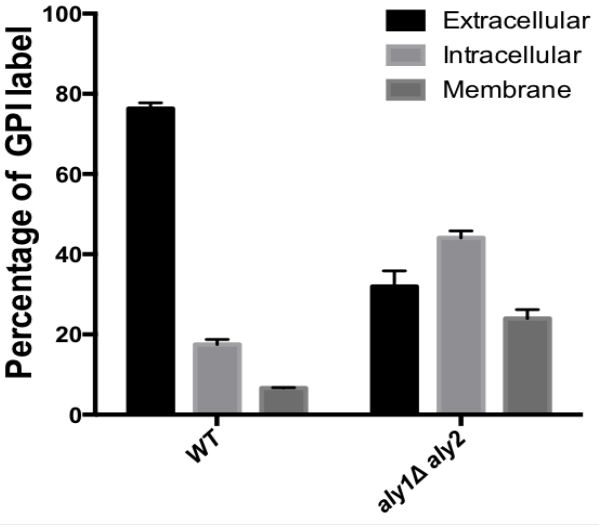

A. 16. *aly1Δaly2Δ* mutant exhibits an increased incorporation of radiolabel into membrane fraction compared to WT.

WT (BY4741) and *aly1Δ aly2Δ* cultures were grown aerobically overnight at 30°C in yeast nitrogen base (YNB) medium altered to lack inositol, contain a low level of KH_2PO_4 (200 μM), and to contain 2% glucose. Amino acid concentrations were as described [88]. The medium lacked inositol (I-) and contained a low KH_2PO_4 level to induce expression of the *GIT1* transporter for GPI uptake. The overnight cultures were diluted to log phase in fresh medium containing a high level of KH_2PO_4 (10 mM P_i) and allowed to double. To begin labeling, 4 ml cultures normalized to OD_{600} =0.2 were spiked with 5μM [^{3}H]GPI (100,00 cpm/ml). The cultures were harvested following aerobic growth at 30°C for 5 hours (OD_{600} range of 1.3-1.5). A membrane fraction, a TCA-extractable intracellular fraction and an extracellular fraction were isolated as described in chapter 2. The percentages of radioactive counts in each fraction were determined using a liquid scintillation counter. Lipids were extracted from the membrane fraction and separated by TLC. Radioactive (American Radiolabeled Chemicals Inc.) and nonradioactive (Avanti Polar Lipid) phosphatidylinositol (PI) standards were used to verify the migration of PI on the TLC plate. The transport data indicate *aly1Δ aly2Δ* mutants display increased Git1 transport activity. Since the inositol moiety of the Git1 substrate, GPI, is used for the synthesis phosphatidylinositol (PI), we wished to examine how loss of Aly and Aly2 would impact the flux of label from exogenously supplied ^{3}H-GPI to ^{3}H-PI in the absence of *GIT1* overexpression. Thus, cells were first grown under low phosphate conditions to induce expression of *GIT1*. For the labelling period, cells were shifted to high phosphate conditions, where *GIT1* expression is transcriptionally and posttranscriptionally, downregulated. As shown in A. 15, an *aly1Δ aly2Δ* mutant incorporates a greater percentage of label form exogenous GPI into the cell as both a TCA-extractable (water-soluble) fraction and into a particulate membrane fraction as compared to wild type over the labeling period. Consistent with this, roughly 2.5 more ^{3}H-PI was found in *aly1Δaly2Δ* as compared to wild type when lipids were extracted from the membrane fractions and resolved by TLC. This result is consistent with increased stability, and hence activity, of Git1 at the plasma membrane of *aly1Δ aly2Δ* cells during the labeling period. It's important to note that the PI detected is not a measure of total PI, but the [^{3}H]PI derived from exogenously supplied [^{3}H]GPI. Data represent average ± SD of three individual cultures (biological triplicates).

Common Strain table

	Strain	Genotype	Reference
JPV 399	WT, BY4742	BY4742; *MATα his3Δ1 leu2Δ0 lys2Δ0 ura3Δ0*	Research Genetics
JPV 788	*gpc1*Δ	BY4742; *gpc1::KanMX*	This study
JPV 125	*gde1*Δ	BY4742; *gde1::KanMX*	This study
JPV 834	*gde1*Δ *gpc1*Δ	JPV 125; *gpc1::URA3*	This study
JPV 272	*cho2*Δ *pct1*Δ	BY4742; *cho2:: KanMX pct1::LEU2*	This study
JPV 839	*cho2*Δ *pct1*Δ *gpc1*Δ	JPV 272; *gpc1::URA3*	This study
JPV 271	*opi3*Δ *cho2*Δ	BY4742; *cho2:: KanMX opi3::LEU2*	Strain database
JPV 828	*opi3*Δ *cho2*Δ *gpc1*Δ	BY4742; *cho2:: KanMX opi3::LEU2 gpc1::HPHmx*	Strain database
JPV 841	*pct1*Δ *gpc1*Δ	JPV 788; *pct1::LEU2*	This study
JPV 269	*cho2*Δ	BY4742; *cho2::KanMX*	Research Genetics
JPV680	*plb1*Δ *plb2* Δ*plb3* Δ *nte1* Δ	*his3Δ1 leu2Δ0 met15Δ0 ura3Δ0 plb1::hph,plb2::KanMX,plb3::nat,nte1::*ble*1*	Strain Database
JPV 827	*plb1*Δ *plb2* Δ*plb3* Δ *nte1* Δ *gpc1* Δ	*his3Δ1 leu2Δ0 met15Δ0 ura3Δ0 plb1::hph,plb2::KanMX,plb3::nat,nte1::ble1, gpc1::LEU2*	Strain database
JPV 270	*pct1*Δ	BY4742; *pct1::LEU2*	Research Genetics
JPV 832	*ale1*Δ	*Mat* ***a:*** *his3Δ1 leu2Δ0 met15Δ0 ura3Δ0 ale1::KANMX*	[52]
JPV 833	*ale1*Δ *gpc1*Δ	JPV 832; *gpc1::KANMX*	[52]
JPV 846	*WT+GPC1-3xHA*	BY4742; *GPC1-3xHA*	This study

References

1. Duina, A. A., Miller, M. E., and Keeney, J. B. (2014). Budding yeast for budding geneticists: A primer on the *Saccharomyces cerevisiae* Model System. *Genetics 197*: 33-48.
2. Breslow, D.K. and Weissman, J.S. (2010). Membranes in balance: mechanisms of sphingolipid homeostasis. *Molecular Cell. 40*: 267-279.
3. Covino, R., Ballweg, S., Stordeur, C., Michaelis, J.B., Puth, K., Wernig, F., …Ernst R (2016). A eukaryotic sensor for membrane lipid saturation. *Molecular Cell. 63*: 49-59.
4. Panaretou, B. and P. (2006). Piper, isolation of yeast plasma membranes. *Methods in molecular biology. 313*: 27-32.
5. Henry, S.A., Kohlwein, S.D., and Carman, G. M. (2012). Metabolism and regulation of glycerolipids in the yeast *Saccharomyces cerevisiae*. *Genetics. 190*, 317-349.
6. Klug, L. and Daum, G. (2014). Yeast lipid metabolism at a glance. *FEMS Yeast Research*. *14*: 369-388.
7. Patton, J.L. and Lester, R.L. (1991). The phosphoinositol sphingolipids of *Saccharomyces cerevisiae* are highly localized in the plasma membrane. *Journal of Bacteriology. 173*: 3101-3108.
8. Dickson, R.C., Nagiec, E.E., Wells, G.B., Nagiec M. M., and Lester, R. L. (1997). Synthesis of mannose-(inositol-P)2-ceramide, the major sphingolipid in *Saccharomyces cerevisiae*, requires the *IPT1* (YDR072c) gene. *The Journal of Biological Chemistry. 272*: 29620-2965.
9. Strahl, T. and Thorner, J. (2007). Synthesis and function of membrane phosphoinositides in budding yeast, *Saccharomyces cerevisiae*. *Biochimica et Biophysica Acta. 1771*: 353-404.
10. Schneiter, R., Brügger, B., Sandhoff, R., Zellnig, G., Leber, A., Lampl, M., . . . Kohlwein, S. D. (1999). Electrospray ionization tandem mass spectrometry (ESI-MS/MS) analysis of the lipid molecular species composition of yeast subcellular membranes reveals acyl chain-based sorting/remodeling of distinct molecular species en route to the plasma membrane. *Journal of Cell Biology. 146*: 741-754.
11. Chen, M., Hancock, L.C., and Lopes, J.M. (2007). Transcriptional regulation of yeast phospholipid biosynthetic genes. *Biochimica et Biophysica Acta. 1771*: 310-321.
12. Carman, G.M. and Han, G.S. (2009). Regulation of phospholipid synthesis in yeast. *Journal of Lipid Research. 50*: 69-73.
13. Rajakumari, S., Grillitsch, K., and Daum, G. (2008). Synthesis and turnover of non-polar lipids in yeast. *Progress in Lipid Research. 47*: 157-171.
14. Kurat, C.F., Wolinski, H., Petschnigg, J., Kaluarachchi, S., Andrews, B., Natter, K., and Kohlwein, S. D. (2009). Cdk1/Cdc28-dependent activation of the major triacylglycerol lipase Tgl4 in yeast links lipolysis to cell-cycle progression. *Molecular Cell. 33*: 53-63.
15. Petschnigg, J., Wolinski, H., Kolb., D., Zelinig., G., Kurat, C. F., Natter, K., Kohlwein, S.D. (2009). Good fat, essential cellular requirements for triacylglycerol synthesis to maintain membrane homeostasis in yeast. *The Journal of Biological Chemistry. 284*: 30981-30993.
16. Henry, S.A. and Patton-Vogt, J.L (1998). Genetic regulation of phospholipid metabolism: yeast as a model eukaryote. *Progress in Nucleic Acid Research and Molecular Biology. 61*: 133-179.
17. Nikawa, J., Kodaki, T., and Yamashita, S. (1987). Primary structure and disruption of the phosphatidylinositol synthase gene of *Saccharomyces cerevisiae*. *The Journal of Biochemistry. 262*: 4876-4881.

18. Baile, M.G., Lu, Y.W., and Claypool, S.M. (2014). The topology and regulation of cardiolipin biosynthesis and remodeling in yeast. *Chemistry and Physics of Lipids. 179*: 25-31.
19. Kodaki, T. and Yamashita, S. (1987). Yeast phosphatidylethanolamine methylation pathway. Cloning and characterization of two distinct methyltransferase genes. *The Journal of Biochemistry. 262*: 15428-15435.
20. Gaspar, M.L, Aregullin, M. A., Jesch, S. A., and Henry, S. A. (2006). Inositol induces a profound alteration in the pattern and rate of synthesis and turnover of membrane lipids in *Saccharomyces cerevisiae*. *The Journal of Biological Chemistry. 281*: 22773-22785.
21. Carman, G.M. and Han, G.S. (2011). Regulation of phospholipid synthesis in the yeast *Saccharomyces cerevisiae*. *Annual Review of Biochemistry. 80*: 859-883.
22. Henry, S.A., Gaspar, M.L., and Jesch, S.A. (2014). The response to inositol: regulation of glycerolipid metabolism and stress response signaling in yeast. *Chemistry and Physics of Lipids*. *180*: 23-43.
23. Eide, D.J. (2009). Homeostatic and adaptive responses to zinc deficiency in *Saccharomyces cerevisiae*. *The Journal of Biochemistry. 284*: 18565-18569.
24. Aloulou, A., YB, A., Bezzine, S., Gargouri, Y., and Gelb, M. H. (2012). Phospholipases: an overview. *Methods in Molecular Biology. 861*: 63-85.
25. Patton-Vogt, J. (2007). Transport and metabolism of glycerophosphodiesters produced through phospholipid deacylation. *Biochimica et Biophysica Acta.*, *1771*: 337-342.
26. Lee, K.S., Patton, J. L., Fido, M., Hines, L. K., Kohlwein, S.D., Paltauf, F., …Levin, D. E. (1994). The *Saccharomyces cerevisiae PLB1* gene encodes a protein required for lysophospholipase and phospholipase B activity. *The Journal of Biological Chemistry. 269*: 19725-19730.
27. Merkel, O., Fido, M., Mayr, J. A., Pruger, H., Raab, F., Kohlwein, S.D and Paltauf, F. (1999). Characterization and function *in vivo* of two novel phospholipases B/lysophospholipases from *Saccharomyces cerevisiae*. *The Journal of Biological Chemistry. 274*: 28121-28127.
28. Fernandez-Murray, J.P., Gaspard, G., Jesch, S. A., and McMaster, C. R. (2009). *NTE1*-encoded phosphatidylcholine phospholipase b regulates transcription of phospholipid biosynthetic genes. *The Journal of Biological Chemistry. 284*: 36034-36046.
29. Almaguer, C., Fisher, E., and Patton-Vogt, J. (2006). Posttranscriptional regulation of Git1p, the glycerophosphoinositol/glycerophosphocholine transporter of *Saccharomyces cerevisiae*. *Current Genomics. 50*: 367-375.
30. Patton-Vogt, J.L. and Henry, S.A. (1998). *GIT1,* a gene encoding a novel transporter for glycerophosphoinositol in *Saccharomyces cerevisiae. Genetics. 149*: 1707-1715.
31. Fisher, E., Almaguer, C., Holic, R., Griac, P., and Patton-Vogt, J. (2005). Glycerophosphocholine-dependent growth requires Gde1p (YPL110c) and Git1p in *Saccharomyces cerevisiae*. *The Journal of Biological Chemistry*. *280*: 36110-36117.
32. Zheng, B., Berrie, C., Corda, D., and Farquhar, M. (2003). *GDE1*/MIR16 is a glycerophosphoinositol phosphodiesterase regulated by stimulation of G protein-coupled receptors. *Proceedings of the National Academy of Sciences of the United States of America. 100*: 1745-1750.
33. Yamashita, A., Hayashi, Y., Ito, M., Oka, S., Tanikawa, T., …Sugiura, T. (2014). Acyltransferases and transacylases that determine the fatty acid composition of

glycerolipids and the metabolism of bioactive lipid mediators in mammalian cells and model organisms. *Progress in Lipid Research. 53*: 18-81.

34. Smart, H.C., Mast, F. D., Chilije, M. F., Tavassoli, M., Dacks, J. B., and Zaremberg, V. (2014). Phylogenetic analysis of glycerol 3-phosphate acyltransferases in opisthokonts reveals unexpected ancestral complexity and novel modern biosynthetic components. *PLoS One. 9*: e110684.
35. Martin, C.E., Oh, C.S., and Jiang, Y. (2007). Regulation of long chain unsaturated fatty acid synthesis in yeast. *Biochimica et Biophysica Acta*. *1771*: 271-285.
36. De Smet, C.H., Vittone, E., Scherer, M., Houweling, M., Liebisch, G., Brouwers J. F., de Kroon, A.,I. (2012). The yeast acyltransferase Sct1p regulates fatty acid desaturation by competing with the desaturase Ole1p. *Molecular Biology of the Cell. 23*: 1146-1156.
37. Jasieniecka-Gazarkiewicz, K., Demski, K., Lager, I., Stymne, S., and Banas, A. (2016). Possible role of different yeast and plant lysophospholipid:acyl-CoA acyltransferases (LPLATs) in acyl remodelling of phospholipids. *Lipids. 51*: 15-23.
38. Renne, M.F., Bao, X., Smet, C.H., and de Kroon, A. (2015). Lipid acyl chain remodeling in yeast. *Lipid Insights. 8*: 33-40.
39. Riekhof, W.R., Gijón, M.A., Zarini, S., Murphy, R.C., and Voelker, D.R. (2007). Lysophosphatidylcholine metabolism in *Saccharomyces cerevisiae*: the role of P-type ATPases in transport and a broad specificity acyltransferase in acylation. *The Journal of Biological Chemistry. 282*: 36853-36861.
40. Riekhof, W.R., James, W., Jones, J. L. and Voelker, D. R. (2007). Identification and characterization of the major lysophosphatidylethanolamine acyltransferase in *Saccharomyces cerevisiae. The Journal of Biological Chemistry. 282*: 28344-28352.
41. Chen, Q, Kazachkov, M., Zheng, Z., and Zou, J. (2007). The yeast acylglycerol acyltransferase *LCA1* is a key component of Lands cycle for phosphatidylcholine turnover. *FEBS Letters. 581*: 5511-5516.
42. Stahl, U., Stalberg, K., Stymne, S., and Ronne, H. (2008). A family of eukaryotic lysophospholipid acyltransferases with broad specificity. *FEBS Letters. 582*: 305-309.
43. Le Guedard, M., Bessoule, J.J., Boyer. V., Ayciriex. S., Velours. G., Kulik. W.,… Testet. E. (2009). *PSI1* is responsible for the stearic acid enrichment that is characteristic of phosphatidylinositol in yeast. *FEBS Journal. 276*: 6412-6424.
44. Joshi, A.S., Zhou, J., Gohil, V., Chen, S., and Greenberg, M. (2009). Cellular functions of cardiolipin in yeast. *Biochimica et Biophysica Acta*. *1793*: 212-218.
45. Claypool, S.M., McCaffery, J.M., and Koehler, C.M. (2006). Mitochondrial mislocalization and altered assembly of a cluster of Barth syndrome mutant tafazzins. *Journal of Cell Biology. 174*: 379-390.
46. Horvath, S.E., Wagner, A., Steyrer, E., and Daum, G. (2011). Metabolic link between phosphatidylethanolamine and triacylglycerol metabolism in the yeast *Saccharomyces cerevisiae*. *Biochimica et Biophysica Acta*. *1811*: 1030-1037.
47. Dahlqvist, A., Stahl. U., Lenman. M., Banas. A., Lee. M., Sandager. L.,… Stymne. S. (2000). Phospholipid:diacylglycerol acyltransferase: an enzyme that catalyzes the acyl-CoA-independent formation of triacylglycerol in yeast and plants. *Proceedings of the National Academy of Sciences of the United States of America*. *97*: 6487-6492.
48. Oelkers, P., Tinkelenberg, A., Erdeniz, N., Cromley, D., Billheimer, J.T., Sturley, S.L. (2000). A lecithin cholesterol acyltransferase-like gene mediates diacylglycerol esterification in yeast. *The Journal of Biological Chemistry. 275*: 15609-15612.

49. Stalberg, K., Neal A. C., Ronne, H., and Stahl, U. (2008). Identification of a novel GPCAT activity and a new pathway for phosphatidylcholine biosynthesis in *S. cerevisiae*. *Journal of Lipid Research. 49*: 1794-1806.
50. Lager, I., Glab, B., Chen, G., Banas, A., and Stymne, S. (2015). Novel reactions in acyl editing of phosphatidylcholine by lysophosphatidylcholine transacylase (LPCT) and acyl-CoA:glycerophosphocholine acyltransferase (GPCAT) activities in microsomal preparations of plant tissues. *Planta. 241*: 347-358.
51. Moser, R., Aktas, M., and Narberhaus, F. (2014). Phosphatidylcholine biosynthesis in *Xanthomonas campestris* via a yeast-like acylation pathway. *Molecular Microbiology. 91*: 736-750.
52. Glab, B., Beganovic, M., Anaokar, S., Hao, M.S., Rasmusson, A.G., Patton-Vogt, J., ...Lager, I. (2016). Cloning of Glycerophosphocholine Acyltransferase (GPCAT) from Fungi and Plants: a novel enzyme in phosphatidylcholine synthesis. *The Journal of Biological Chemistry. 291*: 25066-25076.
53. Kim, H., Melen, K., and von Heijne, G. (2003). Topology models for 37 *Saccharomyces cerevisiae* membrane proteins based on C-terminal reporter fusions and predictions. *The Journal of Biological Chemistry. 278*: 10208-10213.
54. Hishikawa, D., Hashidate, T., Shimizu, H., and Shindou, H. (2014). Diversity and function of membrane glycerophospholipids generated by the remodeling pathway in mammalian cells. *Journal of Lipid Research. 55*: 799-807.
55. Lands, W.E. (1960). Metabolism of glycerolipids. The enzymatic acylation of lysolecithin. *The Journal of Biological Chemistry. 235*: 2233-2237.
56. Okuyama, H., Yamada, K., and Ikezawa, H. (1975). Accepton concentration effect in the selectivity of acyl coenzyme A: U aclglycerylphosphorylcholine acyltransferase system in rat liver. *The Journal of Biological Chemistry. 250*: 1710-1713.
57. Wagner, S. and Paltauf, F. (1994). Generation of glycerophospholipid molecular species in the yeast *Saccharomyces cerevisiae*. Fatty acid pattern of phospholipid classes and selective acyl turnover at *sn-1* and *sn-2* positions. *Yeast. 10*: 1429-1437.
58. Tanaka, K., Fukuda, R., Ono, Y., Eguchi, H., Nagasawa, S., Nakatani, Y., …Ohta, A. (2008). Incorporation and remodeling of extracellular phosphatidylcholine with short acyl residues in *Saccharomyces cerevisiae*. *Biochimica et Biophysica Acta*. *1781*: 391-399.
59. Murphy, R.C. and Gaskell, S.J. (2011). New applications of mass spectrometry in lipid analysis. *The Journal of biological chemistry. 286*: 25427-25433.
60. De Smet, C.H., Cox, R., Brouwers, J.F., and de Kroon, A.I. (2013). Yeast cells accumulate excess endogenous palmitate in phosphatidylcholine by acyl chain remodeling involving the phospholipase B Plb1p. *Biochimica et Biophysica Acta*. *1831*: 1167-1176.
61. Renne, M.F. and de Kroon, A. (2017). The role of phospholipid molecular species in determining the physical properties of yeast membranes. *FEBS Letters. 592*: 1330-1345.
62. de Kroon, A.I., Rijken, P.J., and De Smet, C.H. (2013). Checks and balances in membrane phospholipid class and acyl chain homeostasis, the yeast perspective. *Progress in Lipid Reseasrch. 52*: 374-394.
63. Antonny, B., Vanni, S., Shindou, H., and Ferreira, T. (2015). From zero to six double bonds: phospholipid unsaturation and organelle function. *Trends in Cell Biology. 25*: 427-436.
64. Chen, X., Hyatt, B. A., Mucenski, M.L., Mason, R. J, and Shannon, J. M. (2006). Identification and characterization of a lysophosphatidylcholine acyltransferase in alveolar

type II cells. *Proceedings of the National Academy of Sciences of the United States of America*. *103*: 11724-11729.
65. Rong, X., Albert, C.J., Hong, C., Duerr, M.A., Chamberlain, B. T., Tarling, E. J.,… Tontonoz, P. (2013). LXRs regulate ER stress and inflammation through dynamic modulation of membrane phospholipid composition. *Cell Metabolism. 18*: 685-697.
66. Rong, X., Wang, B., Dunham, M. M., Hedde, P. N., Wong, J.S., Gratton, E., Tontonoz, P. (2015). Lpcat3-dependent production of arachidonoyl phospholipids is a key determinant of triglyceride secretion. *Elife. 4:* e06557.
67. Sohlenkamp, C. and Geiger, O. (2016). Bacterial membrane lipids: diversity in structures and pathways. *FEMS Microbiology Review. 40*: 133-159.
68. Jain, S., Caforio, A., and Driessen, A.J. (2014). Biosynthesis of archaeal membrane ether lipids. *Frontiers in Microbiology. 5*: 641.
69. Lagace, T.A. and Ridgway, N.D. (2013). The role of phospholipids in the biological activity and structure of the endoplasmic reticulum. *Biochimica et Biophysica Acta*. *1833*: 2499-2510.
70. Li-Beisson, Y., Shorrosh, B., Beisson, F., Andersson, M.X., Arondel, V., Bates, P.D., Ohirogge, J. (2013). Acyl-lipid metabolism. A*rabidopsis Book. 11*: e0161.
71. Cheng, L., Bucciarelli, B., Liu, J., Zinn, K., Miller, S., Patton-Vogt, J., … Vance, C.P. (2011). White lupin cluster root acclimation to phosphorus deficiency and root hair development involve unique glycerophosphodiester phosphodiesterases. *Plant Physiology. 156*: 1131-1148.
72. Dawson, R.M. (1955). The role of glycerylphosphorylcholine and glycerylphosphorylethanolamine in liver phospholipid metabolism. *The Journal of Biological Chemistry. 59*: 5-8.
73. Kennedy, E.P. and Weiss, S.B. (1956). The function of cytidine coenzymes in the biosynthesis of phospholipides. *The Journal of Biological Chemistry. 222*: 193-214.
74. Krogh, A., Larsson, B., Heijne, G., and Sonnhammer, E.L. (2001). Predicting transmembrane protein topology with a hidden Markov model: application to complete genomes. *Journal of Molecular Biology. 305*: 567-580.
75. Bafor, M., Smith, M.A., Stobart, K., and Stymne, S. (1991). Ricinoleic acid biosynthesis and triacylglycerol assembly in microsomal preparations from developing castor-bean (Ricinus communis) endosperm. *The Journal of Biological Chemistry. 280*: 507-514.
76. Almaguer, C., Cheng, W., Nolder, C., and Patton-Vogt, J. (2003) Glycerophosphoinositol, a novel phosphate source whose transport is regulated by multiple factors in Saccharomyces cerevisiae. *The Journal of Biological Chemistry. 279*: 31937-31942.
77. Siltberg-Liberles, J., Grahnen, J.A., and Liberles, D.A. (2011). The evolution of protein structures and structural ensembles under functional constraint. *Genes (Basel). 2*: 748-762.
78. Jones, A.M., Xuan, Y., Xu, M., Wang, R. S., Ho, C. H., Lalonde, S., …Frommer, W. B. (2014). Border control--a membrane-linked interactome of Arabidopsis. *Science. 344*: 711-716.
79. Chen, G., Woodfield, H. K., Pan, X., Harwood, J.L., and Weselake, R. J. (2015). Acyl-trafficking during plant oil accumulation. *Lipids. 50*: 1057-1068.
80. Liu, Y., Wang, G., and Wang, X. (2015). Role of aminoalcoholphosphotransferases 1 and 2 in phospholipid homeostasis in Arabidopsis. *Plant Cell. 27*: 1512-1528.
81. Bishop, A. C., Ganguly, S., Solis, N. V., Cooley, B. M., Jensen-Seaman, M. I., Filler, S. G.,...Patton-Vogt, J. (2013). Glycerophosphocholine utilization by *Candida albicans*: role

of the Git3 transporter in virulence. *The Journal of Biological Chemistry. 288*: 33939-33952.
82. Notari, L., Baladron, V., Aroca-Aguilar, J. D., Balko, N., Heredia, R., Meyer, C.,... Becerra, S. P. (2006). Identification of a lipase-linked cell membrane receptor for pigment epithelium-derived factor. *The Journal of Biological Chemistry. 281*: 38022-38037.
83. Guan, R., Lager, I., Li X., Stymne, S., and Zhu, L. H. (2014). Bottlenecks in erucic acid accumulation in genetically engineered ultrahigh erucic acid *Crambe abyssinica. Journal of Plant Biotechnology. 12*: 193-203.
84. Bligh, E.G. and Dyer, W.J. (1959). A rapid method of total lipid extraction and purification. *Canadian Journal of Biochemistry and Physiology. 37*: 911-917.
85. Notredame, C., Higgins, D.G., and Heringa, J. (2000). T-Coffee: A novel method for fast and accurate multiple sequence alignment. *Journal of Molecular Biology. 302*: 205-217.
86. Tamura, K. Stecher, G., Peterson, D., Fillipski, A., and Kumar, S. (2013). MEGA6: Molecular Evolutionary Genetics Analysis version 6.0. *Molecular Biology of Evolusion. 30*: 2725-2729.
87. Hanscho, M., Ruckerbauer, D.E., Chauhan, N., Hofbauer, H.F., Krahulec, S., Nidetzky, B.,… Natter, K. (2012). Nutritional requirements of the BY series of *Saccharomyces cerevisiae* strains for optimum growth. *FEMS Yeast Research. 12*: 796-808.
88. Surlow, B.A., Cooley, B. M., Needham, P.G., Brodsky, J.L., and Patton-Vogt, J. (2014). Loss of Ypk1, the yeast homolog to the human serum- and glucocorticoid-induced protein kinase, accelerates phospholipase B1-mediated phosphatidylcholine deacylation. *The Journal of Biological Chemistry. 289*: 31591-31604.
89. Ernst, R., Ejsing, C.S. and Antonny, B. (2016). Homeoviscous adaptation and the regulation of membrane lipids. *Journal of Molecular Biology. 428*: 4776-4791.
90. Laplante, M. and Sabatini, D.M. (2009). An emerging role of mTOR in lipid biosynthesis. *Current Biology. 19*: 1046-1052.
91. Lee, J.C., Simonyi, A., Sun, A., and Sun, G. (2011). Phospholipases A2 and neural membrane dynamics: implications for Alzheimer's disease. *Journal of Neurochemistry. 116*: 813-819.
92. Marchan, R., Lesjak, M. S., Stewart, J. D., Winter, R., Seeliger, J., and Hengstler, J. G. (2012). Choline-releasing glycerophosphodiesterase *EDI3* links the tumor metabolome to signaling network activities. *Cell Cycle. 11*: 4499-4506.
93. Cornell, R.B. and Ridgway, N.D. (2015). CTP:phosphocholine cytidylyltransferase: Function, regulation, and structure of an amphitropic enzyme required for membrane biogenesis. *Progress in Lipid Research. 59*: 147-171.
94. Fagone, P. S., and Jackowski, S. (2013). Phosphatidylcholine and the CDP-choline cycle. *Biochimica et Biophysica Acta. 1831*: 523-532.
95. Sreenivas, A., Patton-Vogt, J., Bruno, V., Griac, P., and Henry, S. (1999). A role for phospholipase D (Pld1p) in growth, secretion, and regulation of membrane lipid synthesis in yeast. *The Journol of Biological Chemistry. 273*: 16635-16638.
96. Fernandez-Murray, J.P. and McMaster, C.R. (2005). Glycerophosphocholine catabolism as a new route for choline formation for phosphatidylcholine synthesis by the Kennedy pathway. *The Journal of Biological Chemistry. 280*: 38290-38296.
97. Dowd, S.R., Bier, M.E, and Patton-Vogt, J.L. (2001) Turnover of phosphatidylcholine in *Saccharomyces cerevisiae*. The role of the CDP-choline pathway. *Journal of Biological Chemistry. 276*: 3756-3763.

98. Ejsing, C.S., Sampaio, J. L., Surendranath, V., Duchoslav, E., Ekroos, K., Klemm.,… Shevchenko, A. (2009). Global analysis of the yeast lipidome by quantitative shotgun mass spectrometry. *Proceedings of the National Academy of Sciences of the United States of America*. *106*: 2136-2141.
99. Boumann, H.A., Damen, M.J., Versluis, C., Heck, A. J., de Kruijff, B., and de Kroon, A.I. (2003). The two biosynthetic routes leading to phosphatidylcholine in yeast produce different sets of molecular species. Evidence for lipid remodeling. *Biochemistry. 42*: 3054-3059.
100. Elble, R. (1992). A simple and efficient procedure for transformation of yeasts. *Biotechniques. 13*: 18-20.
101. Amberg, D.C., Burke, D., and Strathern, J. (2005). Methods in yeast genetics: a cold spring harbor laboratory course mannual. Cold Spring Harbor Laboratory Press.
102. Wykoff, D.D. and O'Shea, E.K. (2001). Phosphate transport and sensing in *Saccharomyces cerevisiae. Genetics. 159*: 1491-1499.
103. Longtine, M.S., McKenzie, A., Demarini, D.J., Shah, N. G., Wach, A., Brachat, A.,...Pringle J. R. . (1998). Additional modules for versatile and economical PCR-based gene deletion and modification in *Saccharomyces cerevisiae. Yeast. 14*: 953-961.
104. Schneider, B.L., Steufert, W., Yanq, Q. H., and Futcher, A. B. (1995). Use of polymerase chain reaction epitope tagging for protein tagging in *Saccharomyces cerevisiae. Yeast. 11*: 1265-1274.
105. Yang, K. and Han, X. (2011). Accurate quantification of lipid species by electrospray ionization mass spectrometry - Meet a key challenge in lipidomics. *Metabolites. 1*: 21-40.
106. Smith, C.A., Want, E. J., O'Maille, G, Abagyan, R., and Siuzdak, G. (2006). XCMS: processing mass spectrometry data for metabolite profiling using nonlinear peak alignment, matching, and identification. *Analytical Chemistry. 78*: 779-787.
107. Ausubel, F.M. (1999). *Short Protocols in Molecular Biology*. Wiley and Sons Inc.
108. Pfaffl, M.W. (2001). A new mathematical model for relative quantification in real-time RT-PCR. *Nucleic Acids Research. 29*: e45.
109. Livak, K.J. and Schmittgen, T.D. (2001). Analysis of relative gene expression data using real-time quantitative PCR and the $2^{(-DDC(T))}$ Method. *Methods. 25*: 402-408.
110. Volland, C., Urban-Grimal, D., Geraud, G., and Haguenauer-Tsapis, R. (1994). Endocytosis and degradation of the yeast uracil permease under adverse conditions. *The Journal of Biological Chemistry. 269*: 9833-9841.
111. Almaguer, C., Mantella, D., Perez, E., and Patton-Vogt, J. (2003). Inositol and phosphate regulate *GIT1* transcription and glycerophosphoinositol incorporation in *Saccharomyces cerevisiae. Eukaryotic Cell. 2*: 729-736.
112. Hofbauer, H.F., Schopf, F. H., Schleifer, H., Knittelfelder, O. L., Pieber, B., Rechberger, G. N., …Kohlwein, S. D. (2014). Regulation of gene expression through a transcriptional repressor that senses acyl-chain length in membrane phospholipids. *Developmental Cell. 29*: 729-739.
113. Hofbauer, H. F., Schopf, F. H., Schleifer, H., Knittelfelder, O. L., Pieber, B., Rechberger, G.N., …Kohlwein, S. D. (2014). Acyl-chain remodeling of dioctanoyl-phosphatidylcholine in *Saccharomyces cerevisiae* mutant defective in *de novo* and salvage phosphatidylcholine synthesis. *Biochemical and Biophysical Research Communications. 445*: 289-293.

114. Morisada, S., Ono, Y., Kodaira, T., Kishino, H., Ninomiya, R., Mori, N.,... Fukuda, R. (2018). The membrane-bound O-acyltransferase Ale1 transfers an acyl moiety to newly synthesized 2-alkyl-sn-glycero-3-phosphocholine in yeast. *FEBS Letters. 592*: 1829-1836.
115. Lands, W.E. (1965). Lipid Metabolism. *Annual Review of Biochemistry. 34*: 313-346.
116. Jain, S., Stanford, N., Bhagwat, N., Seiler, B., Costanzo, M., Boone, C. and Oelkers, P. (2007). Identification of a novel lysophospholipid acyltransferase in *Saccharomyces cerevisiae. The Journal of biological chemistry. 282*: 30562-30569.
117. Benghezal, M., Roubaty, C., Veepuri, V., Knudsen, J., and Conzelmann, A. (2007). *SLC1* and *SLC4* encode partially redundant acyl-coenzyme A 1-acylglycerol-3-phosphate O-acyltransferases of budding yeast. *The Journal of Biological Chemistry. 282*: 30845-30855.
118. Tamaki, H., Shimada, A., Ito, Y., Ohya, M., Takase, J., Miyashita, M., …Kumagai H. (2007). *LPT1* encodes a membrane-bound O-acyltransferase involved in the acylation of lysophospholipids in the yeast *Saccharomyces cerevisiae. The Journal of biological chemistry. 282*: 34288-34298.
119. Klose, C., Surma, M. A., Gerl, M.J., Meyenhofer, F., Shevchenko, A., and Simons, K. (2012). Flexibility of a eukaryotic lipidome--insights from yeast lipidomics. *PLoS One. 7*: e35063.
120. Casanovas, A., Sprenger, R. R., Tarasov, K., Ruckerbauer, D. E., Hannibal-Bach, H. K., Zanghellini, J,... Ejsing, C. S. (2015). Quantitative analysis of proteome and lipidome dynamics reveals functional regulation of global lipid metabolism. *The Journal of Biological chemistry. 22*: 412-425.
121. Donahue, T.F. and Henry, S.A. (1981). myo-Inositol-1-phosphate synthase. Characteristics of the enzyme and identification of its structural gene in yeast. *The Journal of Biological Chemistry. 256*: 7077-7085.
122. Salsaa, M., Case, K., and Greenberg, M.L. (2017). Orchestrating phospholipid biosynthesis: phosphatidic acid conducts and Opi1p performs. *The Journal of Biological Chemistry. 292*: 18729-18730.
123. Hoppen, J., Repenning, A., Albrecht, A., Geburtig, S., and Schuller, H. J. (2005). Comparative analysis of promoter regions containing binding sites of the heterodimeric transcription factor Ino2/Ino4 involved in yeast phospholipid biosynthesis. *Yeast. 22*: 601-613.
124. Robinson, K.A. and Lopes, J.M. (2000). Survey and summary: *Saccharomyces cerevisiae* basic helix-loop-helix proteins regulate diverse biological processes. *Nucleic Acids Research. 28*: 1499-1505.
125. Reimand, J., Vaquerizas, J.M., Todd, A.E., Vilo, J., and Luscombe, N.M. (2010). Comprehensive reanalysis of transcription factor knockout expression data in *Saccharomyces cerevisiae* reveals many new targets. *Nucleic Acids Research. 38*: 4768-4777.
126. Zhu, X. and Keeney, S. (2015). High-resolution global analysis of the influences of Bas1 and Ino4 transcription factors on meiotic DNA break distributions in *Saccharomyces cerevisiae. Genetics. 201*: 525-542.
127. do Canto, A., Robalo, J. R., Santos, P. D., Carvalho, A. J. P., Ramalho, J. P. P., and Loura, L. M. S. (2016). Diphenylhexatriene membrane probes DPH and TMA-DPH: A comparative molecular dynamics simulation study. *Biochimica et Biophysica Acta. 1858*: 2647-2661.
128. Kaeberlein, M. (2010). Lessons on longevity from budding yeast. *Nature. 464*: 513-519.

129. Burhans, W.C. and Weinberger, M. (2009). Acetic acid effects on aging in budding yeast: are they relevant to aging in higher eukaryotes?. *Cell Cycle. 8*: 2300-2302.
130. Farrugia, G. and. Balzan, R. (2012). Oxidative stress and programmed cell death in yeast. *Frontier Oncology. 2:* 64.
131. Hai, B., Zhao, Q., Deveau, M., and Liu, F. (2018). Delivery of sonic hedgehog gene repressed irradiation-induced cellular senescence in salivary glands by promoting DNA repair and reducing oxidative stress. *Theranostics. 8*: 1159-1167.
132. Hannun, Y.A. and Obeid, L.M. (2017). Sphingolipids and their metabolism in physiology and disease. *Nature Reviews Molecular Cell Biology. 19*: 175-191.
133. Hannun, Y.A. and Obeid, L.M. (2008). Principles of bioactive lipid signalling: lessons from sphingolipids. *Nature Reviews Molecular Cell Biology. 9*: 139-150.
134. Tams, R. N., Cassilly, C. D., Anaokar, S., Brewer, W. T., Dinsmore, J. T., Chen, Y. L.… Reynolds, T. B. (2019). Overproduction of phospholipids by the Kennedy Pathway Leads to Hypervirulence in *Candida albicans*. *Frontiers in Microbiology. 10*: 86.